

Design and Dynamic Modeling of a Solar Electric Boat Power System

by

Mohammad Abu Abdullah Al Mehedi

A Thesis Submitted to the
School of Graduate Studies
in Partial Fulfillment of the Requirements for the Degree of

Master of Engineering (Electrical)

Faculty of Engineering and Applied Science

Memorial University of Newfoundland

May 2021

St. John's

Newfoundland and Labrador

Canada

ABSTRACT

This thesis describes the system required for a solar electric boat power system with energy storage and a DC gas generator for sailing the boat at 10km/h with 20people. Details of existing diesel engine-driven boats in a river in Bangladesh were collected for the system design. Sizing assessment, sensitivity analysis, and optimization of required power are performed in HOMER. The system's equipment is modeled in MATLAB Simulink platform and simulated to know the dynamic performance of system components. An Arduino-based basic control system also was proposed for the solar boat. The proposed system was simulated in Tinkercad.com web-based software to check the live functionality of the designed control system. Power system instruments were proposed, including solar PV panel, PMDC motor and driver, generator, lead-acid battery, circuit breaker, busbar, and a programmable display device to measure battery voltage and capacity and display data. Additionally, navigation instruments were proposed for measuring water depth, boat speed, and water temperature and display the values on a monitor. The projected payback period was calculated for the recommended solar boat. PV/diesel/battery hybrid power system is compared with PV/battery and the traditional diesel-only power system in this research. Economic analysis indicates that the proposed solar boat design is the best option for rivers in Bangladesh.

ACKNOWLEDGEMENT

I would like to express my gratitude to Dr. Tariq Iqbal for his comprising inspiration and support in accomplishing research in electrical engineering. Without his direction, supervision, patience, insightful comments, immense knowledge, and encouragement, I would not finish this thesis. I am grateful to the Memorial University of Newfoundland to pursue my Master of Engineering degree.

I would like to thank my wife, Nehelina Yeasmin, for her continuous assistance, patience, and encouragement throughout the coursework and research work.

I would like to thank the National Student Loans Service Centre (NSLSC), NL, Canada, for providing the student loan and funding to continue my study.

I would like to acknowledge most profound gratefulness and affection to my lovely kids Amelia Al Mehedi and Aydin Al Mehedi, sisters, and extended family members for their constant support and sacrifice, also friends in St. John's Campus for their devotion and accompany.

Finally, I would like to dedicate this thesis to my parents (Mohammad Abdul Aziz Mian and Zohora Begum).

Table of Contents

Abstract	I
Acknowledgment	II
List of Tables	VII
List of Figures	VIII
List of Abbreviations	XI
List of Symbols	XIII
Chapter 1: Introduction & Literatura Review	1
1.1 Why Solar Electric Power Boat	1
1.2 Currently Used Boats in Bangladesh	1
1.3 Typical River Boats in Bangladesh	2
1.4 Prospectus of Solar Energy in Bangladesh	2
1.5 System Components of Solar PV Powered Boat	4
1.5.1 Solar Photovoltaic (PV) Array	4
1.5.2 Solar Charge Controller (SCC)	6
1.5.3 Battery Bank (BB) for Solar System	7
1.6 Electric Motor for Boat Propulsion	8
1.7 Literature Review	9
1.8 Research Objectives	18
Chapter 2: Sizing of Solar Power System for a Boat	19
2.1 Introduction	19
2.2 Design Overview of Solar Boat	19
2.3 Boat Components Sizing	20
2.3.1 Boat Dimensioning	20
2.3.2 Solar Boat's Speed and Power Demand Computation	21

I	Solar Boat's Hull Speed Calculation	21
II	Solar Boat's Power Demand Calculation	22
III	Boat Parameters Briefly	23
IV	Boat Motor Selection	23
2.4	Sizing the Solar Power System	24
2.4.1	Power Consumption Demands	24
2.4.2	Solar Panel Specification	25
2.5	System Architecture	26
2.6	Daily Load Profile Assessment	27
2.7	Resource Assessment	28
2.8	Technical Details of the Generator	30
2.9	Technical Details of the Battery	30
2.10	Solar Charge Controller	32
2.11	Optimization Techniques	32
2.12	Dispatch Strategy and Constraints	34
2.13	Optimized Sizing for Meeting Boat Load Demand	34
2.13.1	Optimized Hybrid PV/Diesel/Batt System	35
2.14	Proposed Design to Fix PV Array on Boat's Roof	37
2.15	Summary	38
Chapter 3: Dynamic Modeling of the Proposed System in Simulink		39
3.1	Introduction	39
3.2	Simulink Model of Proposed System	39
3.3	Solar Irradiance and Temperature Signal for the Dynamic Model	40
3.4	PV Array Design in Simulink	41
3.4.1	Mathematical Derivation of Solar Cell	42
3.4.2	PV Array Simulink Model	45
3.5	Maximum Power Point Tracking (MPPT)	45
3.5.1	The Perturbation and Observation (P & O) Method	46
3.6	Boost Converter	47

3.7	Bus Bar	47
3.8	Constant voltage (48V to 50V) dropper (CVD) to load	49
3.9	Battery Bank	50
3.9.1	Battery Charge Controller (BCC)	51
3.9.2	Battery Discharge Controller (BDC)	51
3.10	DC Generator	52
3.11	Permanent Magnet DC Motor (PMDC)	53
3.11.1	PMDC Motor Driver	55
3.12	Switching Controller for DC Generator and PMDC Motor	56
3.13	Flow Chart of Working Principle of the Dynamic System	57
3.14	Analysis of the MATLAB Simulation Result of the Proposed System	57
3.15	Summary	68
Chapter 4: Proposed Instrumentation Design and Control Mechanism		69
4.1	Introduction	69
4.2	Proposed Instruments for the Proposed System	69
A	Proposed Power System Instruments	69
B	Proposed Control Mechanism	70
C	Proposed Display System Instruments (Cockpit of the boat)	70
4.3	Proposal for Measuring, Collecting, and Displaying Data of the Proposed System	70
4.4	Proposed Equipment	71
4.4.1	Permanent Magnet Direct Current (PMDC) Motor	71
4.4.2	Variable Speed Control Driver	71
4.4.3	Maximum Power Point Tracker (MPPT)	72
4.4.4	Proposed Main Distribution Board (MDB)	73
4.5	Proposed Switching Control	73
4.5.1	Proposed Physical Connection Outline	74
4.5.2	Proposed Control Mechanism	76
4.6	Summary	77

Chapter 5: Sensitivity and Economic Analysis	78
5.1 Sensitivity Analysis	78
5.2 The sensitivity of PV/ Diesel/Batt system	79
5.3 Payback Period	83
5.4 Environmental Benefits	84
5.5 Summary	85
Chapter 6: Conclusion and Recommendation	86
6.1 Conclusion	86
6.2 Recommendation	88

List of Tables

TABLE 2. 1: SOLAR BOAT PARAMETER	- 23 -
TABLE 2. 2: ENERGY DEMAND FOR PV SYSTEM	- 24 -
TABLE 2. 3: PV PANEL DATA SHEET [65].....	- 25 -
TABLE 2. 4: SPECIFICATION OF GENERATOR.....	- 30 -
TABLE 2. 5: TROJAN SAGM 06 220 LEAD-ACID BATTERY SPECIFICATION [70]	- 31 -
TABLE 2. 6: TECHNICAL AND ECONOMIC CHARACTERISTICS OF THE SYSTEM COMPONENTS.....	- 32 -
TABLE 2. 7: SUMMARY OF OPTIMIZED RESULTS OF HYBRID POWER SYSTEM CONFIGURATIONS	- 35
-	
TABLE 2. 8: SUMMARY OF HYBRID PV/DIESEL/BATT SYSTEM.....	- 36 -
TABLE 2. 9: THE OPTIMIZED SOLUTION FOR THE BATTERY	- 37 -
TABLE 3. 1: CONSTRAINTS FOR PERTURBATION AND OBSERVATION (P & O) METHOD	- 47 -
TABLE 4. 1: SPECIFICATION OF THE PROPOSED PMDC MOTOR	- 71 -
TABLE 4. 2: SPECIFICATION OF THE DC MOTOR DRIVER [79]	- 72 -
TABLE 4. 3: SPECIFICATION OF THE SELECTED MPPT CHARGE CONTROLLER [78].....	- 73 -
TABLE 4. 4: ARDUINO UNO FUNCTIONS	- 75 -
TABLE 5. 1: SENSITIVITY VARIABLES	- 78 -

List of Figures

FIG.1. 1. CONVENTIONAL FLOOD-BASIN PASSENGER BOAT (FBPB) IN BANGLADESH.....	- 2 -
FIG.1. 2. MONTHLY AVERAGE SOLAR RADIATION PROFILE IN BANGLADESH.....	- 3 -
FIG.1. 3. BANGLADESH PHOTOVOLTAIC POWER POTENTIAL MAP	- 3 -
FIG.1. 4. SOLAR DNI (KWH/M ²) GRAPH IN THE MOST IMPORTANT CITIES IN BANGLADESH.....	- 4 -
FIG.1. 5. MONOCRYSTALLINE SILICON CELL.....	- 5 -
FIG.1. 6. POLYCRYSTALLINE SILICON CELL	- 5 -
FIG.1. 7. NON-CRYSTALLINE SILICON IS PLACED ON A FLEXIBLE MATERIAL TO FORM A THIN FILM CELL	- 6 -
FIG.1. 8. PWM WORKING RANGE CURVE	- 7 -
FIG.1. 9. SUNTECH PANEL'S "I vs V" & "P vs V" CURVE	- 7 -
FIG.2. 1. THE SCHEMATIC DIAGRAM OF A HYBRID-POWERED CATAMARANS TYPE PASSENGER BOAT (CPB).....	- 20 -
FIG.2. 2. CANADIAN SOLAR BAND CS6U-330P MODEL 330W SOLAR MODULE.....	- 25 -
FIG.2. 3. SCHEMATIC LAYOUT OF THE PROPOSED HYBRID ENERGY SYSTEM FOR SOLAR BOAT....	- 27 -
FIG.2. 4. DAILY LOAD PROFILE FOR THE PROPOSED ENERGY SYSTEM OF CATAMARANS BOAT...	- 28 -
FIG.2. 5. MONTHLY AVERAGE SOLAR RADIATION AND CLEARNESS INDEX PROFILE	- 29 -
FIG.2. 6. TIME SERIES SOLAR IRRADIATION AND AMBIENT TEMPERATURE PROFILE.....	- 29 -
FIG.2. 7. TROJAN BRAND 6V, 220AH RATED LEAD-ACID BATTERY.....	- 31 -
FIG.2. 8. STEPS FOR OPTIMAL SIZING OF PV/DIESEL/BATTERY HYBRID ENERGY SYSTEM IN HOMER.	- 33 -
FIG.2. 9. ENERGY SHARE FOR HYBRID PV/DIESEL/BATT SYSTEM OVER A WEEK IN MARCH.	- 36 -
FIG.2. 10. DESIGN TO FIX PV ARRAY ON THE PROPOSED SOLAR BOAT.....	- 37 -
FIG.3. 1. SIMULINK MODEL OF THE PROPOSED SYSTEM IN MATLAB.....	- 39 -
FIG.3. 2. CHOSEN IRRADIANCE FOR SIMULATION SOLAR PV POWER-DRIVEN BOAT.....	- 40 -
FIG.3. 3. CHOSEN TEMPERATURE FOR SIMULATION SOLAR PV POWER-DRIVEN BOAT.	- 41 -
FIG.3. 4. PV ARRAY INPUT PARAMETER IN THE SIMULINK	- 41 -

FIG.3. 5. SOLAR PV CELL EQUIVALENT CIRCUIT DIAGRAM	- 42 -
FIG.3. 6. THE V-I CHARACTERISTICS CURVE OF A SINGLE PV MODULE	- 43 -
FIG.3. 7. THE POWER CURVE OF A SINGLE PV MODULE	- 44 -
FIG.3. 8. PV ARRAY V-I CHARACTERISTIC CURVE FOR VARIOUS SOLAR IRRADIANCES.....	- 44 -
FIG.3. 9. PV ARRAY P-V CHARACTERISTIC CURVE FOR VARIOUS SOLAR IRRADIANCES.....	- 44 -
FIG.3. 10. SOLAR PHOTOVOLTAIC ARRAY SIMULINK BLOCK.....	- 45 -
FIG.3. 11. FLOW-CHART OF PERTURBATION AND OBSERVATION (P & O) METHOD.....	- 46 -
FIG.3. 12. BOOST CONVERTER IN THE SIMULINK MODEL.....	- 47 -
FIG.3. 13. BUS BAR SUBSYSTEM IN THE SIMULINK MODEL.	- 48 -
FIG.3. 14. BUS BAR CONNECTION IN THE SIMULINK MODEL.....	- 48 -
FIG.3. 15. CVD SIMULINK MODEL.	- 49 -
FIG.3. 16. NOMINAL PARAMETER OF THE 48V LEAD-ACID BATTERY IN THE SIMULINK BLOCK. .	- 50 -
FIG.3. 17. DISCHARGE PARAMETER OF THE DESIGNATED LEAD-ACID BATTERY.	- 50 -
FIG.3. 18. BATTERY CHARGE CONTROLLER (BCC) DETAILS IN THE SIMULINK MODEL.	- 51 -
FIG.3. 19. BATTERY DISCHARGE CONTROLLER SIMULINK MODEL.....	- 52 -
FIG.3. 20. DC GENERATOR SIMULINK MODEL.	- 52 -
FIG.3. 21. PMDC MOTOR CONNECTION.	- 54 -
FIG.3. 22. THREE-STEP STARTER TO START THE PMDC MOTOR.....	- 54 -
FIG.3. 23. PERMANENT MAGNET DC MACHINE (PMDc MOTOR) SIMULINK MODEL.....	- 54 -
FIG.3. 24. PMDC MOTOR SPEED CHANGER KNOB	- 55 -
FIG.3. 25. PMDC MOTOR DRIVER SIMULINK BLOCK.....	- 55 -
FIG.3. 26. MOTOR CONTROLLER SIMULINK BLOCKS.....	- 56 -
FIG.3. 27. SWITCHING CONTROLLER SIMULINK MODEL FOR DC GENERATOR AND MOTOR.	- 56 -
FIG.3. 28. FUNCTIONAL FLOW CHART OF THE PROPOSED DYNAMIC SYSTEM IN MATLAB SIMULINK.	- 57 -
FIG.3. 29. GRAPH OF PV IRRADIANCE (W/M ²), PV VOLTAGE (V), PV CURRENT (A), PV MEAN POWER (kW), AND PV DUTY CYCLE AMPLITUDE VERSUS TIME IN SECOND.....	- 62 -
FIG.3. 30. GRAPH OF MOTOR SPEED (RPM), MOTOR ARMATURE CURRENT (A), AND MOTOR TORQUE (N.M) VERSUS TIME IN SECONDS.	- 63 -
FIG.3. 31. GRAPH OF BATTERY STATE-OF-CHARGE, I.E., SOC (%), BATTERY CURRENT (A), AND BATTERY VOLTAGE (V) VERSUS TIME IN SECONDS.	- 65 -

FIG.3. 32. BATTERY CHARGER CHARGING CURRENT (A) AND VOLTAGE (V) VERSUS TIME IN SECOND.....	- 66 -
FIG.3. 33. GENERATOR VOLTAGE (V) VERSUS TIME IN SECOND	- 67 -
FIG.3. 34. GENERATOR CURRENT (A) VERSUS TIME IN SECOND	- 67 -
FIG.4. 1. BATTERY CAPACITY AND VOLTAGE MEASURING AND DISPLAY INSTRUMENT.....	- 70 -
FIG.4. 2. A SUPER MOTOR BRAND 5.0kW 48V 3000RPM BRUSHED PMDC MOTOR.....	- 71 -
FIG.4. 3. PROPOSED PWM VARIABLE SPEED CONTROL DRIVER FOR THE PMDC MOTOR.....	- 72 -
FIG.4. 4. PROPOSED PV ARRAY, BATTERY BANK, GENERATOR AND MOTOR SWITCHING CONTROL WITH CODE.....	- 74 -
FIG.4. 5. PROPOSED BATTERY BANK TO ARDUINO CONNECTION FOR VOLTAGE MONITORING.	- 75 -
FIG.4. 6. PROPOSED CONNECTION AMONG ARDUINO, BB, GENERATOR, PV, AND MOTOR.	- 77 -
FIG.5. 1. THE SENSITIVITY OF SOLAR RADIATION AND DIESEL FUEL PRICE FOR PV/DIESEL/BATT SYSTEM ON COE.....	- 80 -
FIG.5. 2. THE SENSITIVITY OF SOLAR RADIATION AND DIESEL FUEL PRICE FOR PV/DIESEL/BATT SYSTEM ON NPC.....	- 80 -
FIG.5. 3. EFFECTS OF PROJECT LIFETIME AND PV MODULE CAPITAL COSTS FOR PV/DIESEL/BATT SYSTEM ON COE.....	- 81 -
FIG.5. 4. EFFECTS OF PROJECT LIFETIME AND PV MODULE CAPITAL COSTS FOR PV/DIESEL/BATT SYSTEM ON NPC.....	- 81 -
FIG.5. 5. EFFECTS OF PROJECT DISCOUNT AND INFLATION RATE FOR PV/DIESEL/BATT SYSTEM ON COE.	- 82 -
FIG.5. 6. EFFECTS OF THE INFLATION RATE AND DISCOUNT FOR PV/DIESEL/BATT SYSTEM ON NPC.	- 83 -
FIG.5. 7. SIMPLE PAYBACK PERIOD (SPBP) GRAPH OF THE PROPOSED SYSTEM	- 84 -

List of Abbreviations

Index	Contents
FBPB	Flood-basin passenger boat
SPB	Solar Powered Boat
BFG	Boat Function Governance
DNI	Direct Normal Irradiation
DC	Direct Current
AC	Alternating Current
PV	Photovoltaic
GHI	Global Horizontal Irradiance
V	Voltage
I	Current
PWM	Pulse Width Modulation
MPPT	Maximum Power Point Tracking
BB	Battery Bank
SOC	State of Charge
AGM	Absorbent Glass Mat
DoD	Depth of Discharge
CC	Constant Current
CV	Constant Voltage
CVD	Constant Voltage Dropper
PMDC	Permanent Magnet Direct Current Motor
RPM, rpm	Revolutions Per Minute
CPB	Catamarans Type Passenger Boat
DH	Draft Height
HOMER	Hybrid Optimization and Multiple Energy Resources
NASA	National Aeronautics & Space Administration
DG	Diesel Generator
NPC	Net Present Cost

COE	Cost of Electricity
MATLAB	Matrix Laboratory
P & O	Perturbation and Observation
D	Duty Cycle
IGBT	Insulated-Gate Bipolar Transistor
PID	Proportional–Integral–Derivative Controller
BCC	Battery Charge Controller
BDC	Battery Dis-Charge Controller
NO	Normally Open
NC	Normally Close
COM	Common
CB	Circuit Breaker
MCB	Main Circuit Breaker
GND	Ground
LED	Light Emitting Diode
O & M	Operation & Maintenance
SPBP	Simple Payback Period

List of Symbols

Index	Contents
CIGS	Copper Indium Gallium Diselenide
CdTe	Cadmium Telluride
a-Si	Amorphous Silicon
kWh	Kilowatt-Hours
kW	Kilowatt
lb	Pound
Ah	Ampere-hour
km	Kilometer
A	Ampere
V	Voltage
hr	Hour
s	Second
N.m	Newton-Meter
W_p	Watts Peak
P_{max}	Nominal Max. Power
V_{mp}	Operating Voltage at Max. PowerPoint
I_{mp}	Operating Current at Max. PowerPoint
V_{oc}	Open Circuit Voltage
I_{sc}	Short Circuit Current
I_L	Light Generated Current
I_D	Diode Saturation Current
R_s	Series Resistance
R_{SH}	Shunt Resistance
n_l	Diode Ideality Factor
K	Boltzmann constant
q	Electron charge
Ncell	Number of cells connected in series in a module
T	Cell temperature

I_d	Diode current
V_d	Diode Voltage
$U(t)$	PID control variable
$K(p)$	Proportional Gain
$e(t)$	Error Value
K_i	Integral Gain
de	Change in Error Value
dt	Change in Time
F	Field Terminal
T_L	Shaft Torque
R_f	Field Resistance
L_f	Field Inductance
ω	Motor Speed (rad/s)
P_{rated}	Motor Rated Power
N_{rated}	Motor Rated Rotation
K	Gain
R_a	Armature Resistance
L_a	Armature Inductance
J	Total Inertia ($Kg.m^2$)
B_m	Viscous Friction Co-Efficient
T_f	Coulomb Friction Torque (N.m)

Chapter-1

Introduction & Literature Review

1.1 Why Solar Electric Power Boat

Global warming and climate change are the most critical concerns that the world is chasing nowadays. The utilization of solar energy is one of the best solutions to overcome, as it does not generate any harmful contaminants leading to global warming. Bangladesh is a South Asian developing country. Either the petrol engine or diesel engine is typically used to operate country boats. A recent trend in boating is the use of electric power for driving a boat [1]. The average solar radiation in Bangladesh is around 4-6.5 kWh/m²/d, with the peak in April and the lowest in December [2]. Solar energy use can assist in energy independence, long-term financial benefits, and a degree of reliability and security [3]. Henceforth, solar power-driven electric boats for water transportation can be a part of clean transportation.

1.2 Currently Used Boats in Bangladesh

I have considered Bangladesh, a country in South Asia, to design a solar electric boat power system. Bangladesh is a land of rivers, and lakes, where water transportation is an essential means of communication. During the rainy season, many roads are obstructed, basically from July to October, when rivers water rise on average 4 meters (12 feet), which also can disrupt school for nearly a million students. So, country boats are still the primary transportation means in the widespread inland waterway [4]. Around 800 rivers, including tributaries, flow through the country. More than 700,000 boats are on the waterway. Approximately 60% are diesel engine driven, and 150 types of flood-basin fishing boats, cargo boats, and passenger boats exist [5]. Most water vessels are driven by fossil fuels like, diesel which creates huge ecological problems for water, air, and waterside inhabitants. The appropriate use of renewable energy sources, particularly solar energy, could resolve the issue, and recently there are many country boats driven by only solar power [6] [7].

1.3 Typical River Boats in Bangladesh

A flood-basin passenger boat (FBPB) is considered as a model for the economic feasibility study, load analysis, and designing solar PV system to drive an FBPB on the Buriganga River for the transportation of around 10 to 12 passengers at a time from one riverbank to the opposite riverside and for tourism as well. The existing FBPB is driven by a diesel engine running at 4knots (7.5km/h) and takes 12-15minutes to cross the buriganga river (**Fig.1.1**). The mentioned water transport system has been used for shuttling offices, marketing, and merchandising business. Subsequently, the frequency of boat travel decreases considerably in the evening. Tourism will be taken into consideration to design the solar-powered boat (SPB). Henceforward, SPB could be able to operate after dawn using the onboard battery.



Fig.1. 1. Conventional Flood-basin passenger boat (FBPB) in Bangladesh

1.4 Prospectus of Solar Energy in Bangladesh

Bangladesh is a subtropical country with more than 300 sunny days a year. Henceforth, PV panels could produce a significant amount of electricity for any kind of appliance. Though in Bangladesh, solar radiation differs concerning season, it receives average solar radiation of 4 – 6.5 kWh/m²/d with peak amount in April and the lowest amount in December with air temperature 23.4 °C - 26.5 °C and optimum tilt of PV modules 22° - 27° (**Fig.1.2**) [2] [8].

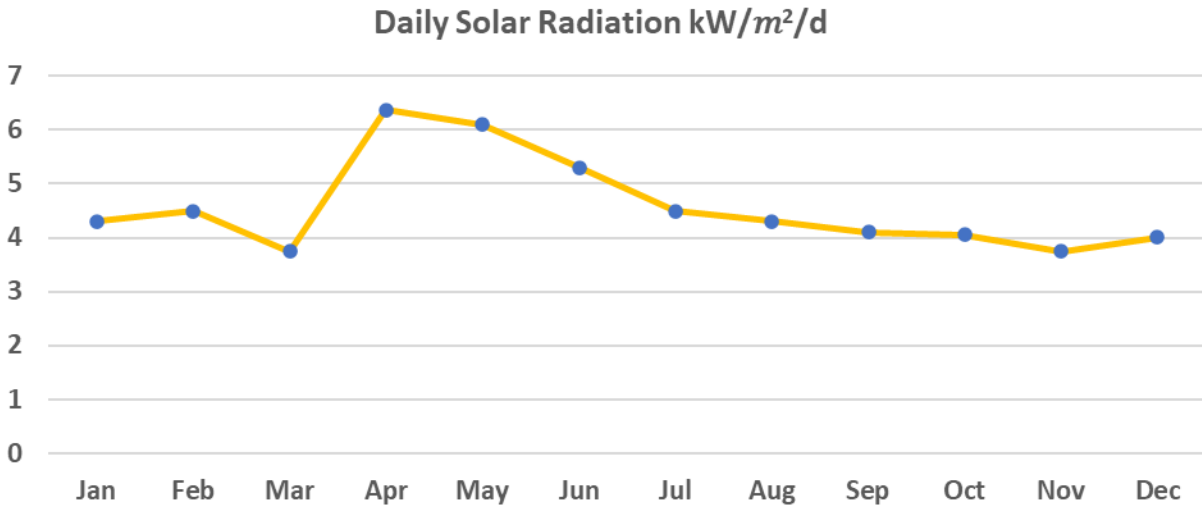


Fig.1. 2. Monthly average solar radiation profile in Bangladesh

Six meteorological stations exist in Bangladesh. According to meteorological stations, a map of Photovoltaic power potentiality has given in **Fig.1.3.**

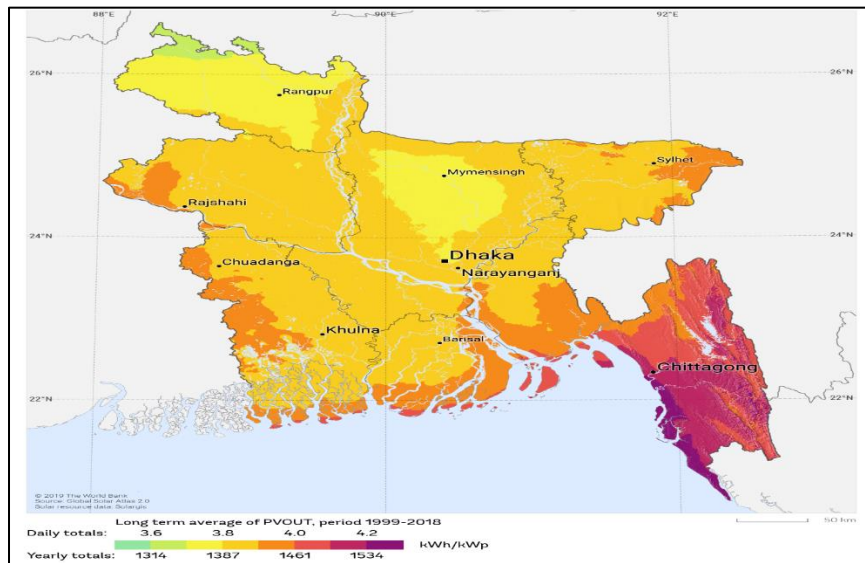


Fig.1. 3. Bangladesh photovoltaic power potential map

The graph of solar Direct Normal Irradiation (kWh/m²) in several most important cities in Bangladesh has been mentioned in **Fig.1.4.**

Direct Normal Irradiation (DNI) data for different places in Bnagladesh

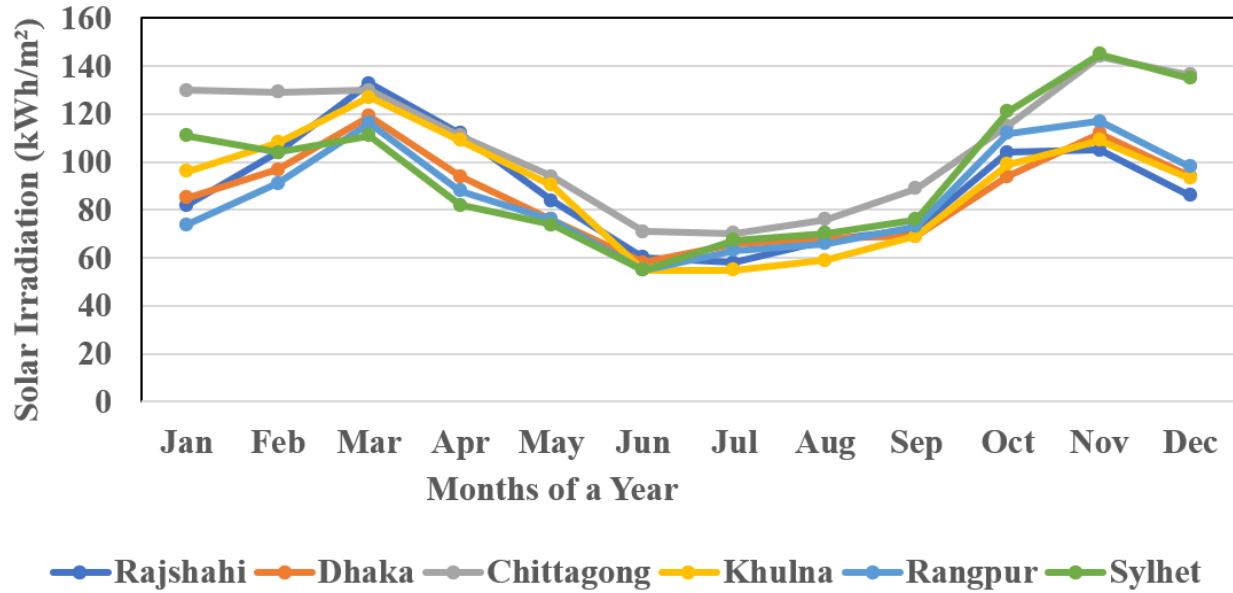


Fig.1. 4. Solar DNI (kWh/m²) graph in the most critical cities in Bangladesh

1.5 System Components of Solar Powered Boat

Solar PV system includes different components chosen according to the system type, site location, and applications. The major components for solar PV powered boat are:

1.5.1 Solar Photovoltaic (PV) Array

Hundreds of photovoltaic cells (solar cells) establish solar photovoltaic (PV) arrays and contain semiconducting properties. PV array is the combination of PV modules. According to the energy demand, PV modules are coupled in series (string) and parallel. While shining sunlight strikes solar cells, it energizes electrons and converts them into electrical current [9].

A conventional PV module consists of 60 or 72 cells in series. In contrast, the 72-cell modules can be configured to behave either as one 24-V module by keeping 72 cells in series or as 12-V modules, which comprises two parallel strings with 36 series cells in each. Polycrystalline silicon cells have been considered, and the sizing of solar PV panels will be performed in the next chapter to do modeling of the solar PV-powered boat. Nowadays, mainly, three kinds of Photovoltaic cell technologies are leading globally [10].

I. Monocrystalline Silicon Cell

It has made from very pure monocrystalline silicon, which forms a single uniform crystal structure. Also, it was the first commercially launched solar cell in the world. This type of cell is beneficial, but the production method is slow. It is more costly in comparison to polycrystalline silicon cells and thin-film cells. **Fig.1.5** reveals the monocrystalline silicon cell.

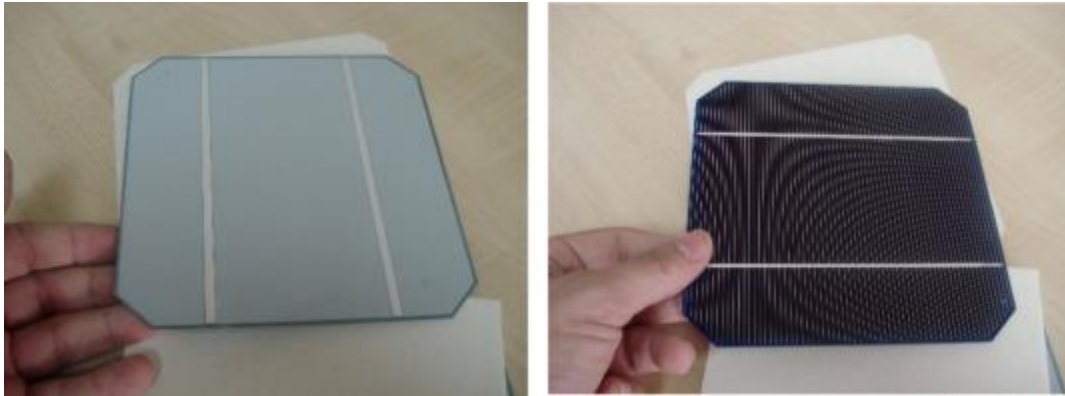


Fig.1. 5. Monocrystalline silicon Cell

II. Polycrystalline Silicon Cell

The polycrystalline (or multi-crystalline) structure consists of several tiny crystal particles, shown in **Fig.1.6**. Though polycrystalline silicon PV cells are less efficient but cheaper, it assists in leading the world PV Cell market in 2015 by producing 70% of Photovoltaic Polycrystalline silicon cells.

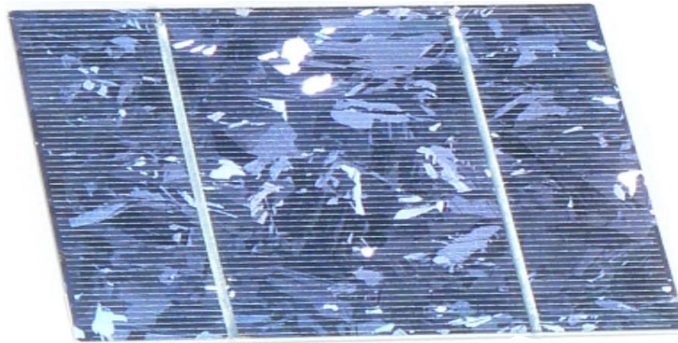


Fig.1. 6. Polycrystalline silicon Cell

III. Thin-film Cell

The photovoltaic cells made from a thin film, such as amorphous silicon (a-Si), are incredibly flexible and viable and significantly lower manufacturing cost but much decreased efficiency. **Fig.1.7** shows the non-crystalline silicon placed on a flexible material to make a thin-film solar panel. Thin-film PV cells are made from copper indium gallium diselenide (CIGS) and cadmium telluride (CdTe), which has more improved efficiency than a-Si.



Fig.1. 7. Non-crystalline silicon is placed on a flexible material to form a thin film cell.

1.5.2 Solar Charge Controller (SCC)

The solar charge controller (SCC) function obtains the maximum power from the available solar power. The harvested power will charge the battery and run the motor in this research. At present, Pulse width modulation (PWM) and Maximum Power Point Tracking (MPPT) solar charge controllers are well recognized in the market. PWM-based SCC controls the PV module's output voltage by adjusting pulse size [11]. The PWM-SCC is suitable for application under a 2kW solar power system. The working range curve for the PWM-SCC is given in **Fig.1.8**. MPPT based SCC extracts the maximum power from a PV module at a specific voltage depends on the required load. MPPT-SCC functions well for more than 2kW solar power systems [11]. Suntech panel's I-V curve and P-V curve has shown in **Fig.1.9** [12].

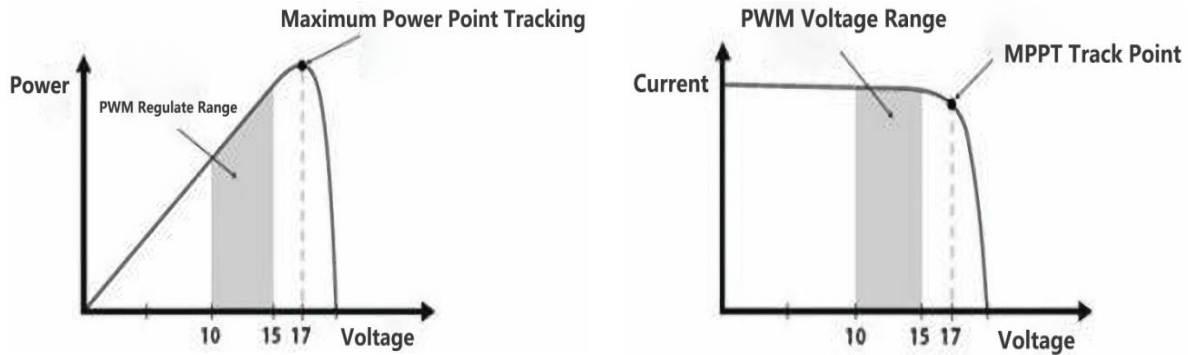


Fig.1. 8. PWM working range curve

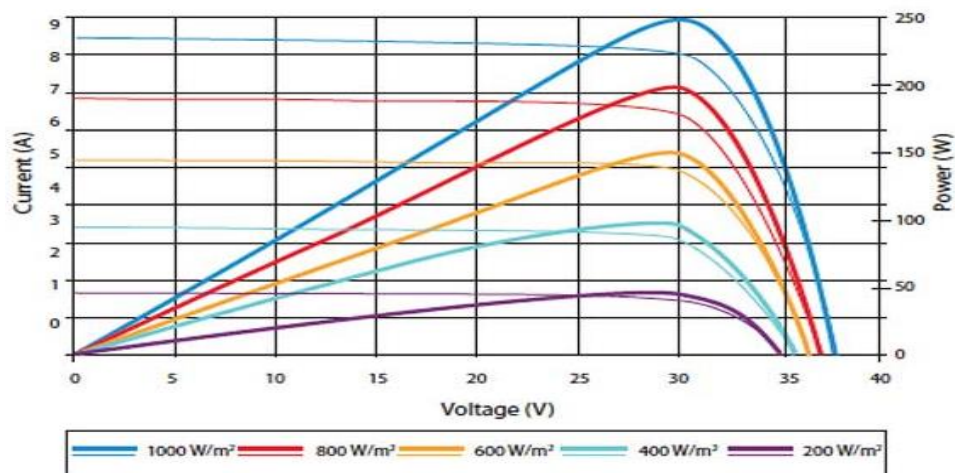


Fig.1. 9. Suntech panel's "I vs. V" & "P vs. V" curve

1.5.3 Battery Bank (BB) for Solar System

To store solar energy in the battery bank needs a battery that gives a small current for a prolonged cycle of time. Solar batteries are classified on the chemical composition of lead-acid, lithium-ion, and saltwater. Among these lithium-ion batteries, the best choice for solar PV system by considering the battery capacity and power ratings, the depth of discharge (DoD), the round-trip efficiency, and the manufacturer & the warranty, although other types are reasonable.

➤ Lead Acid Batteries [13] [14]:

The lead-acid battery technology comprises of Lead-Acid, Absorbent Glass Mat (AGM), and Gel batteries. It has comparatively more minor DoD, a shorter lifecycle, and least expensive

than other kinds of battery. Nowadays, flooded lead-acid battery prices are between \$70/kW-h to \$80/ kW-h, AGM and Gel batteries lie between \$220/ kW-h to \$330/kW-h.

➤ **Lithium-Ion Batteries** [13] [14]:

Lithium-ion batteries are lighter, smaller, more compact, and more robust energy storage devices than lead-acid batteries of the equivalent capacity. It has a greater DoD and extended lifecycle but comparatively costly than lead-acid batteries. At present, the lowest price of lithium-ion battery is offered by the Tesla Powerwall, and the cost is \$505/kW-h.

➤ **Saltwater Batteries** [13] [14]:

Saltwater or sodium-ion batteries are a new technology that is more stable for the solar power storage system. Saltwater batteries are the safest as they can cope with heat perfectly and fully ecological. Also, it has a higher volume of lifecycles and the ability to discharge intensely without hampering lifespan, also does not require maintenance. The price of this battery lies between \$400/ kW-h and \$500/ kW-h.

1.6 Electric Motor for Boat Propulsion

To create propulsion of a boat, need desired power rated motor with approximately 30% surplus of protection [15]. At present, an electric outboard motor is available, which is enormously helpful. It permits slow pace steering to keep the position. The electric outboard motors are made by mixing various components, such as shafts created from high-pitched fiberglass and Stainless steel. It has numerous speed sets for controlling the boat's propulsion, either forward or in reverse. The maximum offered thrust is 55lb, while allowable voltage is 12volt and draw current is 52amp. The electric outboard motor is very much famous for a fishing boat [16]. Henceforth, another type of motor will be the option for using in the tourist boat.

Various types of DC motors are available in the market; among those, three kinds of the electric motor are appropriate for producing the thrust for a solar boat, **i)** DC Shunt Motor (Shunt Wound DC Motor) is a kind of self-excited DC motor. The field windings and armature winding are linked in parallel; thus, the applied voltage is the same for both windings. In general, a Dc shunt motor is built with field windings (stator), an armature (rotor), and a commutator, **ii)** Induction Motor is a rotating transformer. In contrast, the primary transformer refers to the stator

winding, and the second refers to the rotor winding of an induction motor. This device is featured with less expensive, low maintenance cost, easy operation, excellent starting torque, and speed variation. To run an induction motor, need an inverter (DC to AC) and, **iii)** a Brushless direct current motor (BLDC) is constructed without brushes, incorporated with a rotor, a perpetual magnet, and stator. Torque and BLDC motor speed are regulated by supplying a pulse of current to the motor windings through the controller. BLDC motor's performance concerning terminal features, speed control, and boat capacity is acceptable for boat propulsion [15].

1.7 Literature Review

I. Introduction

Various studies related to the expansion and exercise of renewable energy, especially solar-powered boats, have been found in the literature. The electric motorboat Revolution did not move further in the last century due to a lack of technology, energy source, and energy-storing facility in the electrical system. Also, electric motor efficiency was not up to the mark [7]. Solar energy has become the most popular electrical power resource because of advanced, highly efficient solar PV modules [17]. Nowadays, developing countries like Bangladesh are using Solar PV modules to establish the solar home system and massive uses in telecommunication tower in the off-grid areas [6] [7], and worldwide, overall electrification has been practicing by solar PV modules.

II. Literature Study

Kabir et al. [15] described a solar-powered ferry boat in Bangladesh developed to carry 1200kg by converting a conventional ferry boat. This ferry boat was made of local wood. They designed the PV module, motor, and battery storage system but did not report the total control system. Moreover, the water drag force to run the boat is also not discussed.

Mahmud et al. [18] proposed a solar power-driven electric boat for specific load and specific distance movement, but a complete design technique is absent. The light composite material was considered to make a boat. They calculated boat dimensions and hydrodynamics, boat propulsion system, PV capacity, and battery bank size. The boat movement was achieved by

using the motor-driven engine. However, the control system was not reported to keep the constant boat speed while increasing boat passengers.

Postiglione et al. [19] presented a permanent magnet synchronous motor (PMSM) motor-driven zero-emission electric propulsion boat used for public transportation and water sports events. They introduced two PMSM motors, and each engine is rated 12kW and a dc-dc converter for providing steady dc-bus voltage. The boat is a wave penetrating, Catamaran characterized, powered by lithium-ion batteries and the option to charge at the harbor and, partly, with photovoltaic solar panels. This paper has focused on boat speed, duration of power deliver by the battery, does not describe charge control and motor control procedure.

Simonetti et al. [20] proposed an optimistic control technique of a solar-powered vessel driven by an indirect vector-controlled induction motor. To ensure the anticipated method, a trial drive load was coupled and experimented with within the laboratory. This paper does not have sufficient field data regarding solar power and induction motor performance and impact.

Obaid et al. [21] designed an electric boat with a three-phase asynchronous machine powered by solar and diesel hybrid power systems. They used the MPPT system to get maximum PV array output for driving the electric boat. However, a diesel generator was used as secondary power when solar irradiance was inadequate. They also showed the prior solar irradiance forecasting by using a neural network, which assists in planning hybrid power operations for driving the electric boat.

Spagnolo et al. [22] proposed a solar electric tourist boat with advanced management technology for charging and discharging energy storage batteries and could operate pollution-free with a low operating cost. They have used solar PV arrays, battery (45Ah), catamaran boat (14m×5.5m), MPPT controller, boost converter (DC-DC), inverter (DC/AC), charge-discharge controller, and power management controller for the proposed scheme. In a word, it states the integration of pioneering mechanism, engineering method, and intelligible design, safety, and trustworthiness procedures followed in solar boats. It is also observed deficiencies while elaborated the system design.

Campillo et al. [23] tried to discuss the existing tendency of electrification for boat propulsion, assessing the wind and photovoltaic systems. He outlined the electric power system for driving vessels with hybrid power (Generator, battery), only battery, and various resources containing Biofuels, Liquid Natural Gas (LNG), Diesel, FCs, Wind, and PV. Challenge for the improvement of Battery technology to overcome from limited battery range, also battery charging facilities.

Ahmed et al. [24] studied the probability of using PV and wind power on seafaring. The system comprises a PV array, wind turbine, diesel generator, AC/DC converter, DC/AC inverter, and battery storage. They showed that the solar PV panel could be installed on available space in the ship, contributing a significant percentage of energy generation.

Similarly, Reza et al. [25] have analyzed a marine boat powered by solar PV for fishing purposes in Bangladesh using a combination of HOMER, PVsyst software, and manual calculation. The main challenge is to get the maximum output from the solar panel while moving.

J. Hua [26] described the feasibility of renewable energies and their expansion and incorporation for naval transportation. The solar photovoltaic is the first excellent viable and substitutable source to power up the Taiwan maritime industry's commercial vessel. He showed the prosperity of the renewable energy system and the consolidation in the ocean shipment.

Chennai et al. [27] designed a PV/Diesel/Fuel-cell hybrid power system to meet Dubai passengers' main and auxiliary power loads. He used HOMER software for the configuration and simulation. He showed that his proposed architecture is the best eco-friendly hybrid power system, but there is no discussion regarding the investment payback scheme.

Leung et al. [28] designed a PV-powered boat with zero greenhouse gas emissions. They performed case studies (cost savings analysis and reduction of CO₂) by varying solar efficiency. This system saved costs and reduced CO₂ emissions. Also, the author discussed the drawback of the engine-driven boat. Achieve improved battery capacity is the main challenge regarding PV efficiency and its weight.

Chakraborty et al. [29] designed an MPPT based solar PV for fast charging lead-acid battery by using a buck converter and PID controller to fulfill a fishing trawler's power

requirement. The writer used the PIC16F690 microcontroller for buck converter and simulated it in proteus software. The author performed a hardware experiment in the laboratory. However, costing details and a payback period of investment were not reported.

Liu [30] explored a model to reduce CO₂ and NO_x gas emissions and enhanced energy productivity by deploying solar PV and storage systems on a ship. Battery aging and the aftermath of solar irradiance fluctuation are minimized. It has been disclosed that the projected energy storage system could save the battery replacement 25% to 35% at least.

Tamunodukobipi et al. [31] introduced a naval boat powered by the solar PV system. This study used an electric motor for boat thrust, storage battery bank (235Ah, 12V). They faced a challenge for installing solar PV arrays due to lack of space because the proposed system either increases the boat hull's width and length or recharges the battery from the land power grid.

Sayidul Mursalin et al. [32] defined their designed solar boat, but a complete design technique is absent. The boat momentum was achieved by using the motor-driven engine. The boat was also made of light mass composite materials and was not established by changing an existing boat. A motor-driven engine is used for the propulsion of the boat.

Ru-Min Chao et al. [33] mapped out vessel propulsion powered by a standalone distributed photovoltaic system. He has used MPPT technology, power optimizer (PO), the PV power controller, motor controller, Battery management system (BMS), and UART for onboard control for integrating the system. The main challenge is the weight of the Battery bank and replacement cost. The system has been experimented with by reform a PV boat sailing at Love River, Kaohsiung City, Taiwan.

Peter Joore et al. [34] developed solar boats for drifting long distances. He proposed the design and progress of a solar boat for a precise race. Also, a history of the solar boat for notable rivalry and recommendation has been made for future boat design. This paper did not explain design methodology, only a set of project information had been provided in this paper.

Soumya Dasa et al. [35] proposed a country boat powered by a stand-alone photovoltaic system. Buck-Boost converter has been used to simplify the power system and to make stable the economic factor. When excessive voltage is produced from PV array, Chopper operates in buck

mode, and when voltage is lower than reference, chopper functioning in the boost mode to boost up the voltage at a precise value. They used the PV panel for essential shedding to protect the boat passengers from direct sunlight and rain. This technique helps to reduce whole boat weight as well as saving energy and increased passenger capacity.

Aseem Kumar Sharma et al. [36] described the solar photovoltaic system and financial return policy's strength to deploy on a passenger ferry boat in Indian national waterways. The methodology that has been considered for concluding is evaluation of the Indian National Waterways status, incorporation of Solar PV boats, benefits & disputes of the Model and prospective of MW, financial profits & drop rate of greenhouse gas emission by exploiting Solar Photo Voltaic boats, also the world-wide expansion of solar Photo Voltaic technology for boats. This paper does not discuss unified codes, specifications, and Guidelines concerning Solar PV ferries. The main challenge is to implant the solar module directly on the fiber frame boat to lessen the vessel weight.

Waleed Obaid et al. [37] have designed a hybrid power for an electric boat. He used the wind turbine system, solar PV panels scheme, and polymer electrolyte membrane (PEM) fuel cell as the first, second and third renewable energy source to generate power to operate the AC motor for the proposed electric boat. The projected electric boat has been simulated and evaluated by using SIMULINK. Various solar irradiance and wind speed were considered perfect switching, unceasing operation among the hybrid power system mechanism, and constant speed during the experiment. There is no information regarding the motor control system and the impact of variable speed on the power source.

Waleed Obaid et al. [38] [39] offered a scheme of hybrid power system for the electric boat which consists of solar PV panels including MPPT technology, hydrogen storage tank, polymer electrolyte membrane (PEM) fuel cell with water electrolyzer to generate hydrogen and diesel engine coupled with the synchronous machine. He used a weather forecasting system by using Neural Network to achieve solar irradiance by collecting temperature, humidity, wind speed data from the environment, and a fuzzy logic-based battery management system to control fuel flow in the fuel cell relying on battery charge level. Finally, the system has been validated by using

MATLAB SIMULINK. The designed system has been tested with various weather condition by keeping constant speed of boat but not with variable speed.

Sajib Chakraborty et al. [40] discussed the potentiality of solar power implementation on a fishing vessel's free space in Chittagong territory, Bangladesh. He surveyed 200nos of the fishing trawler to collect data of free roof-top space, solar fixed tilt angle to get the maximum solar radiation throughout the year, and power output from the PV panel. This paper does not discuss Life Cycle Cost Analysis and MPPT implementation.

N. A. S. Salleh et al. [41] discussed the probability of using green energy from solar PV and wind for grid-connected charging electric vessels in Kuala Terengganu. He used the various configuration of a wind turbine, Solar PV, converter, Battery, and grid power in HOMER software for simulation. He found the cost-effective & high performed configuration is hybrid grid-PV. There is no information for a solar tracking system to get the maximum output power.

Richard Leiner [42] introduced an emission-free hybrid-powered boat for marine operation. In contrast, solar photovoltaic cells are used to produce Hydrogen gas through an electrolyzer and stored in the tank to operate fuel cells for generating electric power by ensuring optimal use of hydrogen via an energy management system. Also deployed Information management system for collection data remotely by GSM technology. The main challenge is the fuel cell's safe operation and the maximum allowable pressure, and the storage battery's forecasting energy level.

Bankar Jaydip Dilip et al. [43] designed an efficient water transportation system. In contrast, boats are powered from solar photovoltaic cells, which are mounted on the canal surface and charged the battery bank. Boats collect power through the traction method from the overhead line connected to the battery bank. The prime challenge is the maintenance, and if there is any fault raise in the line, all traction boats will be out of service.

Thiago B. Soeiro [44] offered momentum and a charging system of solar-powered electric boats using power electronics. The system is designed with interleaved high-frequency half-bridge digital converters retaining interphase transformer and Gallium Nitride FET semiconductors. He has simulated all hardware in the laboratory. The result showed that the interphase transformers

and GaN FETs converter perform efficiently, and the best result is achieved at the high operating frequency. To troubleshoot power electronics devices, need a highly trained technician.

Nuno Fonseca et al. [45] examined that a tiny electric ship could mitigate power requirements from the fuel cell, solar, and batteries' distributed energy sources. The proposed scheme includes an electric motor, solar photovoltaic array, fuel cell, and battery bank, and it serves the power necessity independently. According to the study, a small-sized electric vessel could run in summer by achieving power from a solar PV array only if the ship is not immensely challenging.

Margaritou Maria D. et al. [46] studied the emissions from Sea-borne ships and the method of lessening the exhaust emission by installing onboard hybrid energy system solar Photovoltaic array and wind turbine optimistically.

Hai Lan et al. [47] explored a power-up ship strategy by a hybrid power system that incorporates a Diesel generator, Battery backup system, and Solar PV array. In this study, minimal asset price, fuel price, and greenhouse gas emissions have been considered to design an off-grid power system by hybrid power. It also examined how the PV module's output varies concerning temperature and solar irradiation change. Finally, the net present cost (NPC) to generate power from the combination of solar PV modules and a Diesel generator is higher than the hybrid power production system.

Alexandros Glykas et al. [48] studied the solar hybrid power system's installation and cost-benefit system on the commercial oceanic ship. They discussed the probability of solar photovoltaic array installation in the ship's ship and the payback period by saved gasoline. The main challenge of increasing oil price, which elongates the payback time and found 10% to 15% increased annual oil cost tends to payback period in-between 16years to 27years. Further investigation is required to design, integrate, test, control systems, and cost assessment of renewable energy systems in the cruise ship for marine transport.

R. Tang [49] [50] has outlined for vast utilization of renewable energy in the vessel a novel solar PV array arrangement with maximum power point tracking (MPPT) technology. A control

tactic and meta-heuristic optimization process was deployed to govern MPPT in real-time and found enhanced output power under various atmosphere.

S. Wen et al. [51] [52] studied the fluctuations of power from solar energy. They proposed a promising scheme for a big vessel to implement solar photovoltaic power and the energy storage system. The methodology that has been followed for governing the optimistic energy storage system is decreasing the investment expenses for both energy storage systems and gasoline and drop of emissions. It also considered the weight fluctuation and different operation states of the vessel.

F. Diab et al. [53] studied the achievement and judgment of hybrid renewable energy systems on land and ship. An assessment was performed regarding the planned renewable energy scheme's payback period and observed reduced gasoline consumption and dropped greenhouse gas emissions.

Chaouki Ghenai et al. [54] described the performance of a hybrid power system that includes solar PV, PEM fuel Cell with electrolyzer (hydrogen production) and H₂ storage tank, and Diesel Generator to assist the main and auxiliary power for a cruise ship in Stockholm, Sweden. This study's primary purpose is to make the environment more green and sustainable oceanic transportation by incorporating renewable energy systems in the small and big vessels. He calculated the cruise ship's power load and modeling and simulation to determine the power system's regular and yearly efficiency, production cost, and energy conversion capacity factor during the investigation. The outcome of this investigation exposed that the proposed system is adequate to meet the cruise ship's energy requirement and approach a decent penetration of renewable resources for naval usages.

Janie Ling-Chin et al. [55] studied the consequences of the hybrid power system on roll-on roll-off freight vessels. In contrast, the hybrid power system is integrated with diesel gen-sets, solar PV arrays, battery banks, cold ironing, propellers and thrusters, motors, transformers, VFDs, AC-AC converters, inverters, and rectifiers. In this study life cycle of equipment and environmental issues were analyzed. They burned marine diesel oil and discharged CO, CO₂, particulate matter, hydrocarbons, NO, and SO₂ to get the maximum impact of the conventional power system in the ship and compared the result with new build hybrid power system and decided

that the proposed scheme have considerable influence on eco system, biological resources, and humanity, henceforth appropriate administration was highlighted.

R.D. Geertsma et al. [56] reviewed the model for managing hybrid power and momentum of intelligent vessels. He categorized the vessel according to the power structure, including a hybrid power supply (solar PV and others), battery bank, ignition, and electrochemical and thrust topology. Advance control techniques for hybrid power systems and ship propulsion systems were established and finally determined that the proposed system could reduce gasoline use and radiations by 10% to 35%, reduce noise, and improve power availability. The main challenge is to combine the total control system, and further research requires crucial incorporation.

Tim Gorter [57] proposed a solar racing boat. In this study, he optimized the solar boat by optimizing the propeller to achieve maximum boat propulsion from the available solar power by considering hull resistance with various speeds and the best possible electric engine efficiency. The result was compared with a similar race boat but not optimized and observed 15% increased efficiency. The primary deficiency is to design a drive train for a PV boat as the optimized solar boat may not work correctly if different voltage (if solar PV output is not constant) and torque is applied.

Satish Babu et al. [58] proposed a solar power system to fill the fishing trawlers' onboard power requirement. The objective was to obtain a stable ecological power and reduce existing costs. ADSGAF company surveyed and calculated onboard load and fuel consumption of Indian fishing boats. With the BOBP-IGO company's assistance, the proposed system has been installed and commissioned for trial and ensured it is more pollution-free, energy-efficient, profitable, and balanced. They suggested further research and testing achieve a perfect integration of the solar PV module's structural and electronic equipment in the fishing boat.

Ahmad Nasirudina et al. [59] planned a scheme to optimize the solar-powered vessel, and the objective was to find out the solar PV system with the least expense. The golden search section algorithm methodology was used to gain the lowest propulsion power from the current ship design, a catamaran traveler used in Taiwan. The simplex algorithm was used to seize the photovoltaic system to get the PV array and battery with the least expense. After the simulation, it was found that the optimal vessel is extra lean and more minor impulsion power (just about 1.75%), and offers

greater photovoltaic power, reduced battery capacity, and reduced annual investment expense, which is around 16% of the current vessel. They faced the challenge of overcoming the weight of PV modules and battery banks and did not consider the impact of solar irradiance fluctuation.

K. Yigita et al. [60] explored a modern energy management method using various techniques and procedures. The objective was to lessen the ecological effects and obtain a balanced power utilization in a vessel and harbor. This study used renewable energy sources, energy storage systems, grid power at the coast, and various marine gasoline for both vessels and harbor. It was seen that the chosen energy management techniques are profitable for harbor, vessel, and the further growth of balanced towns.

The above literature shows that proper equipment sizing for the solar-powered electric boat could harvest maximum solar power from the existing solar irradiance. The solar boat can save the environment. Furthermore, installing renewable energy systems, particularly solar PV systems and storage systems in a boat, further study must optimize daily to yearly energy generation, greenhouse gas emissions, and pay-back periods of investment.

1.8 Research Objectives

The research objective is given in below:

- ✓ Design a solar power system for a riverboat in Bangladesh.
- ✓ Develop a dynamic model of the boat power system in Simulink.
- ✓ Propose a basic control system for a low-cost solar boat and
- ✓ Complete a sensitive economic analysis of a solar electric boat.

Chapter-2

Sizing of Solar Power System for a Boat

2.1 Introduction

Either petrol engine or diesel engine typically operates country boats. Moreover, few practices exist of the hybrid power system for boat propulsion, which combines fossil fuel and clean energy (solar photovoltaic panel, wind energy, fuel cells). Recently, the world is thinking about green power and seeking to stay away from fossil fuels. Henceforth, the best option is electric thrust for driving a boat [1]. The electric propulsion system consists of onboard batteries to store charge from clean energy (solar photovoltaic panel, wind energy, fuel cells) for creating thrust by an electric motor. Hereafter, the solar-powered boat is the most excellent option and viable for the electric propulsion of passenger ferry boats in the river. The equipment could achieve the best result of harvesting maximum solar power from the existing solar irradiance, battery charging, and controlling thrust economically by proper sizing.

2.2 Design Overview of Solar Boat

An electric motor (which is rated 5kW, 3000rpm) drives a boat powered by a hybrid power system, which includes solar PV (10.6kW), DC gas generator (1.6kW), and battery bank (440Ah) is the perfect solution for a conventional water boat. The Catamarans-type passenger boat (CPB), made of fiberglass polyester material, 12m in length and 4.8m in width, has been considered. The CPB speed is measured 10km/h (5.4knots), and it could carry 20passengers at a time. The schematic diagram of a hybrid-powered CPB is shown in **Fig.2.1**. Solar Photo Voltaic (PV) panel will be installed in such a way so that it could work as an energy source and roof of this proposed system boat simultaneously. A 140A rated MPPT controller controls PV power, and its output is connected to the battery through constant current (CC) 25A and constant voltage (CV) 49V charge controller and boost converter. The dc gas generator is connected to the battery bank (BB). BB is linked to the Motor Speed Controller (MSC) through the overcurrent protection device (140A rated DC relay). Motor ON/OFF manual switch is proposed between Motor speed controller and motor.

Finally, the DC motor transmit mechanical rotative power to the boat propeller via coupler and shaft mechanism, while the Switch is in an ON state.

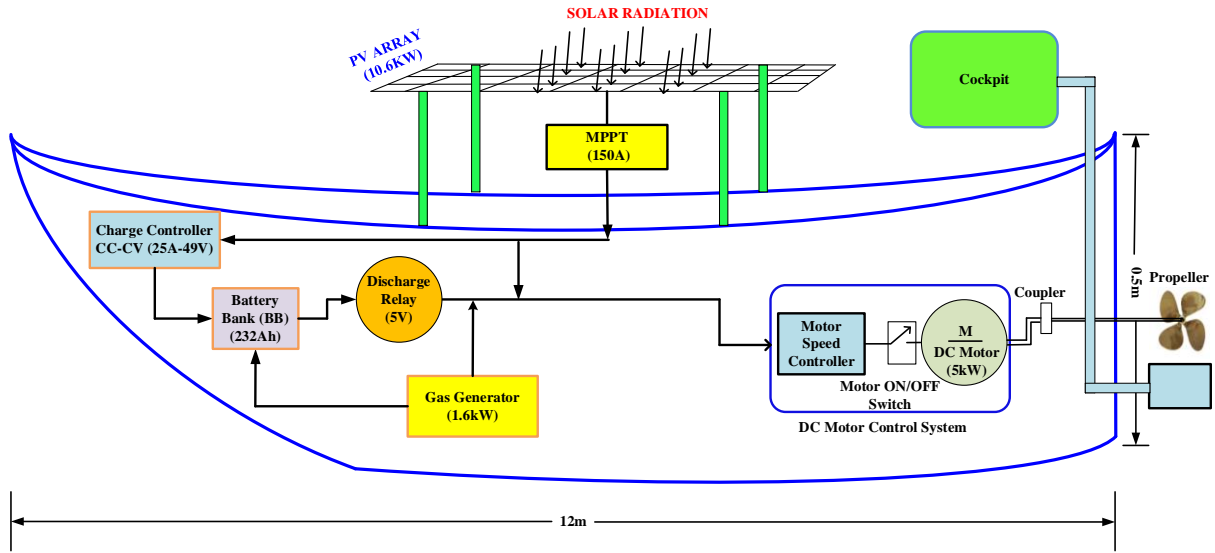


Fig.2. 1. The schematic diagram of a hybrid-powered Catamarans type passenger boat (CPB)

2.3 Boat Components Sizing

The selected main components are the boat dimension, speed, power demand, motor sizing, battery sizing, solar photovoltaic panel sizing, solar charge controller, and generator. The complete design and proper sizing calculation are given step by step below. A HOMER optimization tool has been applied for all the simulation and analysis of the data for solar PV panel, battery, and generator sizing.

2.3.1 Boat Dimensioning

The CPB, which is made of fiberglass polyester material, has been considered. The CPB is 12m in length, width 4.8m by considering 40% of boat length, and calculated draft height 0.04m. For safely boat journey in good weather, the thumb rule to calculate the capacity of the boat, i.e., passenger capacity (assume each, on average weighing 68kg) [61] [62]:

$$\text{Passenger capacity} = (L \times W)/15 = 41 \text{ person}$$

For this research, we have considered 20passengers at a time which is equivalent to 1360kg.

Where, L= Boat length in feet

W=Boat width in feet

To calculate the power required to propel the boat at design speed, need to calculate total displacement water by boat at full load condition, and it is calculated accordingly,

Displacement of water = total Load

= Passenger weight + boat infrastructure weight + battery weight

Displacement of water = 2400kg

2.3.2 Solar Boat's Speed and Power Demand Computation

The proposed hybrid power-driven boat's hull speed is 15.58km/hr, and the existing diesel engine driven country boat speed usually is from 7km/hr to 12km/hr to cross the Buriganga river in Bangladesh. Also, solar PV-powered boat speed is around 10 km/hr in Bangladesh [63]. PV panel size needs to be increased to supply the necessary power for designing higher speed, affecting the said sized boat's stability while sailing. Therefore, the boat speed of 10km/hr (5.4 knots) has been chosen, which is sufficient to cross the river, and medium distance tourism purposes and the computation method has given below:

I. Solar Boat's Hull Speed Calculation

For a catamaran hull shape boat, the conditions are no wind challenge or no current, and the hull is tidy and obstruction-free. Otherwise, the probability of excessive drag, the conceptual boat speed, or the maximum allowable safest speed defines according to the below **Equation (2.1)** [64]:

$$Hull\ Speed = 1.34 * \sqrt{(LWL)} \quad 2.1$$

Whereas,

LWL = The length at the water line = 39.37ft

From Equation (3),

$$\text{Hull Speed} = 1.34 * \sqrt{39.37}$$

$$\Rightarrow \text{Hull Speed (maximum allowable)} = 8.41\text{knots} = 15.58\text{km/hr}$$

Hereafter, **the boat speed has considered 5.4 knots (10km/hr) to proceed with the research.**

II. Solar Boat's Power Demand Calculation

For a catamaran hull shape boat, the conditions are no wind or no current, and the hull is tidy and object-free. Otherwise, the probability of excessive drag, the necessary conceptual horsepower to achieve hull speed, defines according to the below **Equation (2.2)** [64].

$$\text{Motor power (Horsepower)} = (\text{Displacement}) / ((150)^2 / (\text{Hull Speed})^2)$$

2.2

Where, Displacement = 2400kg = 5291lb

Hull Speed = 5.4 knots=10km/hr

We get, From **Equation (2.2)**,

$$\text{Horsepower} = 5291 / ((150)^2 / 5.4^2) = 6.86\text{hp}$$

Henceforth,

$$\text{Motor power} = 6.86 * 746\text{watt}; [1\text{hp} = 746\text{watt}]$$

Motor power $\cong 5.0\text{kW}$

III. Boat Parameters Briefly

Solar boat parameters at a glance have shown in **Table 2.1**.

Table 2. 1: Solar Boat Parameter

Boat Hull Type	Catamarans type passenger boat (CPB)
Boat materials	Fiber Glass Polyester materials
The gross weight of the boat (full load capacity)	2400kg (5291lb)
Passenger on board	20 people
Boat length	12m (39.37ft)
Boat beam (the transverse distance between the outer sides of the boat)	4.8m (15.75ft)
Draft height (DH)	0.04m (0.13ft)
Boat depth	0.5m (1.64ft)
The displaced volume of water	2.41m ³
Displacement of water by fully loaded boat	2400kg (5291lb)
Maximum and the safest Hull speed	15.58km/hr (8.41knots)
Considered Hull speed	10km/hr (5.4knots)
Maximum boat speed by propeller and propeller efficiency	10.06km/hr (5.43knots), 99.43%

IV. Boat Motor Selection

Various DC motors are available in the market, like DC shunt motor, Brushless DC, and Induction motor. To run an induction motor, need an inverter (DC to AC) and driver to control speed, also high maintenance cost, which is opposed to using it. DC shunt motor could serve the purpose, but the risk is brushed that could be badly-behaved in the field when it will be depreciated because of frequent utilization.

A 5.0kW 48V 3000rpm permanent magnet DC motor has been considered as the system bus voltage is 48V and 3000rpm for the designed propeller (12inch pitch, slip 40%, and gear ratio 3:1) to achieve a designated boat operating speed of 10km/hr.

Also, the PM DC motor generates revolving torque by alternating phase current concerning time for the motor's commutation method, and the system is known as controlled commutation by electronic means. PMDC motors are also represented as trapezoidal permanent magnet motors.

2.4 Sizing the Solar Power System

Solar Photovoltaic (PV) system is a very reliable and clean source of electricity that can suit a wide range of applications such as a boat, telecommunication, residence, industry, agriculture, livestock, etc. The Battery bank, PV, and generator have been evaluated manually to compare with HOMER software. The following steps are necessary to size the solar photovoltaic system:

2.4.1 Power Consumption Demands

Power consumption demand has been calculated by the following **Equation (2.3)** [15]:

$$\text{Energy demand} = \text{Load}(kW) * \text{Time}(hr) \quad 2.3$$

Table 2.2 represents the daily energy demand for a PV system of the electrical device and loads operated from the Solar Photovoltaic (PV) system, obtained by calculating **Equation (2.3)**. These are obtained by optimizing power consumption and lessen power demands by adjusting light, motor, and computer ON/OFF time.

Table 2. 2: Energy demand for PV system

Equipment	Current (A)	Voltage (V)	Run Time (hr)	Power (kW)	Energy Consumed (kWh)
BLDC Motor	104	48	8	5.00	40.00
Light-1	1.25	48	1	0.06	0.06
Light-2	0.83	48	3	0.04	0.12
Cockpit control and others	5.00	48	8	0.24	1.92
Total Load	44.58	48	20	5.34	42.10

2.4.2 Solar Panel Specification

A polycrystalline Canadian solar panel brand CS6U-330P model, 72-cell, 330 Watts, and 1.96m x 0.992m solar panel is considered by counting PV panel efficiency and price for PV size calculation. **Fig.2.2** reveals the Canadian solar band CS6U-330P model 330W solar module, and the datasheet, i.e., brief specification of PV panel, is given in **Table 2.3**.

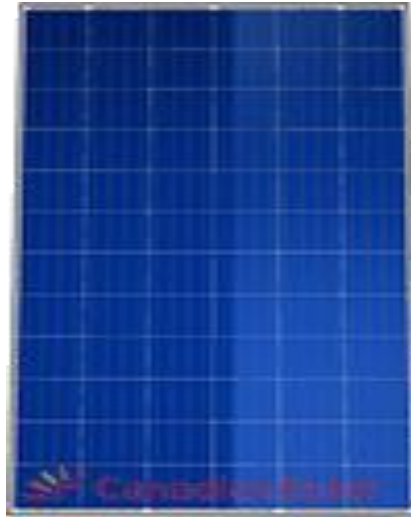


Fig.2. 2. Canadian solar band CS6U-330P model 330W solar module

Table 2. 3: PV panel data sheet [65]

Brand	Canadian solar panel
Electrical data	
CSI model no.	CS6U-330P
Nominal Max. Power (Pmax)	330W
Opt. Operating Voltage (Vmp)	37.2V
Opt. Operating Current (Imp)	8.88A
Open Circuit Voltage (Voc)	45.6V
Short Circuit Current (Isc)	9.45A
Module Efficiency	16.97%
Operating Temperature	-40°C ~ +85°C
Max. System Voltage	1000 V (IEC) or 1000 V (UL)

Max. Series Fuse Rating	15A
Power Tolerance	0 ~ + 5 W
Mechanical data	
Cell Type	Poly-crystalline, 6 inch
Cell Arrangement	72 (6 × 12)
Dimensions	1960 × 992 × 40 mm (78.7 × 39.1 × 1.57 in)
Weight	22.4 kg (49.4 lbs)
J-Box	IP68, 3 diodes
Cable	4.0 mm ² (IEC), 12 AWG (UL), 1160 mm (45.7 in)
Connector	T4 series (IEC / UL)
Temperature Characteristics	
Temperature Coefficient (P _{max})	-0.41 % / °C
Temperature Coefficient (V _{oc})	-0.31 % / °C
Temperature Coefficient (I _{sc})	0.05 % / °C
Nominal Module Operating Temperature	43±2 °C

2.5 System Architecture

A schematic layout of the proposed hybrid power system for a boat is shown in **Fig.2.3**. In this study, PV modules are used to produce baseload demand. In contrast, a diesel generator is also used as a standby option when there is an insufficient supply of electricity from PV due to solar inaccessibility, thus increasing its reliability. The excess energy from PV modules and diesel generators is charged to the battery and used to supply the load demand until it reaches its minimum state of charge (SOC). The system does not need any bi-directional converter since there are no AC components.

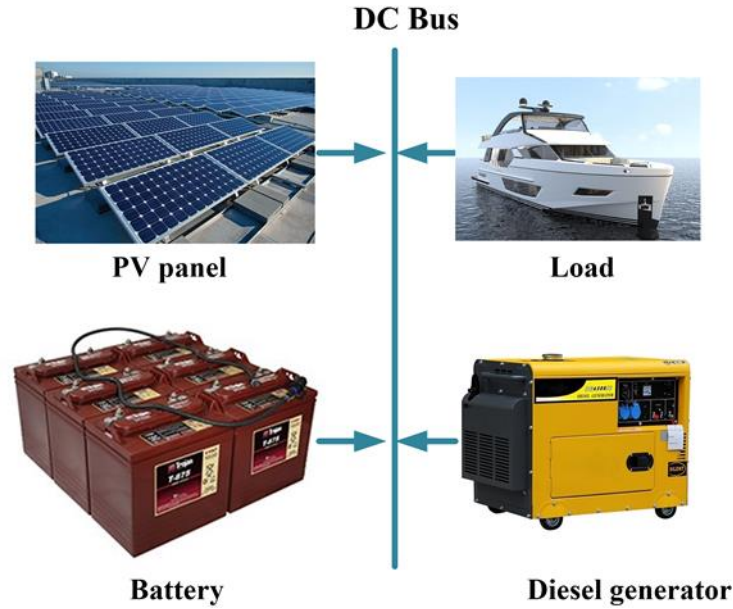


Fig.2. 3. Schematic layout of the proposed hybrid energy system for solar boat

2.6 Daily Load Profile Assessment

The load demand consists of the motor, light, control system, computer, and miscellaneous. **Table 2.2** shows the load demand for a catamarans boat in climatic conditions of Bangladesh. Following the load consumption in HOMER software, some hypothesis that solar boat will be in operation 08hours in a day and starts the journey from 08:00 am stopped at 04:00 pm while the boat is in rest 01:00 pm. The daily load profile for the boat is presented in **Fig.2.4**. In this research, a small PMDC motor with a capacity of 5 kW is considered to propel the boat at 10km/hr, where the constant daily load demand is 42.10 kWh with an average load of 1.75 kW and peak load demand 5.34 kW. In the simulation undertaken, the load demand is considered constant irrespective of the proposed hybrid system season. A residential load is selected in HOMER software, which produces a monthly average data profile based on **Table 2.2**. This total electric load profile is then scaled with the peak load demand of 3.22 kW, the average load of 1.06kW, and the average load demand of 25.38 kWh/d. The annual average energy demand is scaled 25.38kWh/d as the boat will run 220days a year. Additionally, the baseline and scaled load factor are 0.33.

The HOMER scale value parameter has determined by the below **Equation (2.8)** [61] :

$$\text{Scaled value} = \left(\frac{\text{total operating days in a year}}{365 \text{ days}} \right) \times \text{energy demand} \quad (2.8)$$

$$\text{Scaled value} = 25.38 \text{ kWh/d}$$

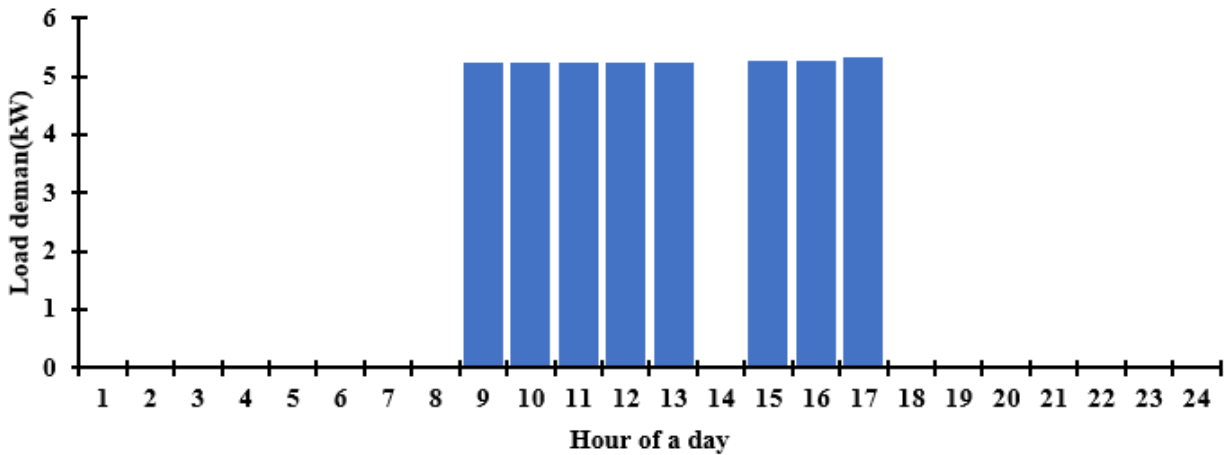


Fig.2. 4. Daily load profile for the proposed energy system of Catamarans Boat

2.7 Resource Assessment

The monthly average solar radiation data and clearness index profile was collected from NASA using the HOMER tool as sufficient measured data was unavailable for the desired location Sadarghat, Bangladesh. It can be seen from **Fig.2.5** that the solar radiation data vary in a range of 4.02 to 5.76 kWh/m²/day, where the scaled annual average value is 4.65 kWh/m²/day with a clearness index of 0.52. It is also noted that high solar radiation periods are observed from February to May with the highest intensity in April (5.76 kWh/m²/day) and the lowest intensity period started from June to December with minimum passion in September (4.02 kWh/m²/day).

Solar Photovoltaic panel sizing [61]

Perfect solar photovoltaic sizing is required to obtain the enhanced performance of the proposed system; hereafter, various parameters have been given as the input of the HOMER

software. In this proposed system, we have studied PV lifetime 25years and no tracking system. The capital cost of PV is examined by \$0.65/W_p [66] [67]. We have considered, there is no replacement cost as the project lifetime has assumed 10years. Evaluating the present market value, operation, and maintenance (O &M) cost is considered \$10.00/year. We have chosen 330 Watts, 24 Volts, and 1.96m x 0.992m polycrystalline **72-cell solar panel**.

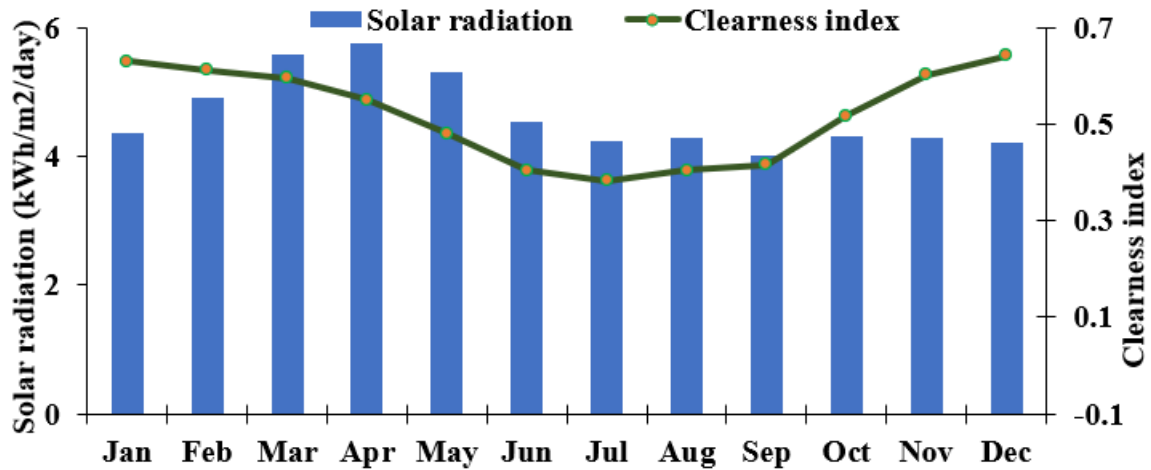


Fig.2. 5. Monthly average solar radiation and clearness index profile

HOMER also created the synthesized 8760 hourly radiation values over the entire year and presented in **Fig.2.6**.

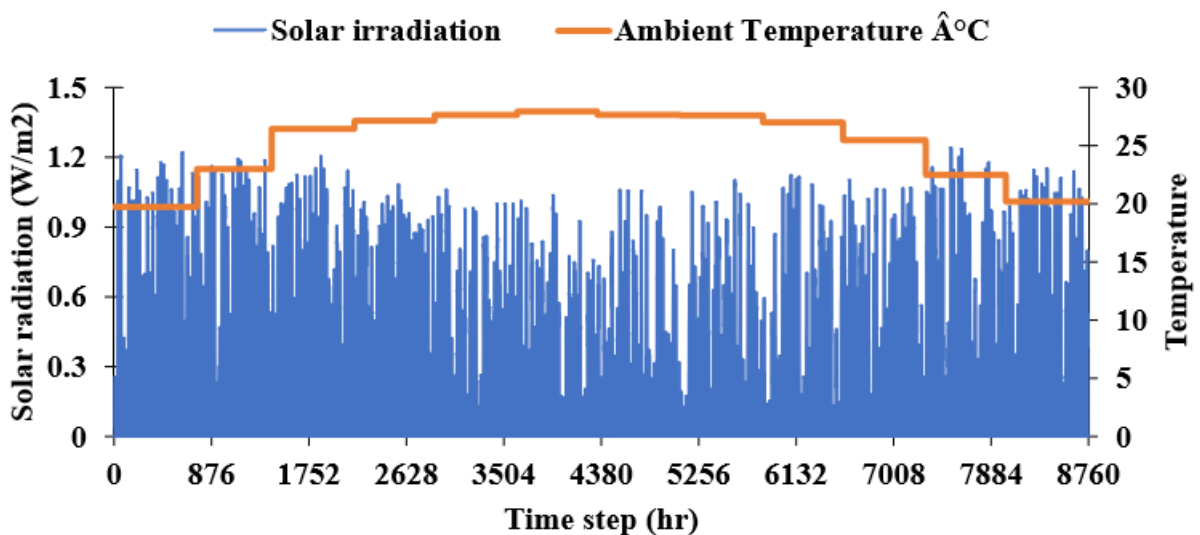


Fig.2. 6. Time series solar irradiation and ambient temperature profile

2.8 Technical Details of the Generator

For the emergency, if the PV output and battery stored energy are insufficient to drive the load, the generator will provide additional power to overcome this situation. In this research, a small-sized Champion 1600W / 2000W inverter generator has considered which has capacity 1.6kW, capital cost \$ 600.00, replacement cost \$400.00, O & M cost \$.05/op.hr , the lifetime of generator 12000hrs and fuel cost \$0.76/lit [69]. The technical specification of the generator has given in **Table 2.4.**

Table 2. 4: Specification of generator

Assembled width, depth, and height (cm)	32,52 and 43
Assembled weight (kg)	21
Generator	Inverter
Noise level (dB)	53
Starting watts (W)	2000
Running watts (W)	1600
Number of 120V outlets	2
Generator starts	Recoil
Half load run time (hr)	5.5
Fuel tank capacity (lit)	4.1

2.9 Technical Details of the Battery

In this study, lead-acid is considered for simulation, which receives surplus energy during charging and provides energy at the time when RE sources are unable to satisfy load requirements. While the solar PV power generation is not sufficient to run the boat motor, then additional power will be delivered by the battery bank in horrible weather conditions while there is no sun. This research has considered a Trojan SAGM 06 220 kinetic battery model with nominal voltage 6.0V, nominal maximum capacity 220Ah (1.32kWh). The capital cost, replacement cost, and O & M cost for a single battery have been considered \$362.00,\$330.00, and \$15.00, respectively [70]. Besides, the battery string size is defined as 48V, which is known as system BUS voltage. Trojan

branded a Lead-acid battery deep cycle series SAGM 06 220 has flashed in **Fig.2.7**, and a brief specification has given in **Table 2.5**.



Fig.2. 7. Trojan brand 6V, 220Ah rated Lead-acid battery.

Table 2. 5: Trojan SAGM 06 220 Lead-acid Battery specification [70]

Model Name	Dimensions (mm)			Weight (kg)	SOC @ Open-Circuit Voltage	
SAGM 06 220	Length	Width	Height		Percentage Charge	6 Volt
	262	179	273		31	100
Electrical Specification					75	6.27
Voltage	Capacity (Ah)		Energy (kWh)		50	6.12
6V	20-Hr		20-Hr		25	5.97
	220Ah		1.32kWh		0	5.82
Charger Voltage Settings (at 77°F/25°C)						
Maximum Charge Current (A)					20% of C ₂₀	
Absorption Voltage (2.40 V/cell)					7.2	
Float Voltage (2.25 V/cell)					6.75	

2.10 Solar Charge Controller

Maximum power point tracking (MPPT) is a system included in charge controllers used for extracting maximum available power from the PV module under certain conditions by regulating voltage and current. Maximum power varies with solar radiation, ambient temperature, and solar cell temperature. The MPPT is rated based on the following calculation [71] :

$$\text{MPPT current rating} = \frac{\text{total required power}}{\text{BUS voltage}} = \frac{5.34\text{kW}}{48\text{V}} = 111.25 \text{ A}$$

To overcome unexpected light reflection factors, 25% more rating is considered for safety.

$$\text{MPPT current rating} = 111.25 + 111.25 * 25\% \cong 140 \text{ A}$$

This analysis judged a charge controller with a capital cost of \$100.00, the replacement cost of \$100.00, O & M cost \$10.00/yearly, and a lifetime of 4years [66] [72].

Input parameters for solar charge controller are given in **Table 2.6** :

Table 2. 6: Technical and economic characteristics of the system components

Components	Capital Cost	Replacement Cost	O&M Cost	Lifetime
PV	\$0.65/W _p	0	\$10.00/year	10yr
Diesel	\$600.00	\$400.00	\$0.05/op.hr	12000hrs
Battery	\$362.00	\$330.00	\$15.00	1,257.40kWh
Controller	\$100.00	\$100.00	\$10.00/year	4years
Discount Rate (%)	8			
Inflation rate (%)	2			
Lifetime	10 year			

2.11 Optimization Techniques

This present study will demonstrate the techno-economic feasibility of a PV/Diesel/Battery hybrid power system for a Catamarans type Boat in Dhaka, Bangladesh. Hybrid Optimization

Model for Electric Renewable (HOMER) is a popular tool to study and design for the hybrid power system to determine optimal sizing of a system by comparing with other possible configuration. The steps followed during the analysis are shown in **Fig.2.8**.

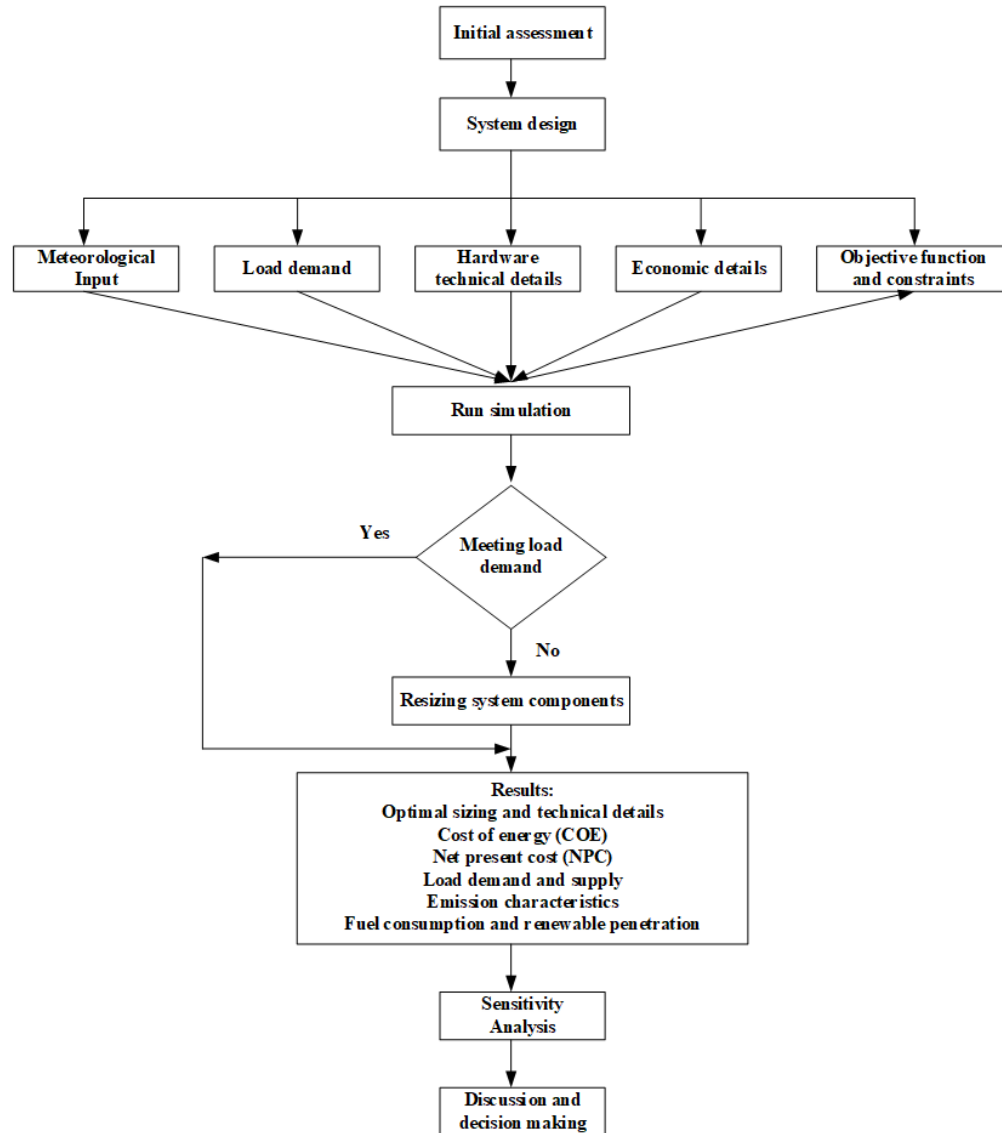


Fig.2. 8. Steps for optimal sizing of PV/Diesel/Battery hybrid energy system in HOMER.

The process of optimization starts with a preliminary assessment and developing system architecture. Then the method identifies the available renewable resources (e.g., solar irradiation, temperature profile, clearness index, etc.) in the selected area, followed by estimating the load requirements, choosing the technical and economic details of system components, and selecting the objective function and necessary constraints. HOMER models the system and suggests the best

configuration. The estimation of load requirements is an essential factor that helps to choose proper hardware components. The financial details include capital costs, replacement costs, Operation and Maintenance costs (O & M) costs, fuel price, and lifetime, whereas the emission details need to assess the environmental analysis. Finally, the sensitivity analysis was performed to observe the influence of input variables on the optimized system.

2.12 Dispatch Strategy and Constraints

HOMER simulates the system components together as a single system in each time step and decides which power source should supply the load at what power level and whether to charge or discharge the batteries. The control system's decision to operate a hybrid energy system occurs every hour based on the energy balance computation.

There are two main operating strategies in HOMER: Load Following (LF) and Cycle Charging (CC) dispatch strategies. In the LF strategy, the PV arrays supply the load, and diesel generators only supply the loads in the absence of PV power. The excess energy from the solar PV charges the batteries. On the contrary, diesel generators meet loads demand and simultaneously charge the batteries in the CC strategy. However, CC generates more excess energy, which increases the total NPC of the system. As a result, LF is the preferred strategy and hence considered in the analysis. In the load dispatch strategy, the load is supplied by the PV. The generator works only when the batteries are discharged to produce enough energy to satisfy the primary load at the least total cost and COE.

2.13 Optimized Sizing for Meeting Boat Load Demand

In this study, the hybrid PV/Diesel/Battery energy system is designed to fulfill the Catamarans Boat's load demand for its proper operation and control. After the technical and economic parameters were set, the system was simulated by the HOMER software tool to optimize the system components according to the load profile. The corresponding results are presented in this section. Later, a sensitivity analysis was performed to observe the system response corresponds to varying input parameters. **Table 2.7** shows the summary of different hybrid configurations with their optimal operating characteristics. It is found that PV/Diesel/Battery is the

optimized system with the minor COE 0.228 \$/kWh. The system is also able to supply the load with maximum renewable penetration of 92.1%.

On the other hand, PV/Battery shows excellent emission characteristics; however, the electricity cost is very high as 0.350 \$/kWh. **Table 2.10** shows the annualized cost summary of different hybrid system configurations. The PV/Diesel/Battery requires a total minimum NPC of only \$15,625, whereas the PV/Battery is the most expensive configuration with NPC \$23,985. The individual results are presented in the following sections.

Table 2. 7: Summary of Optimized Results of Hybrid Power System Configurations

Parameters	PV/Diesel/batt	PV/batt	Diesel only
COE (\$/kWh)	0.228	0.350	0.321
NPC (\$)	15,625	23,985	21,980
Diesel Genset (kW)	1.60	-	4.00
PV module (kW)	10.6	14.8	-
Battery (kWh)	18.5	46.2	-
Genset energy (kWh/yr)	779	-	9,264
PV energy (kWh/yr)	15,990	22,346	-
Diesel consumption (L/yr)	223	-	2914
Excess Energy (kWh/yr)	7,325	12,920	0
Unmet load (kWh/yr)	2.87	6.18	0
Capacity shortage (kWh/yr)	7.93	8.86	0
Renewable fraction (%)	92.1%	100	0

2.13.1 Optimized Hybrid PV/Diesel/Batt System

Optimal design of the PV/Diesel/Batt system for the boat consisting of the different components comprising 10.6 kW PV, 1.6 kW diesel generator, 18.5 kWh storage batteries as best optimized and economic configuration simulated, as presented in **Table 2.7**, also the optimized battery details is shown in **Table 2.9**. Total 32nos. of PV module is required to achieve 10.6kW. HOMER provides this optimized result based on NPC, COE, and initial capital investment. Total Net present cost (NPC), total capital cost, and cost of electricity (COE) of the optimized

PV/Diesel/Batt configuration are \$15,625, \$13,557, and \$0.228/kWh. **Fig.2.9** shows the energy share for hybrid PV/Diesel/batt system over a week in March. It is found that solar PV covers most of the load demand during that period. However, this configuration needs 223 L diesel in an entire year in addition to this PV power. The battery comes into play during the unavailability of renewable sources. The system also generates 7,325 kWh of excess energy after meeting the charging load demand of the battery. The system requires \$13,357 capital cost followed by a replacement cost of \$142 in his lifetime of 10 years. The replacement cost of the system is high due to the limited lifetime throughput of the battery. However, the operating cost is higher than replacement and resource cost as only \$2801. The system has some salvage value of \$1,903 after its operating period. **Table 2.8** shows the energy balance of the hybrid PV/Diesel/Battery system.

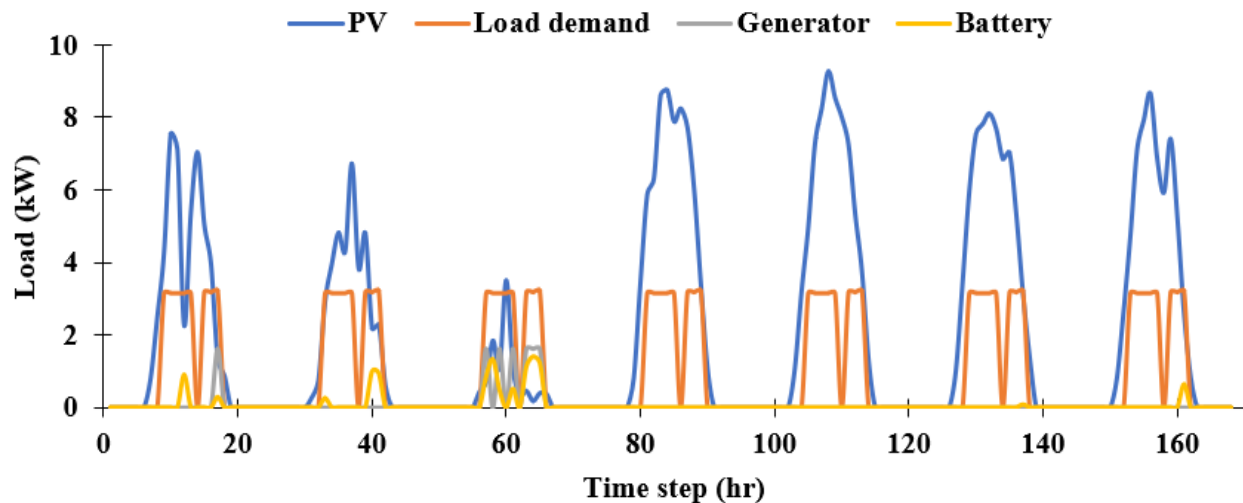


Fig.2. 9. Energy share for hybrid PV/Diesel/batt system over a week in March.

Table 2. 8: Summary of hybrid PV/Diesel/batt system

System sizing		Cost summary		Electrical energy	
PV Module	10.6 kW	COE	0.228 \$/kWh	PV energy	15,990 kWh
Diesel	1.6 kW	NPC	\$15,625	Diesel	779 kWh
Battery	18.5 kWh	Annualized cost	\$2115.00	Total	16,719 kWh

Table 2. 9: The optimized solution for the battery

Quantity	Value	Units	Battery Ratings	Notes
Batteries	16	qty.	6V, 220Ah	Total 440Ah for 48V bus system.
String Size	2	strings		
Bus Voltage	48	V		

2.14 Proposed Design to Fix PV Array on Boat's Roof

The way PV array could fix on the proposed solar boat's roof is given in **Fig.2.12**, and the calculation has presented below:

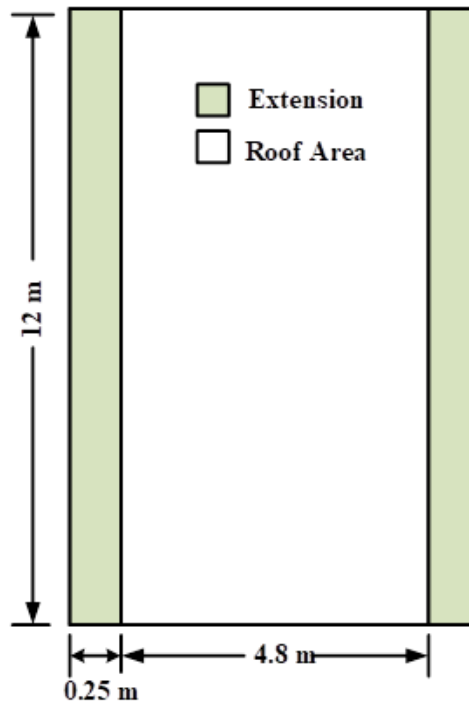


Fig.2. 10. Design to fix PV array on the proposed solar boat.

The area of the boat = $L \times W = (12\text{m}) \times (4.8\text{m}) = 57.6\text{m}^2$

The area of the PV module = $L \times W = (1.96\text{m}) \times (0.992\text{m}) = 1.94\text{m}^2/\text{module}$

Since the solar panel has an area of 1.94 m^2 and the rated capacity is 330 W,

$$\text{The total area required to install 10.6kW PV} = \frac{(10.6 \times 1000w) \times (1.94m^2)}{(330w)} = 62.3m^2$$

Since the roof remains unused, it could be extended to 0.25 m with the help of cantilever support from both sides. Then the total area of the boat after extension will be 63.6m², [(12m) *(4.8m + 0.25m*2)].

Therefore, the roof area with the extension could be able to accommodate the PV panel successfully.

2.15 Summary

System component sizing of PV array, generator, battery bank, and MPPT charge controller is presented for a boat. The PV protection system is protected with a fuse, but surge protection device and PV Grounding will not be used, as the PV module will be installed in the boat and will float on water. Cost analysis has been done by homer software and found the designed system is cost-effective to implement. In the future, hybrid power (PV, fuel cell, and diesel engine) driven boats could be developed, and system size could improve to drive the boat at night and successive two or more cloudy days. The proposed PV/Generator/Battery system comprises clean technologies. It offers close to zero emission during operation since the designated generator will produce only 7.9% of the total electricity required in a year.

The result from HOMER is more precise and optimized. Henceforth, the next chapter, “Dynamic Modeling of the Proposed System in MATLAB Simulink Model,” will be performed based on the HOMER optimized result.

Chapter-3

Dynamic Modeling of the Proposed System in Simulink

3.1 Introduction

The optimized power system includes PV array, Battery, and Diesel Generator and system components. It comprises DC Motor & driver, MPPT controller, Switching Relays, and Battery charge controller designed in MATLAB by using Simulink to analyze the system components' dynamic performance and predict how the scheme will function if implemented real life. Besides, the dynamic simulation will help for instrumentation layout.

3.2 Simulink Model of Proposed System

The Simulink model of the proposed system in MATLAB has shown in **Fig.3.1**.

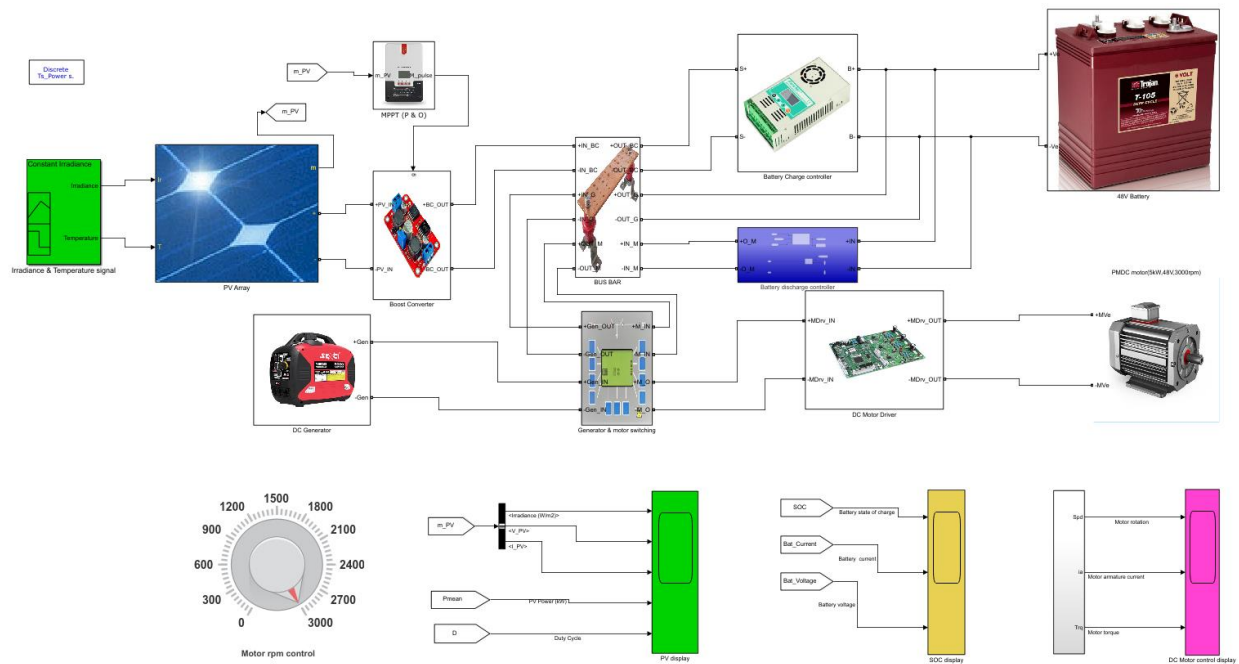


Fig.3. 1. Simulink model of the proposed system in MATLAB.

In the earlier chapter, HOMER provides an optimized solution for the Solar PV-Generator-Battery based system. The proposed scheme for the solar boat is built with an Irradiation and Temperature signal generator, PV array (330Wp/module and total 32 modules), MPPT (P & O),

Boost converter, DC gas generator (1.6kW), PMDC motor rated 5kW and 3000rpm, DC motor driver, 48V lead-acid battery rated 440Ah, Battery charge controller, Battery discharge controller, and Generator & motor switching and BUS bar.

3.3 Solar Irradiance and Temperature Signal for the Dynamic Model

One of the objectives of dynamic modeling and simulation of Solar PV-Generator-Battery based power system in the MATLAB platform for a solar electric boat is to monitor the effect on Battery charging, gash generator, and motor speed status with the change of solar irradiance and temperature within the solar boat operating time, also the performance of battery without PV and generator. The dynamic model will consume many days to compute one solar day while performing simulation as it contains a few complex blocks. Henceforth, the simulation has been done for 40seconds duration to overcome this difficulty. The way solar irradiance and temperature data are selected so that both curves decline and rise in a small portion because of clouds for up to 10sec and is defined as a partial cloud situation. The condition reform to the previous status while clouds back off are defined as an exact sky situation, and it happens from 10sec to 20sec. The entire cloudy case is described while irradiance and temperature value are zero, and it happens from 20sec to 40sec. **Fig.3.2** and **Fig.3.3** represent the irradiance and temperature profiles for 40sec accordingly. The resulting shapes correspond to the change of irradiance and temperature of one solar day.

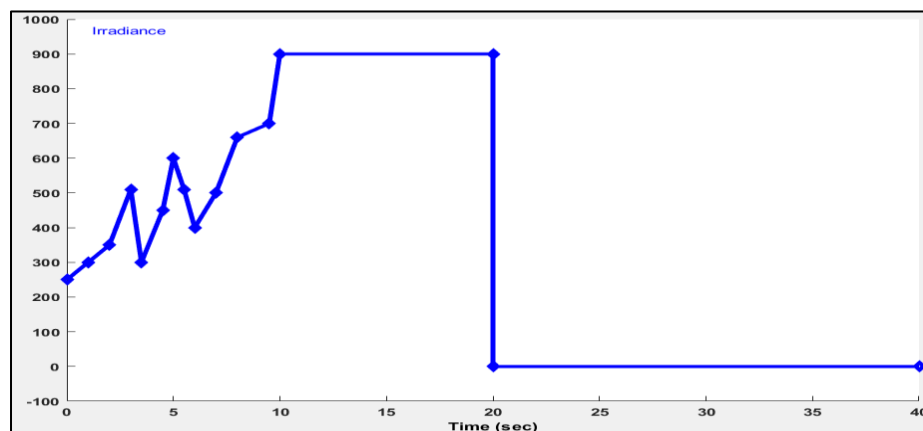


Fig.3. 2. Chosen irradiance for simulation solar PV power-driven boat.

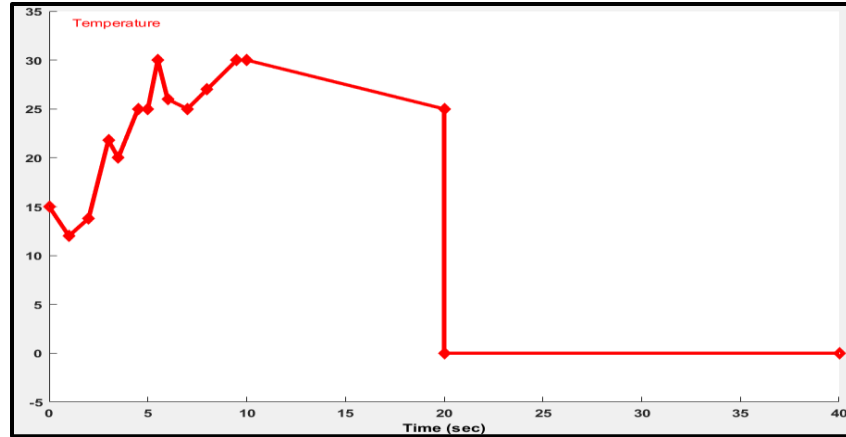


Fig.3. 3. Chosen temperature for simulation solar PV power-driven boat.

The above-explained Solar irradiance and temperature signals are generated in MATLAB Simulink using signal builder for the PV array inputs. The system has been programmed in such a way so that from time $T=0s$ to $T=20s$, only PV and Battery will be delivered power, $T=20s$ to $T=30s$, the only battery will be provided power, i.e., discharged power to the motor, and $T=30s$ to $T=40s$, Gas Generator and Battery bank will be delivered power to the load (dc motor).

3.4 PV Array Design in Simulink

Fig-3.4 is the screenshot of the PV array block parameter, which describes the PV array input parameter in the Simulink PV block.

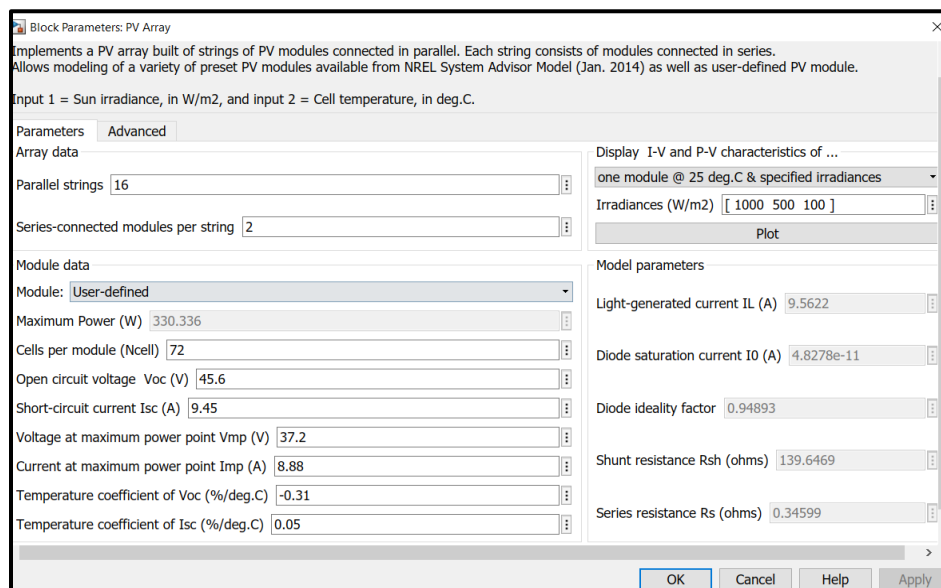


Fig.3. 4. PV array input parameter in the Simulink

It has been found from the HOMER optimization solution that 10.6kWp solar PV is required to generate sufficient power to run the 5kw, 3000rpm rated DC motor and other loads (Light and computer) as well. The total two number of PV string enhances 16parallel and 2series PV module per string, in total 32nos of PV module to achieve the designated power 10.6Wp from the designated 330Wp rated PV module. PV array parameter is used in **Fig.3.4** as stated in **Chapter-2**.

3.4.1 Mathematical Derivation of Solar Cell

The solar PV cell equivalent circuit diagram is shown in **Fig.3.5**, and for the output voltage V and current I , the equivalent equation could express according to **Equation (3.1)**:

$$I = I_L - I_D - \frac{(V + IR_s)}{R_{sh}} \quad 3.1$$

Whereas,

I_L = Light generated current = 9.652A

I_D = Diode saturation current = $1.888e^{(-09)}$ A

R_s = Series resistance = 0.44Ω

R_{sh} = Shunt resistance = 85.739Ω

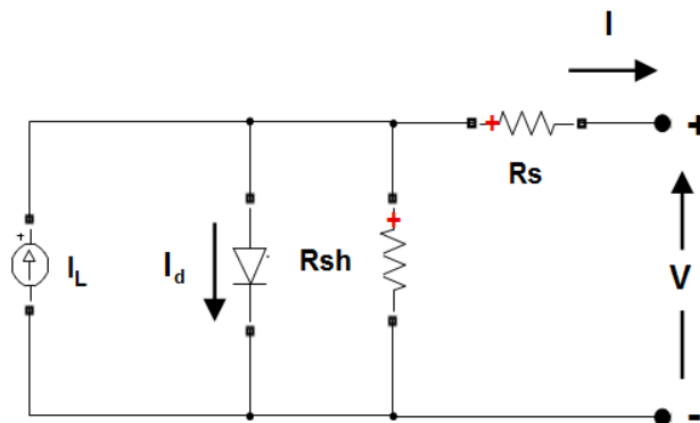


Fig.3. 5. Solar PV cell equivalent circuit diagram

The I-V characteristics of a diode for a particular PV module are expressed by the following **Equation (3.2) and Equation (3.3)**:

$$I_d = I_0 \left[\exp \left(\frac{V_d}{V_T} - 1 \right) \right] \quad 3.2$$

$$V_T = \frac{KT}{q} \times nl \times N_{cell} \quad 3.3$$

Whereas,

nl = diode ideality factor = 1.101

K = Boltzman constant = $1.3806 \times 10^{(-23)}$ J. K⁽⁻¹⁾

q = electron charge = $1.6022 \times 10^{(-19)}$ C

N_{cell} = number of cells connected in series in a module = 72

T = Cell temperature (K)

I_d = diode current (A)

V_d = diode voltage (V)

T, I_d, and V_d values change concerning time in **Equation (3.2) and Equation (3.3)**.

The V-I characteristics curve (**Fig.3.6**) and the power curve graph (**Fig.3.7**) for a single PV module have been obtained after simulation in MATLAB.

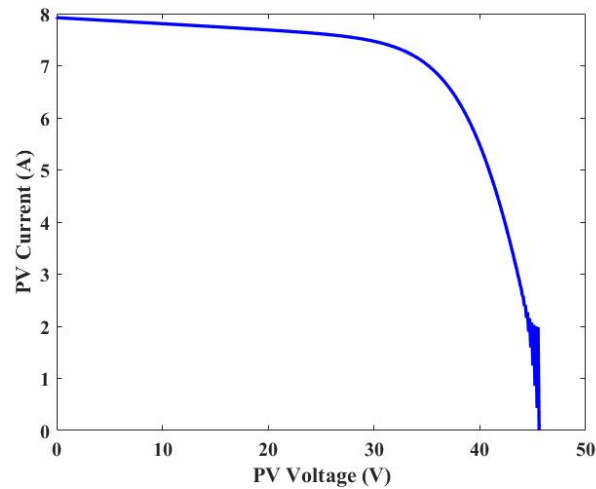


Fig.3. 6. The V-I characteristics curve of a single PV module

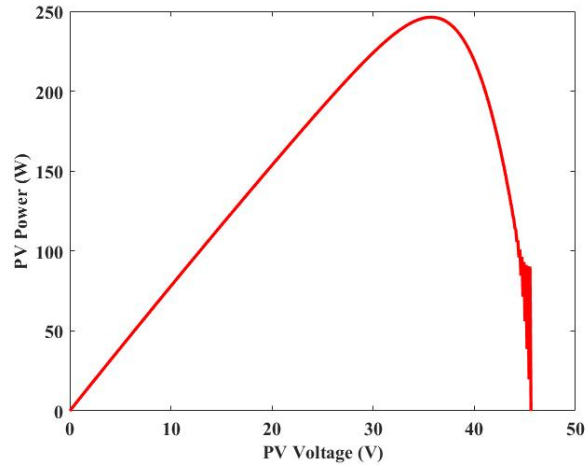


Fig.3. 7. The power curve of a single PV module

The PV array V-I and P-V characteristic curves for various solar irradiances 1000W/m^2 , 500W/m^2 and 100W/m^2 has shown in **Fig.3.8** and **Fig.3.9**, respectively.

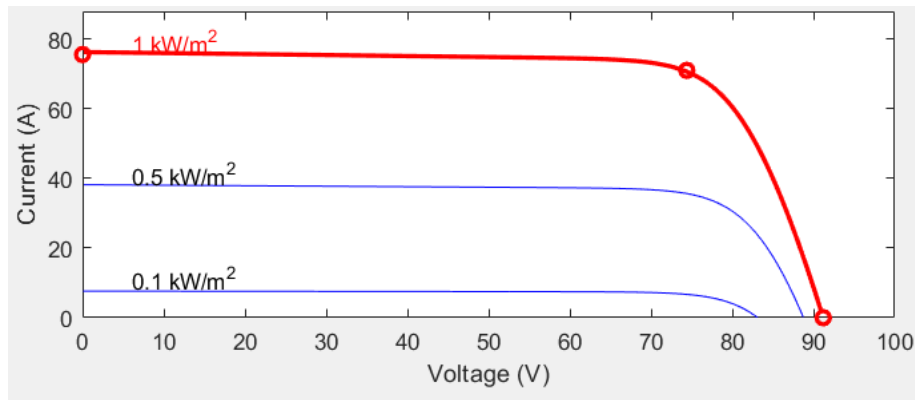


Fig.3. 8. PV array V-I characteristic curve for various solar irradiances

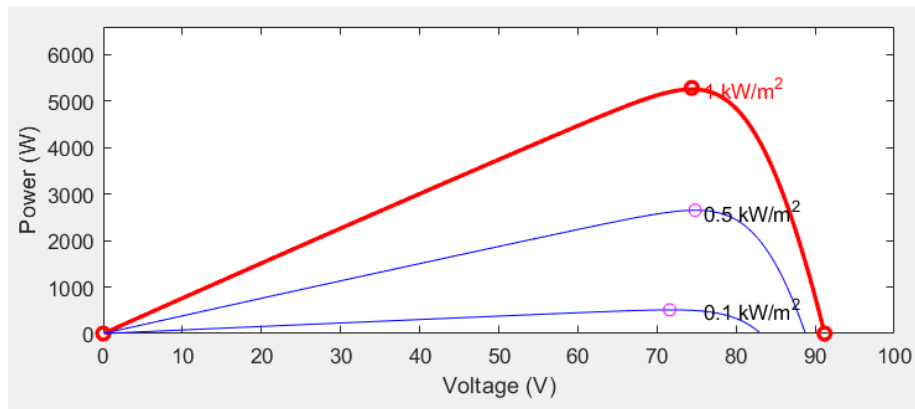


Fig.3. 9. PV array P-V characteristic curve for various solar irradiances

3.4.2 PV Array Simulink Model

The chosen solar photovoltaic (PV) module is Canadian Solar brand, CS-6U-330P model, and the size of each PV module is 330Wp for the MATLAB Simulink model. PV array is constructed in MATLAB by Simulink block, consisting of solar irradiance and temperature-controlled current source, a diode, and resistance in series (R_s) and shunt (R_{sh}). **Fig.3.10** shows the solar Photovoltaic array Simulink block.

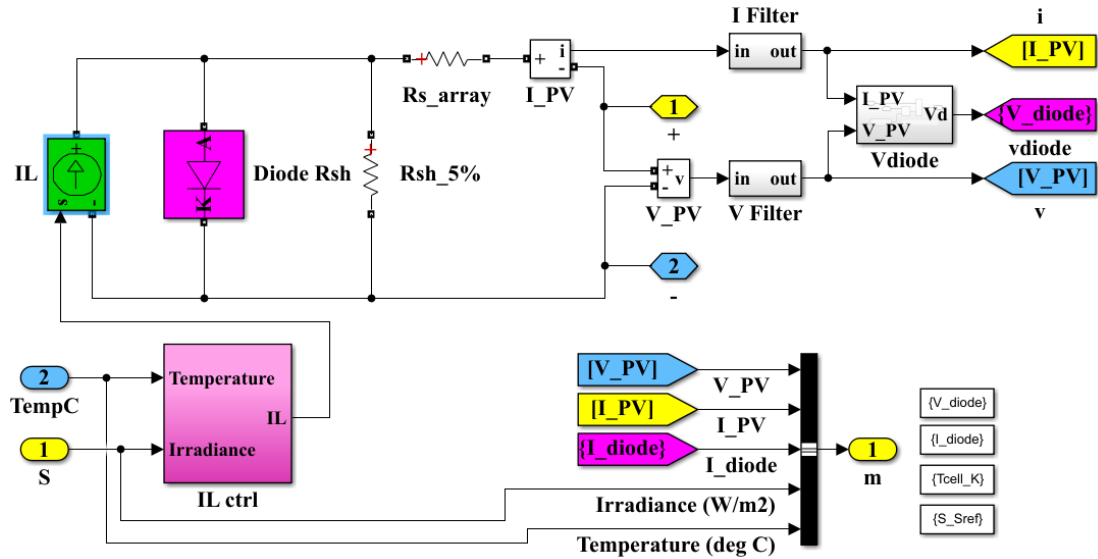


Fig.3. 10. Solar Photovoltaic array Simulink block

3.5 Maximum Power Point Tracking (MPPT)

The variation of solar irradiance, temperature, and sun direction changes the solar photovoltaic (PV) module's electrical output. PV modules have unique PV features regarding a specific PowerPoint for a particular working situation. In a word, the PV module should need to be functioning near to this point so that the PV module output proximate to a maximum power point (MPPT). Under this circumstance, the way PV module operating is known as maximum power point tracking (MPPT), and boosting PV cell application depends on the maximum PV power harvest [73]. The most critical part of an MPPT is its control system and varying duty ratio approach to the maximum PowerPoint. Many techniques were projected to achieve MPPT, such as Perturbation and Observation (P & O), Incremental Conductance (IC), hill-climbing method, neural network, fuzzy logic, and temperature-based, etc., and their assessment has given in [74].

Among these, the most popular algorithms are Incremental Conductance (IC), Perturbation, and Observation (P & O), and the hill-climbing method [75].

3.5.1 The Perturbation and Observation (P & O) Method

The main reason to choose the Perturbation and Observation (P & O) to execute in the proposed system is to offer superior efficiency against the normal atmospheric circumstances. Oscillation and power loss are the significant disadvantages of the P & O method, which arises near the maximum power point due to constant Perturbation. **Table 3.1** reveals the constraint for the Perturbation and Observation (P & O) method. The Perturbation and Observation (P & O) algorithm has been illustrated in **Fig.3.11**.

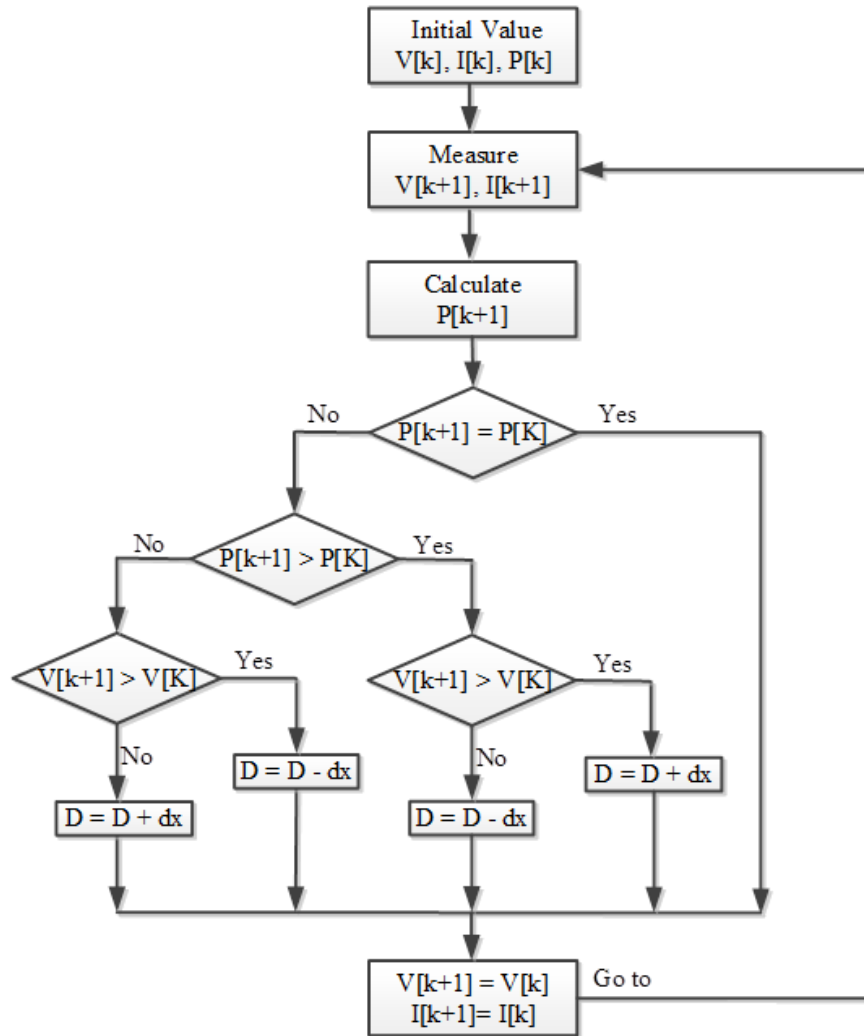


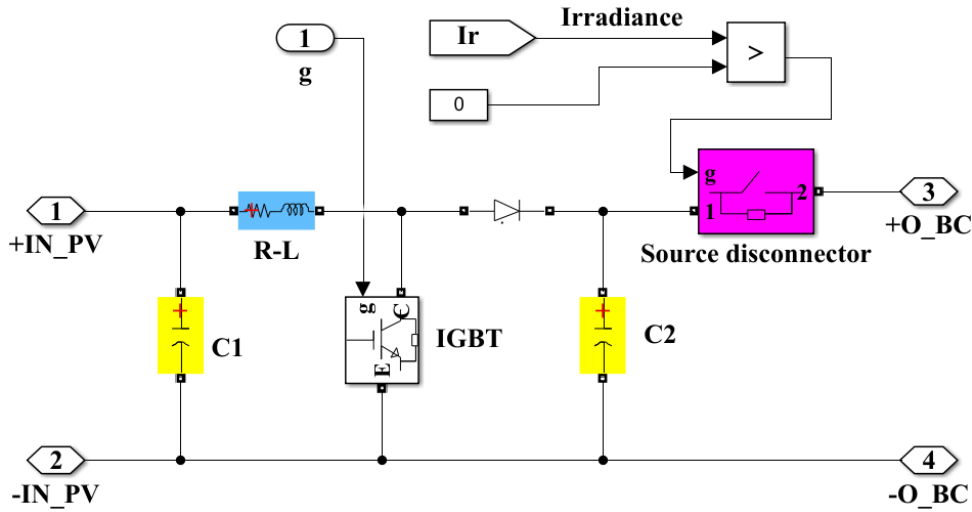
Fig.3. 11. Flow-chart of Perturbation and Observation (P & O) method.

Table 3. 1: Constraints for Perturbation and Observation (P & O) Method

Preliminary value for duty cycle D	0.5
The minimum threshold for duty cycle D	0.4
Maximum threshold duty cycle D	0.6
Increment rate to either increase or decrease	$3e^{-4}$

3.6 Boost Converter:

The boost converter is built with an L-C circuit and an IGBT switching device, whereas the switching function is regulated by the duty cycle (D), and values lie between 0 and 1. MPPT controller generates the duty cycle and then converted into Pulse signal (M_Pulse), which goes to IGBT of Boost converter and hit gate (g) signal. Emitter (E) relates to the negative terminal of PV and Collector (C) connected to PV's positive terminal. The duty cycle, i.e., M_Pulse, is designated as 0.6 by the system to block all firing pulses by implementing an equivalent signal level 1 at input “g” of IGBT in the Simulink prototype, and this method tends to speedier simulation. The Boost converter circuit diagram is shown in **Fig.3.12**.

**Fig.3. 12. Boost converter in the Simulink model.**

3.7 Bus Bar

The Bus Bar is made of a copper bar with protected insulation, which provides input and output connection to avoid joint complexity. Boost converter, DC Gas generator, and DC motor

are linked in IN_BC, IN_G, and O_M ports. On the other hand, the Battery Charge controller and Battery discharge switch are connected in port CC and IN_M. The Simulink model's Bus Bar subsystem is given in **Fig.3.13**, and the Bus Bar connection in the Simulink model in **Fig.3.14**.

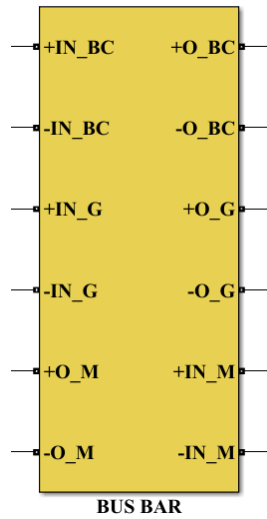


Fig.3. 13. Bus Bar subsystem in the Simulink model.

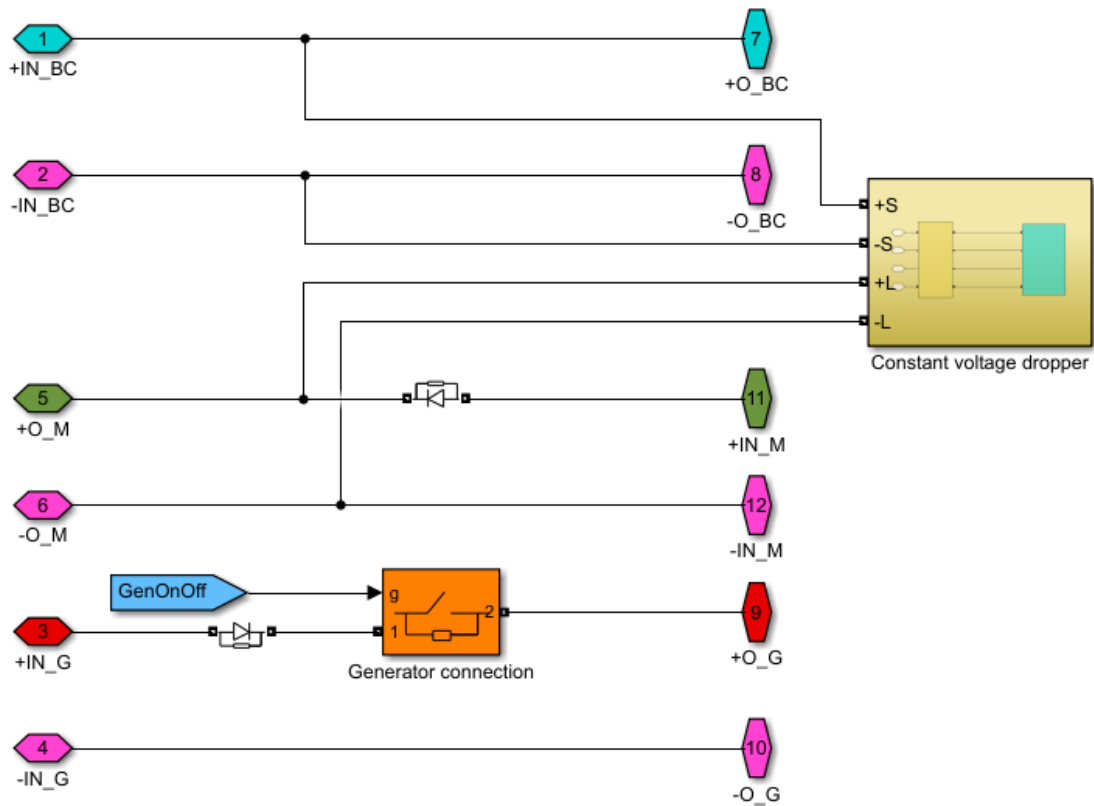


Fig.3. 14. Bus Bar connection in the Simulink model.

3.8 Constant voltage (48V to 50V) dropper (CVD) to load

The constant voltage dropper has been designed with MOSFET, logical operator, inductor, capacitor, and discrete proportional integral derivative (PID) controller. Source relates to the PV system, and load relates to the DC motor. The connection diagram and Simulink model of CVD are shown in **Fig.3.15**.

PID controller works according to the below **Equation (3.4)**:

$$u(t) = K_p e(t) + K_i \int e(t) dt + K_d \frac{de}{dt} \quad (3.4)$$

Whereas,

$u(t)$ = PID control variable

K_p = proportional gain

$e(t)$ = error value

K_i = integral gain

de = change in error value

dt = change in time

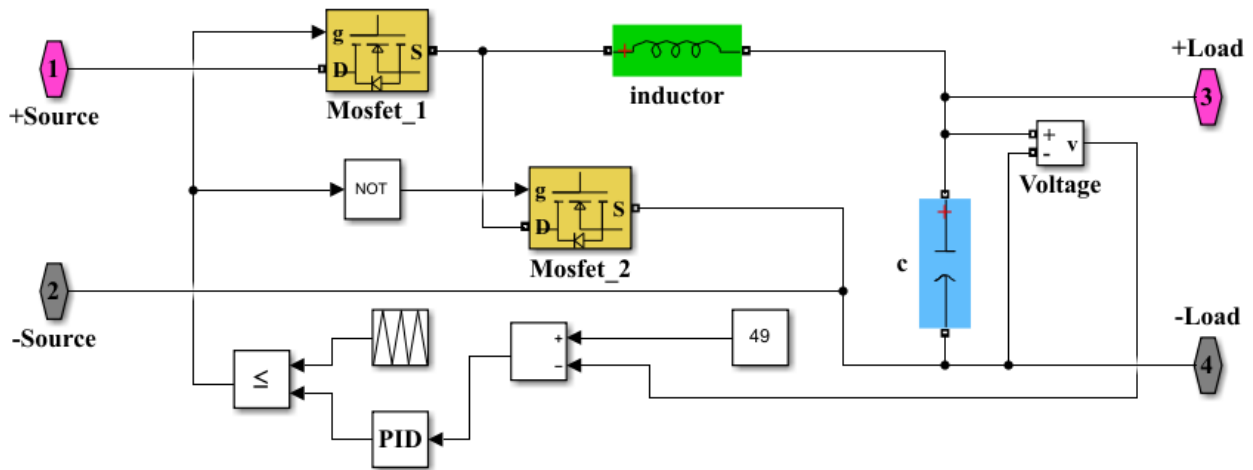
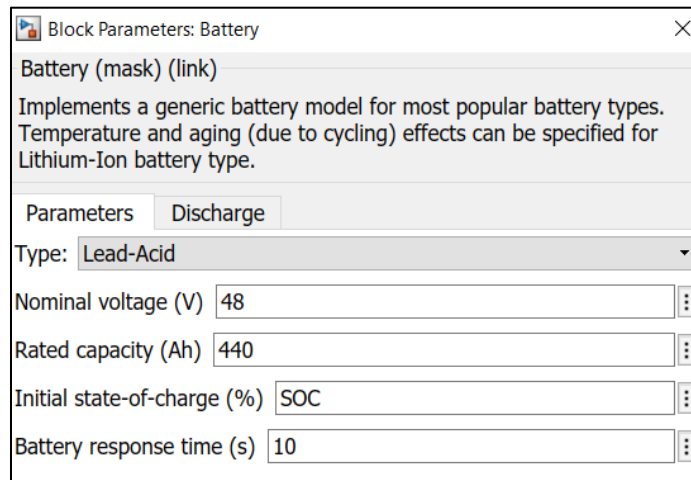


Fig.3. 15. CVD Simulink model.

3.9 Battery Bank

The battery bank (BB) has been assembled up using the lead-acid battery as negligible temperature impact on the battery. BB will provide power to the PMDC motor and charging by solar power & generator. The nominal input parameter of the lead-acid battery in the Simulink block is given in **Fig.3.16**. The discharge parameter is determined from the lead-acid battery's nominal parameters, presented in **Fig.3.17**.



Block Parameters: Battery

Battery (mask) (link)

Implements a generic battery model for most popular battery types. Temperature and aging (due to cycling) effects can be specified for Lithium-Ion battery type.

Parameters Discharge

Type: Lead-Acid

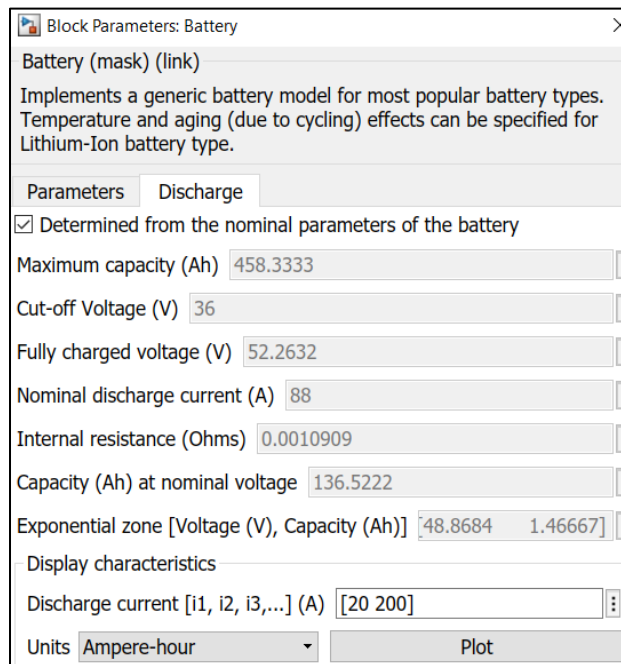
Nominal voltage (V) 48

Rated capacity (Ah) 440

Initial state-of-charge (%) SOC

Battery response time (s) 10

Fig.3. 16. Nominal parameter of the 48V lead-acid battery in the Simulink block.



Block Parameters: Battery

Battery (mask) (link)

Implements a generic battery model for most popular battery types. Temperature and aging (due to cycling) effects can be specified for Lithium-Ion battery type.

Parameters Discharge

☒ Determined from the nominal parameters of the battery

Maximum capacity (Ah) 458.3333

Cut-off Voltage (V) 36

Fully charged voltage (V) 52.2632

Nominal discharge current (A) 88

Internal resistance (Ohms) 0.0010909

Capacity (Ah) at nominal voltage 136.5222

Exponential zone [Voltage (V), Capacity (Ah)] 48.8684 1.46667

Display characteristics

Discharge current [i1, i2, i3,...] (A) [20 200]

Units Ampere-hour Plot

Fig.3. 17. Discharge parameter of the designated lead-acid battery.

3.9.1 Battery Charge Controller (BCC):

The battery charge controller (BCC) has been modeled for charging the battery at constant voltage (49V to 50V) and constant current (25A). The charging current is judged 25A by considering 5.5% of battery capacity 440Ah. BCC consists of a buck converter, two insulated-gate bipolar transistors (IGBT). In contrast, one IGBT is used for source disconnecting and another one to disconnect the load, a PWM generator, an EMI filter, and a programable controller to generate a pulse for source cut-off IGBT, load cut-off IGBT, and PWM generator according to the Battery current (A) and voltage (V) status. Battery charge controller (BCC) details in the Simulink model are shown in **Fig.3.18**.

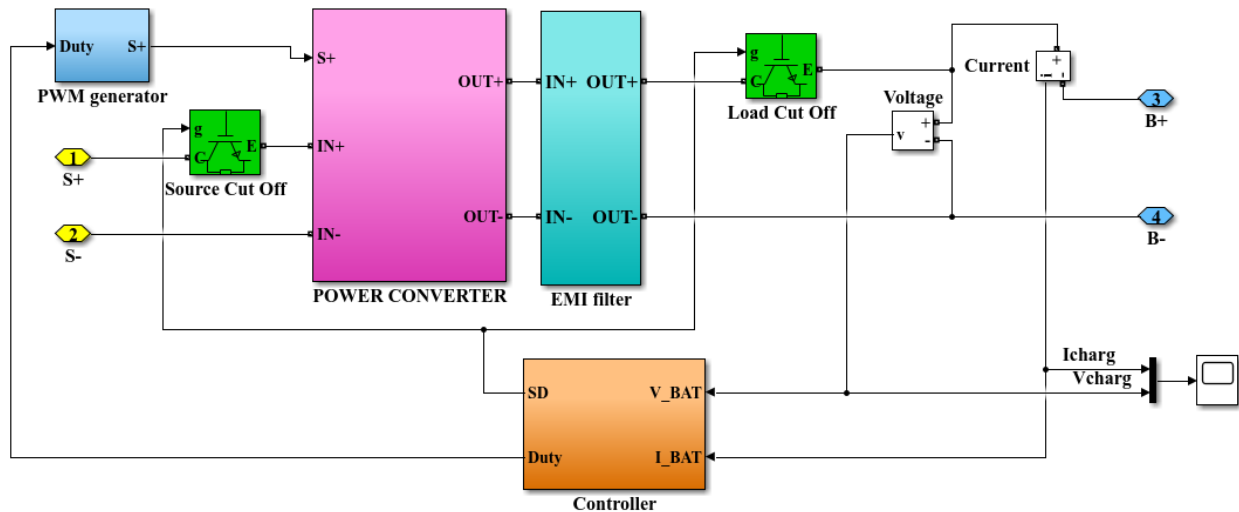


Fig.3. 18. Battery charge controller (BCC) details in the Simulink model.

3.9.2 Battery Discharge Controller (BDC):

The battery will discharge power to the load, i.e., dc motor only, while:

- DC gas generator is either in ON or OFF mode and
- PV array producing power and irradiance less than 700w/m^2
- PV array producing power and irradiance greater than 700w/m^2 and motor speed more than 2500rpm.

The battery discharge controller Simulink model is shown in **Fig.3.19**.

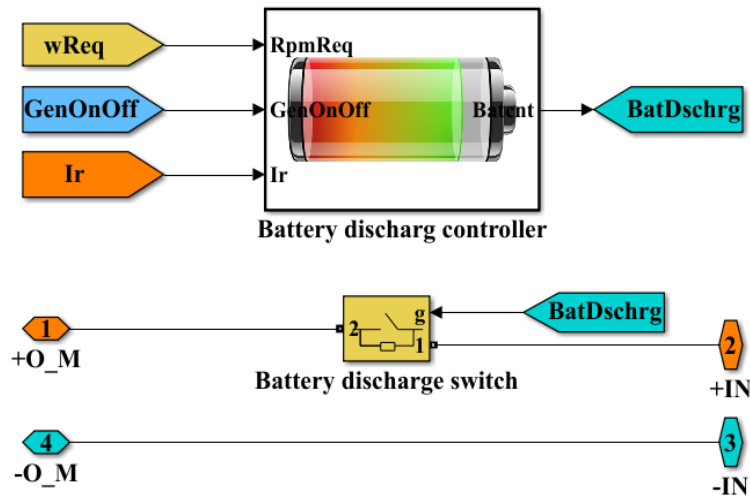


Fig.3. 19. Battery discharge controller Simulink model.

3.10 DC Generator

A wound-field type DC Machine is chosen to form a DC Generator which delivers 1.6kW power to the 48V bus system. A 48V DC voltage has been applied across the field terminal denoted by "F," and a negative value of shaft torque (T_L) implied, which is the mechanical input to operate the DC machine as a DC generator **Fig-3.20**. An $R_f L_f$ circuit illustrates the equivalent field coil circuit. The armature circuit belongs to ports denoted by "A" of the machine block. It is signified by a series $R_a L_a$ branch and placed in series with a Current Measurement block and a Controlled Voltage Source.

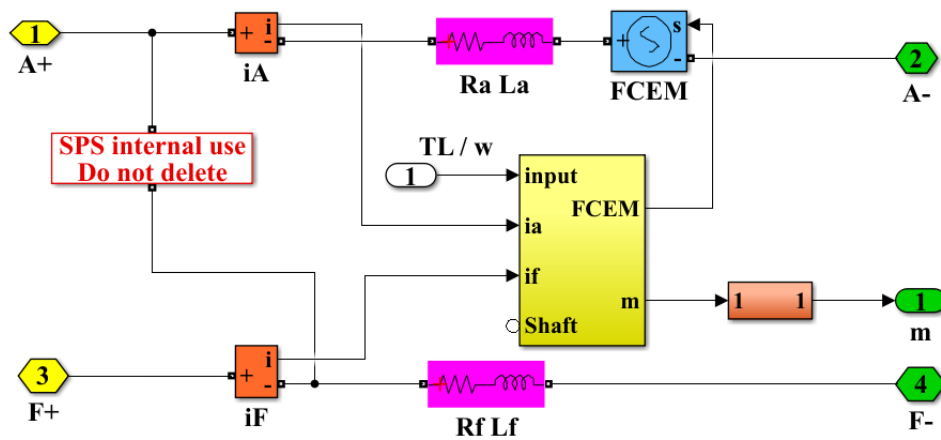


Fig.3. 20. DC Generator Simulink model.

3.11 Permanent Magnet DC Motor (PMDC):

A permanent magnet brushed type DC Machine is chosen to form a DC Motor. A positive value of shaft torque (T_L) implied the mechanical input to operate the DC machine as a DC Motor in **Fig.3.21**. The applied torque (T_L) is proportional to the motor speed ω (rad/s) but through the gain denoted by “K.”

Torque and Gain calculation are given below:

$$T(\text{rated}) = T_L = \frac{P(\text{rated})}{\omega(\text{rated})}$$

Whereas,

$$P_{\text{rated}} = \text{Motor rated power} = 5\text{kW} = 5000\text{watt}$$

$$N_{\text{rated}} = \text{Motor rated rotation} = 3000\text{rpm}$$

$$\omega_{\text{rated}} = N(\text{rated}) \times \left(\frac{60}{2 \times \Pi}\right) = 314.16\text{rad/s}; [\Pi = 3.14]$$

Henceforth,

$$T_L = \frac{5000}{314.16} = 15.915\text{N.m} \cong 16\text{N.m}$$

Also, we know,

$$T_L = K \times (\omega_{\text{rated}})^2$$

$$\text{So, } K = \frac{16}{(314.16)^2} \cong 0.0001612$$

The DC motor's armature is powered through a three-step starter and a switch controlled by the stair generator, and it is shown in **Fig.3.21**. The three-step starter's pulse generator generates a pulse in 0.1s, 0.2s, and 0.3s successively while the motor starts. **Fig.3.22** expresses the Simulink model of a three-step starter to start the engine.

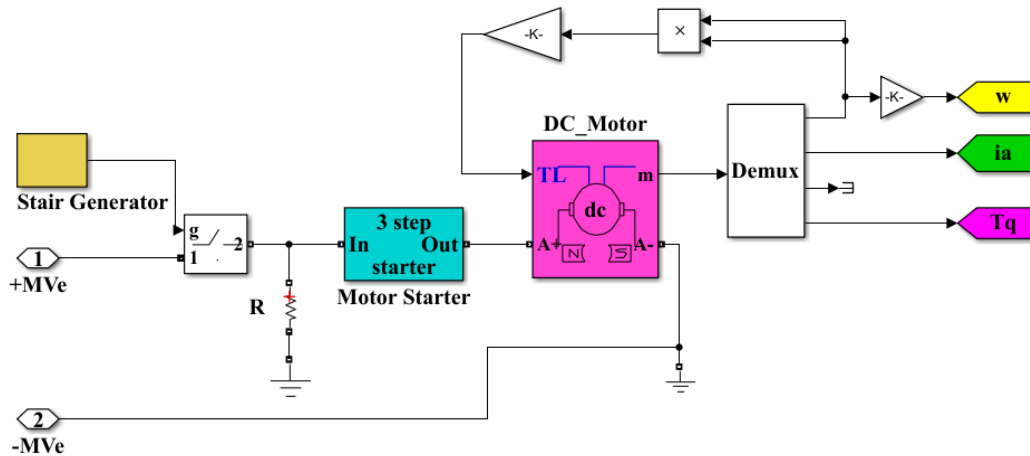


Fig.3. 21. PMDC motor connection.

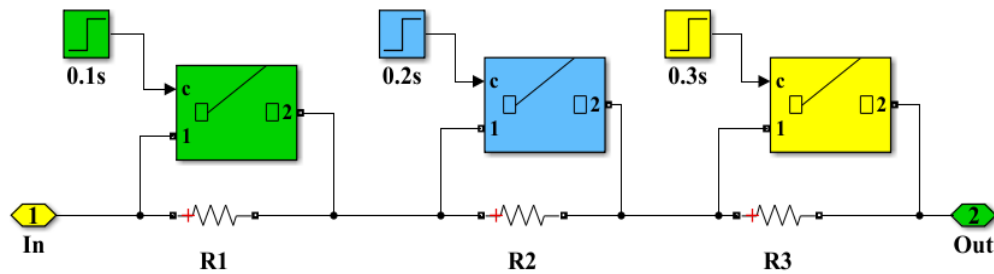


Fig.3. 22. Three-step starter to start the PMDC motor.

The armature circuit belongs to ports denoted by “A” of the machine block. It is signified by a series $R_a L_a$ wing and placed in series with a Current Measurement block and a Controlled Voltage Source. The permanent magnet DC Motor in the Simulink has shown in **Fig.3.23**.

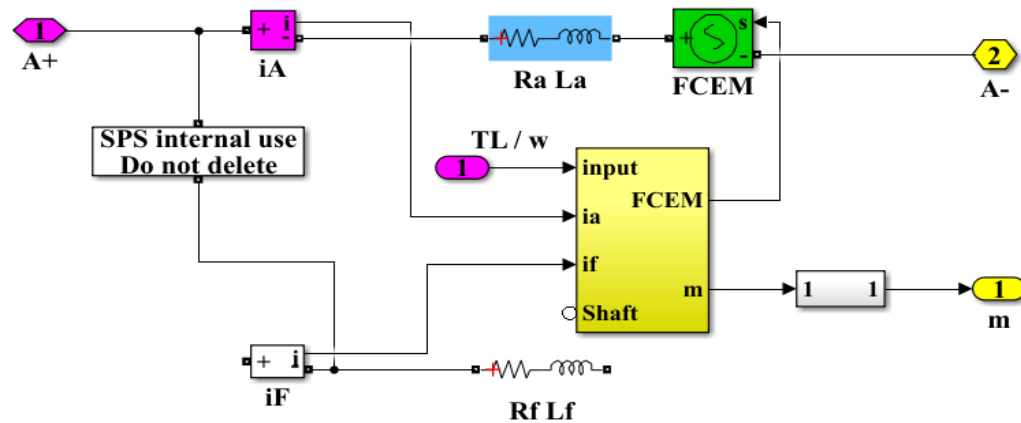


Fig.3. 23. Permanent magnet DC machine (PMDC Motor) Simulink model.

3.11.1 PMDC Motor Driver

The motor driver regulates the motor revolution (rpm) according to the required rpm. The requested rpm could be set using a motor speed changer knob, shown in **Fig.3.24**. The designed PMDC motor can revolve 3000rpm maximum, and by rotating the knob position motor's speed could vary. The motor driver consists of a motor controller, gate driver chopper, and a bridge switch shown in **Fig.3.25**.

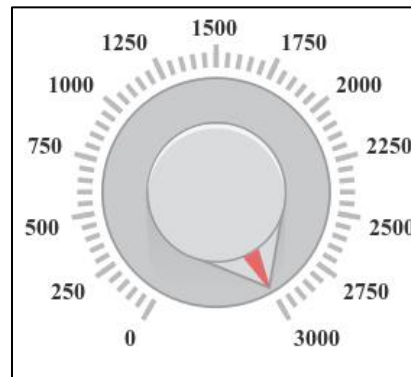


Fig.3. 24. PMDC motor speed changer knob

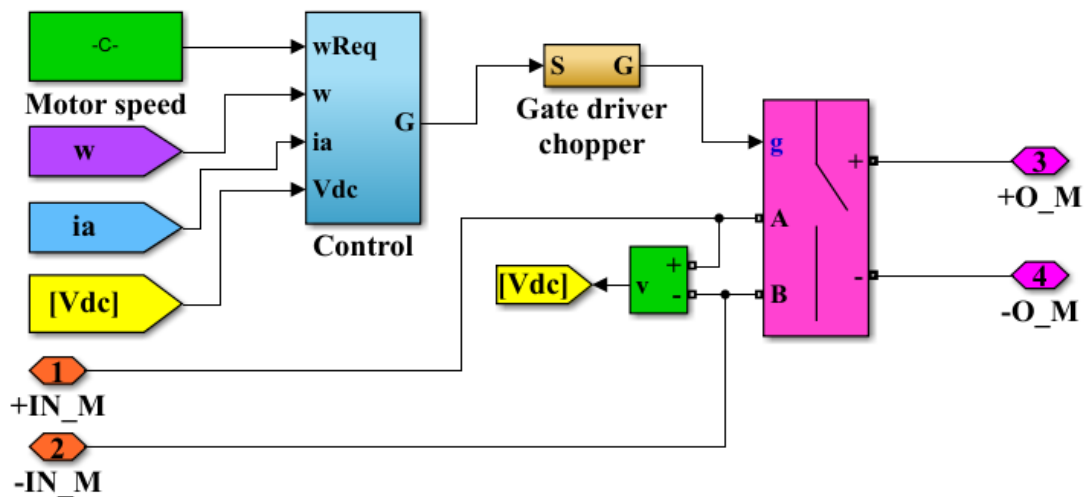


Fig.3. 25. PMDC motor driver Simulink block.

The control system of motor works is based on required motor rpm, actual revolution (ω), armature current, and applied voltage across the bridge circuit terminal. Control system has been developed in Simulink by using rate limiter whereas rising slew rate is 3000rpm/s and falling slew

rate considered -3000rpm/s, one PI controller to control rpm, another rate limiter for linearizing armature current i_A . This DC controller is featured with reset value zero and a PWM generator to generate a final pulse. Motor control Simulink blocks are shown in **Fig.3.26**.

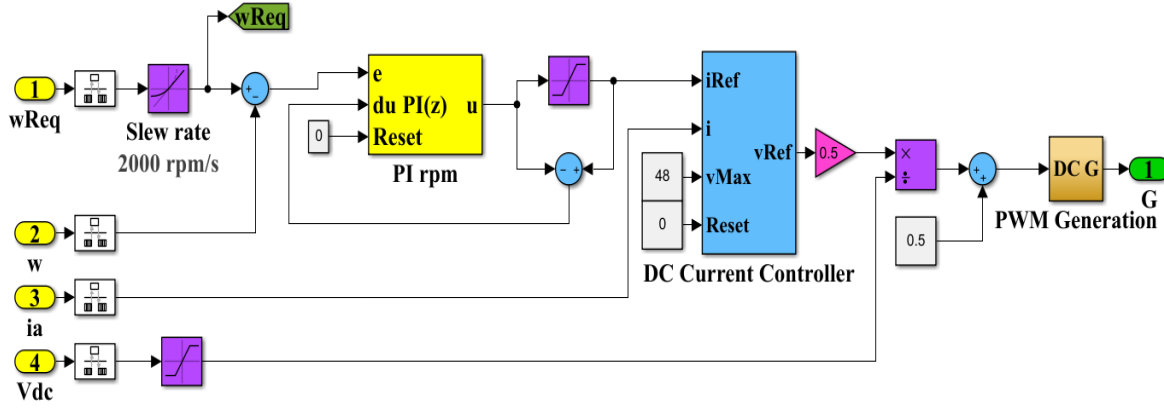


Fig.3. 26. Motor Controller Simulink blocks.

3.12 Switching Controller for DC Generator and PMDC Motor:

According to the state of charge (SOC) status of the battery, DC Motor will always be operational, i.e., ON state, except if SOC value lies under 55%. Simultaneously, $SOC < 55\%$ motor will be disconnected to save the battery from deteriorating. DC Generator will be in service, i.e., operational while $75\% \leq SOC \leq 55\%$ and it will be disconnected if $SOC > 75\%$. The switching Controller for DC Generator and Motor is formed by using four nos. of breaker controlled by an external signal, a signal generator, and a programmed controller. The Switching controller Simulink model for DC Generator and Motor in **Fig.3.27**.

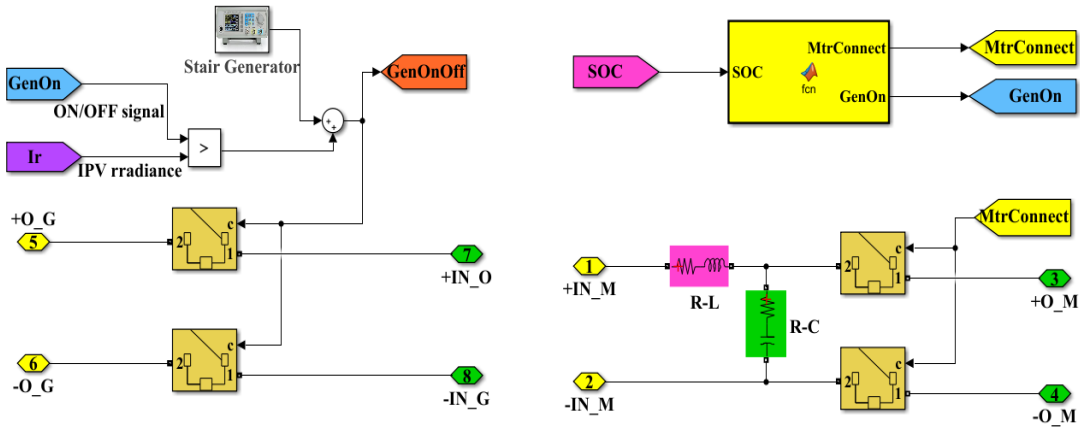


Fig.3. 27. Switching controller Simulink model for DC Generator and Motor.

3.13 Flow Chart of Working Principle of the Dynamic System:

The working principle has been described in the flow chart in the following **Fig.3.28**, which represents the dynamic system's functional flow chart.

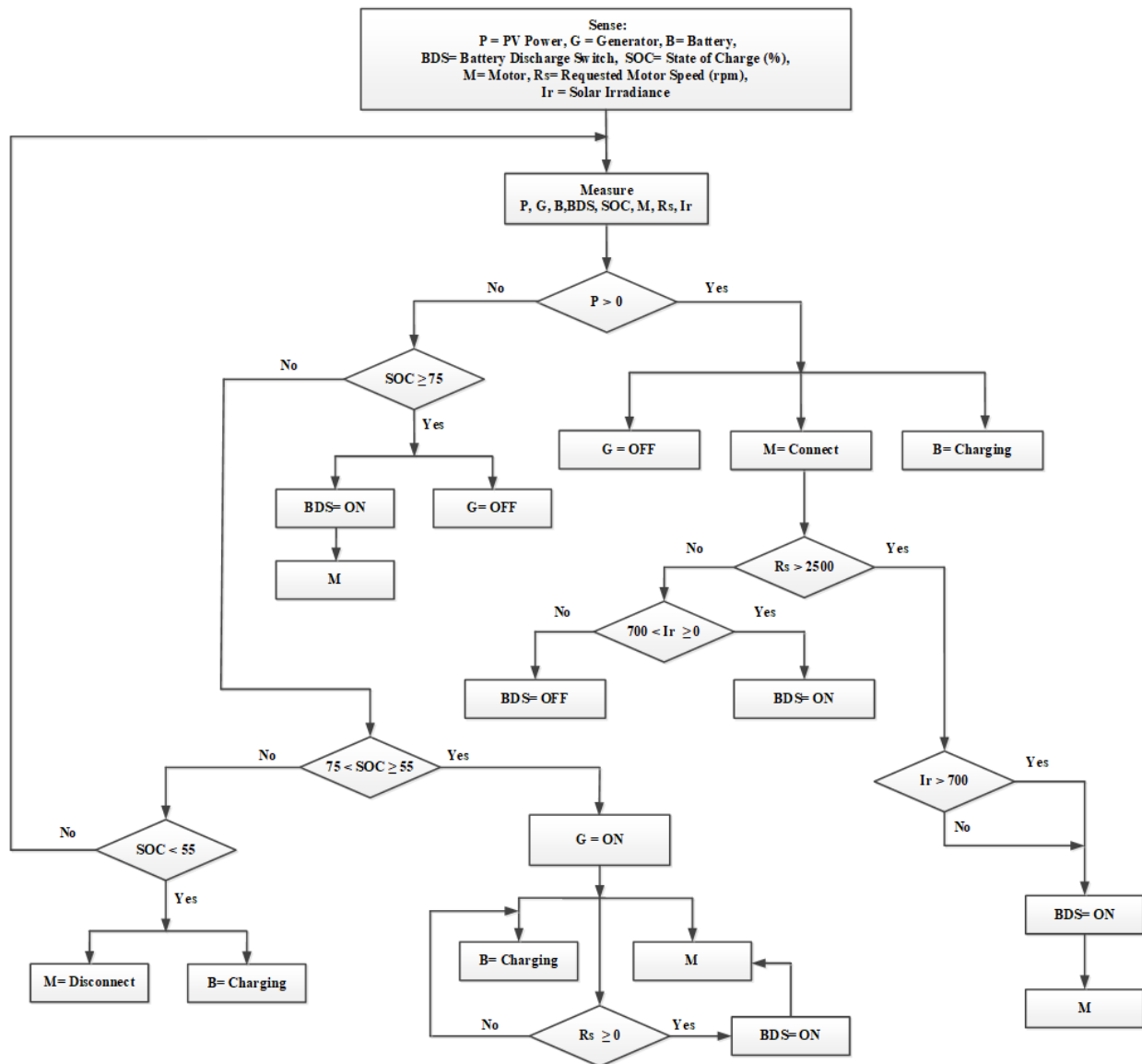


Fig.3. 28. Functional flow chart of the proposed dynamic system in MATLAB Simulink.

3.14 Analysis of the MATLAB Simulation Result of the Proposed System

The MATLAB simulation total time has been considered for 40seconds. In contrast, the first 20seconds (T=0sec to T=20sec) for only PV capability and Battery discharge functionality

observing and the rest of the 20seconds ($T=20\text{sec}$ to $T=40\text{sec}$) for Gas generator and Battery discharge capability observe to run the motor, that is why PV irradiance (W/m^2) turns into zero at $T=20\text{sec}$ to $T=40\text{sec}$. As a result, after $T=20\text{sec}$ PV voltage, current and power becomes zero and remain till the end of the simulation, i.e., $T=40\text{sec}$. Initially, the battery state of charge (SOC%) was chosen 67% for this dynamic simulation, and a 48V lead-acid battery terminal voltage appeared 48.4V. The system has been programmed in such a way so that the gas generator was turned ON at $T=20\text{sec}$, but it was kept disconnect till $T=30\text{sec}$ to examine the battery discharge mode and the capability to operate the motor at the required speed. The gas generator has connected directly with the battery. Henceforth, while the generator is in operation, the battery charge controller showing zero charging current.

After the end of the simulation, it has been concluded that the 48V, 440Ah rated battery serves the desired current to run the motor at desired rpm 0 rpm to 3000 rpm. The designed PV could generate 8.82kW power and charge the battery continually charging current 25A and constant voltage 49V to 50V through the battery charge controller. The system simultaneously operates the rated DC motor (5kW, 3000 rpm) at 3000 rpm. Meanwhile, MPPT trigger pulse according to the PV output voltage.

On the other hand, a 1.6kW rated DC gas generator is also verified. It could concurrently run the motor at a maximum of 2500 rpm and charge the battery at the constant charging current 25A and constant voltage 50V while the motor run 500rpm. While motor speed 1500rpm, then generator could charge the battery but slow charging. DC motor speed control system, i.e., the motor driver has been tested with random speed by varying speed knob at 2500 rpm, 1000 rpm, 1500 rpm, 3000 rpm, 2000 rpm, 2500rpm, 1500rpm, 1000rpm and 500 rpm, respectively, and found that the motor responded according to the requested speed.

Graph of PV irradiance (W/m^2), PV Voltage (V), PV Current (A), PV mean power (kW), and PV Duty cycle amplitude versus time in seconds is shown in **Fig.3.29**.

Graph of Motor speed (rpm), motor armature current (A), and motor torque (N.m) versus time in seconds is shown in **Fig.3.30**.

Graph of Battery state-of-charge, i.e., SOC (%), Battery current (A), and Battery voltage (V) versus time in seconds, is shown in **Fig.3. 31**.

Battery Charger Charging Current (A) and Voltage (V) versus time in seconds are shown in **Fig.3.32**.

Generator Voltage (V) versus time in seconds is shown in **Fig.3.33**, and Generator Current (A) versus time in seconds is shown in **Fig.3.34**.

The MATLAB simulation has explained in four steps and described in the followings:

Step-1: Partial cloudy sky ($T=0\text{sec}$ to $T=10\text{sec}$):

During the interval of $T=0\text{sec}$ to $T=10\text{sec}$, it has been found from the simulation result that, while partial cloudy, PV produced power on an average 3kW, which is not enough because of lower irradiance and temperature to achieve the desired motor speed 2500rpm and to charge the battery as well, consequently, the battery goes to discharge mode to deliver necessary current and motor driver able to latch the motor speed as requested motor speed (rpm) within a short period. When motor speed is set to 1000rpm and 1500rpm, the PV-produced power could run the motor and charge the battery constantly, charging current 25A and voltage 49V. Henceforth, this mode expresses the charge-discharge mode.

Step-2: Clear sky ($T=10\text{sec}$ to $T=20\text{sec}$):

During the interval of $T=10\text{sec}$ to $T=20\text{sec}$, it has been found from the simulation result that, while the sky is clear, PV produced power (8.82kW) is enough because of higher irradiance and temperature to achieve the highest desired motor speed 3000rpm and to charge the battery as well. The system has programmed so that if motor speed exceeds 2500rpm, then battery discharge mode will open to provide supplementary current if necessary and found PV produced power to serve them both, battery charging and run the motor simultaneously. The motor driver can also latch the motor speed as requested motor speed (rpm) within a short period. The battery starts to charge at a constant 25A, and constant voltage lies between 49V to 50V.

Step-3: Completely cloudy sky and only battery back up ($T=20\text{sec}$ to $T=30\text{sec}$):

During the interval of $T=20\text{sec}$ to $T=30\text{sec}$, it has been found from the simulation result that, while the sky is full of cloud, the temperature falls abruptly, and solar irradiance falls to zero.

PV-produced power becomes zero, and the gas generator turns ON. Also, the battery discharge path opens automatically. The generator was still kept disconnected to check the battery bank's capability and found the battery bank starts discharging to run the motor according to the requested speed but is limited to 2500rpm.

Step-4: Completely cloudy sky with Generator (T= 30sec to T= 40sec):

During the interval of T= 30sec to T= 40sec, it has been found from the simulation result that, while the sky is full of cloud, the temperature falls abruptly. Solar irradiance falls to zero, then PV produced power becomes zero, the gas generator turns into ON and starts delivering power to the load (motor and battery), correspondingly, battery discharge path was kept opening and found that the gas generator can charge the battery bank and of operating the motor in required speed.

For PV: T= 0sec to T= 10sec:

We have observed in **Fig.3.29**:

I. Solar irradiance varies from the lowest value 250w/m^2 to 700w/m^2 . PV produced voltage varies from 48.76V to 87.59V, PV produced current range is between 24.28A to 89.86A, PV generated mean power was found 3kW and varied from 2.09kW to 4.67kW. The MPPT duty ratio D was varied from the lowest amplitude 0.4 to the height amplitude 0.6 to trigger the equivalent signal value 0 and 1 in the gate of IGBT of a boost converter.

For PV: T= 10sec to T= 20sec:

We have observed in **Fig.3.29**:

II. Solar irradiance was kept constant 900w/m^2 , PV voltage varies to 87.74V, 78.94V, and 87.9V, the PV current was found 23.5A, 111.3A from and 36.7A, PV generated power was found 2.1kW, 8.82kW, and 3.24kW, from T=10sec to T=11.02sec, T=12sec to T=16.9sec and T=17.68sec to T=19.93sec, respectively. MPPT duty ratio D was latched with the highest amplitude 0.6 to trigger the equivalent signal value 1 in the gate of IGBT of a boost converter. PV power variation is noted. Because of the variation of motor speed, i.e., motor armature current

drawing and battery charging current in a word, PV responds according to the system's power requirement.

For PV: $T=20\text{sec}$ to $T=40\text{sec}$:

We have observed in **Fig.3.29**:

III. Solar irradiance turned into 0W/m^2 at $T=20\text{s}$. Consequently, PV voltage, PV current, PV generated mean power falls into zero lines instantly from their corresponding values till the end of the simulation ($T=40\text{s}$). MPPT duty ratio D was turned into the lowest amplitude 0.4 , which is equivalent to zero triggers, and kept latch until the simulation come to an end.

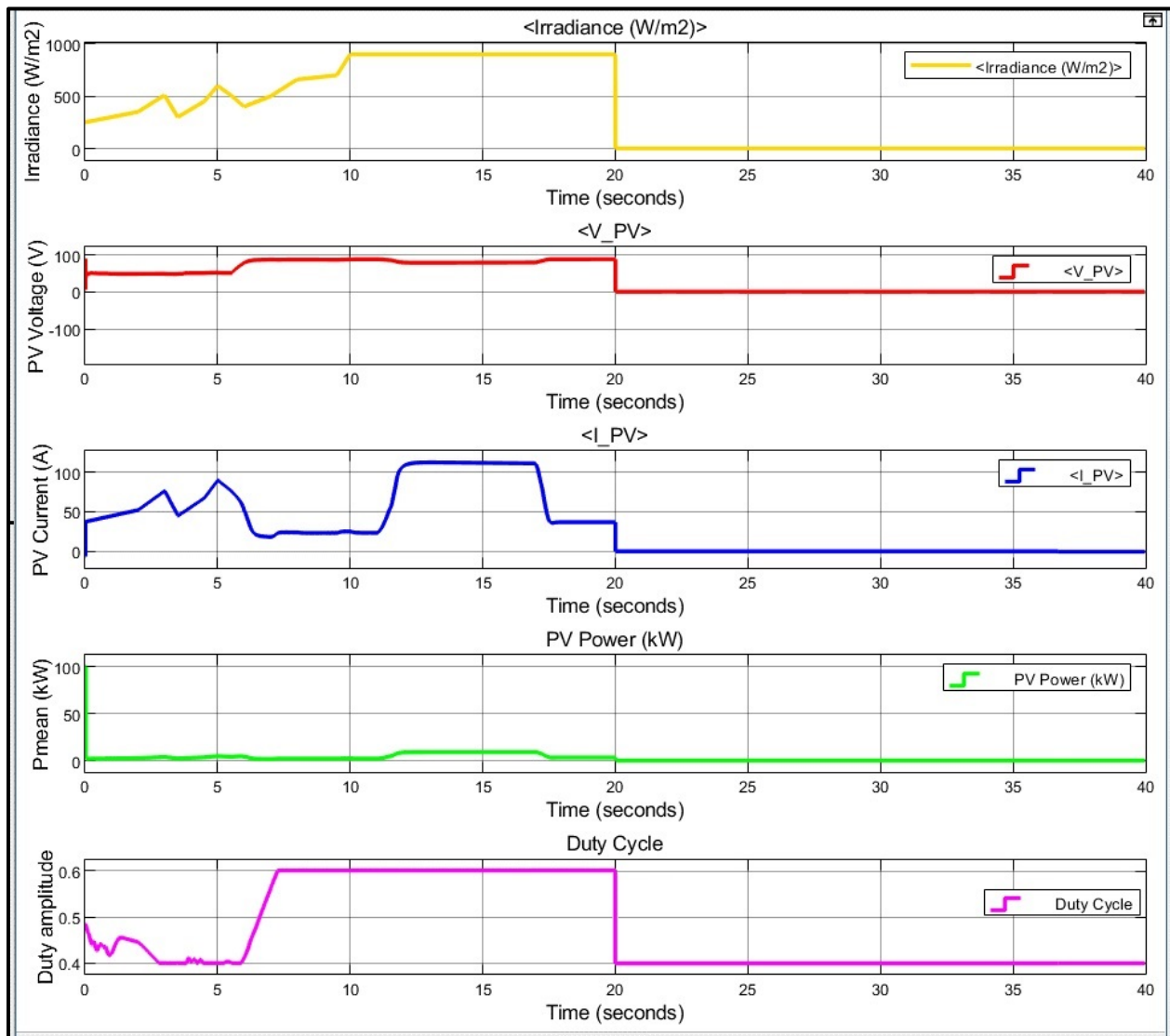


Fig.3. 29. Graph of PV irradiance (W/m²), PV Voltage (V), PV Current (A), PV mean power (kW), and PV Duty cycle amplitude versus time in second.

For DC motor: $T=0\text{sec}$ to $T=10\text{sec}$:

We have observed in **Fig.3.30**:

I. The light green curve (the annotation: Motor rotation2), which is masked by the black curve (the annotation: Motor rotation1), is the measured speed of the motor and the black color curve is the requested motor speed curve. The requested speed was knobbed to 2500rpm that is hooked by the measured speed within 1.35sec, while the motor armature was drawn current 95A, and the mechanical torque was measured 11.14N.m. Also, motor speed was changed to 1000rpm and then 1500rpm, and found the motor driver handle the motor speed as requested rpm quickly.

For DC motor: $T=10\text{sec}$ to $T=20\text{sec}$:

We have observed in **Fig.3.30**:

II. The requested speed was knobbed to 1500rpm, the highest 3000rpm and 2000rpm, hooked by the measured speed within 793.84ms, while the motor armature was drawn current 34.55A, 137A, and 61.43A respectively, also the mechanical torque was measured 4.05N.m, 16.08N.m, and 7.22N.m correspondingly. Hereafter, the motor driver able to handle the motor speed as requested rpm in a short time.

For DC motor: $T=20\text{sec}$ to $T=30\text{sec}$:

We have observed in **Fig.3.30**:

III. The requested speed was knobbed from 2000rpm to 2500rpm and 1500rpm, hooked by the measured speed within 348.06ms and 669.34ms respectively, while the motor armature was drawn current 95A and 34.55A correspondingly. Also, the mechanical torque was measured at 4.05N.m and 11.14N.m, respectively. Hereafter, the motor driver able to handle the motor speed as requested rpm in a short time.

For DC motor: $T = 30\text{sec}$ to $T = 40\text{sec}$:

We have observed in **Fig.3.30**:

IV. The requested speed was knobbed from 1500rpm to 1000rpm and 500rpm, which is hooked by the measured speed within 374.83ms, while the motor armature was drawn current 14.76A and 3.6A correspondingly. Also, the mechanical torque was measured at 1.73N.m and 0.43N.m, respectively. Hereafter, the motor driver able to handle the motor speed as requested rpm in a short time.

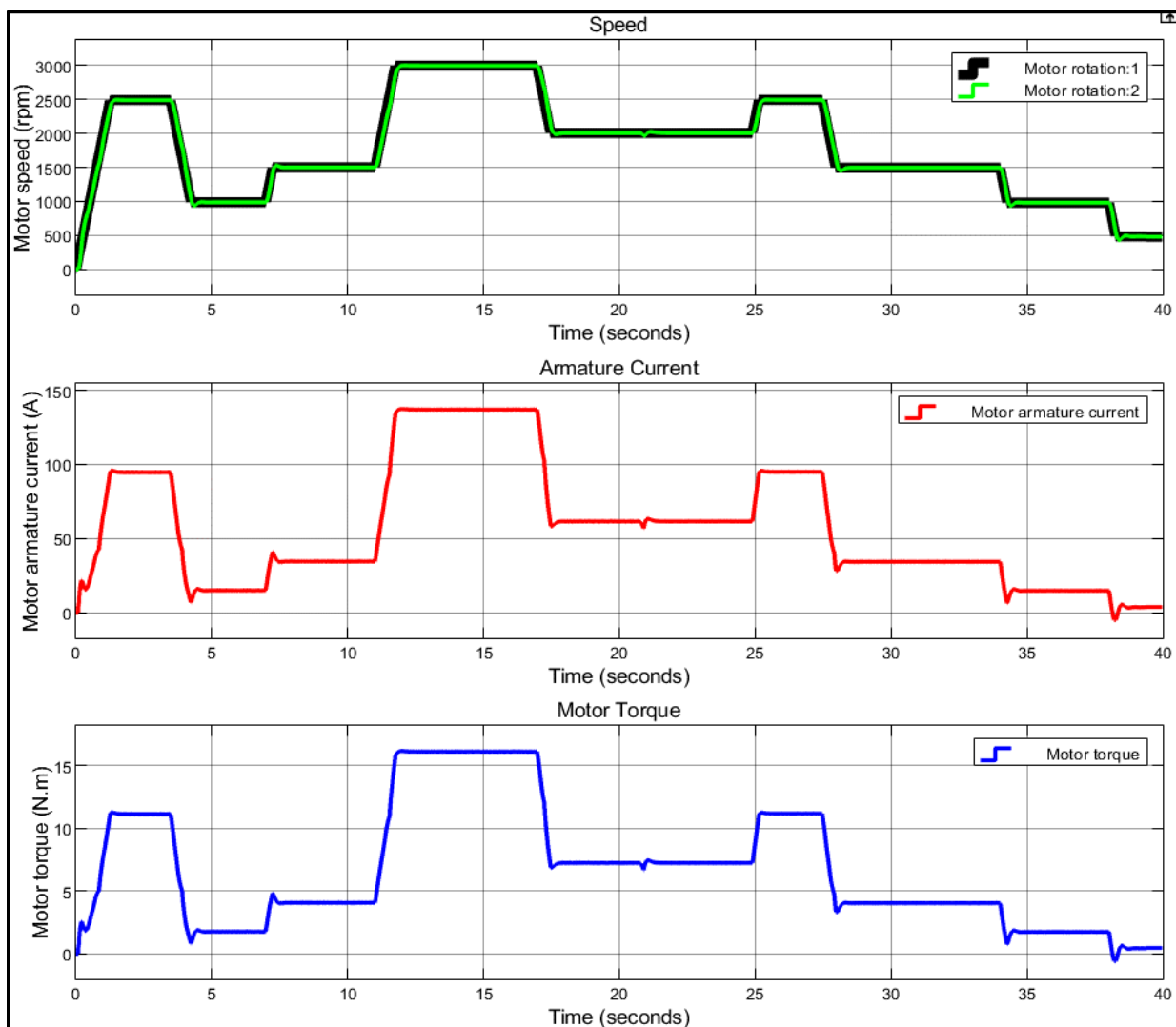


Fig.3. 30. Graph of Motor speed (rpm), motor armature current (A), and motor torque (N.m) versus time in seconds.

For Battery: $T=0\text{sec}$ to $T=10\text{sec}$:

We have observed in **Fig.3.31**:

I. Battery state-of-charge (SOC%) was decreased by $9.143\text{e-}3\%$ at $T=3.5\text{sec}$. Battery discharge current was on average 35A, and voltage was almost unchanged 48.3V. Henceforth, the battery is in discharge mode during the mentioned interval, and there is no flow of charging current observed in the battery charger in **Fig.3.32**. $T=3.5\text{sec}$ to $T=5.5\text{sec}$ is the transition period. $T=5.5\text{sec}$ to $T=10\text{sec}$, battery SOC starts increasing, and the battery starts charging with constant current 25A, and constant voltage 49V and SOC reached 67.18%.

For Battery: $T=10\text{sec}$ to $T=20\text{sec}$:

We have observed in **Fig.3.31**:

II. Battery state - of - charge (SOC%) was increased to 67.05%. Battery current was detected -25.25A, constantly flowing. The negative value of current implies that the battery is charging. Battery voltage was significantly increased to 50.19V. Moreover, the battery is in charge mode during the mentioned interval. There is constant charging current 25.5A remarked.

The charging voltage was found in between 49V to 50V in the battery charger in **Fig.3.32**.

For Battery: $T=20\text{sec}$ to $T=30\text{sec}$:

We have observed in **Fig.3.31**:

III. Battery state - of - charge (SOC%) was decreased from 67.05% to 67.00%. The battery was discharging current at the rate of 40.04A from $T=20\text{sec}$ to $T=24.75\text{sec}$, 87A from $T=24.75\text{sec}$ to $T=27.37\text{sec}$, and 16.39A from $T=28.01\text{sec}$ to $T=30\text{sec}$. The positive value of current implies that the battery is discharging. Battery voltage was noticed significantly decrease from 50.19V to 48.89V.

Moreover, the battery is in discharge mode during the mentioned interval, and there is no charging current remarked in the battery charger in **Fig.3.32**.

For Battery: $T=30\text{sec}$ to $T=40\text{sec}$:

We have observed in **Fig.3.31**:

IV. Battery state - of - charge (SOC%) was increased from 67% to 67.02%, during the period $T=30\text{sec}$ to $T=40\text{sec}$, Battery current turned into negative value and lay between -18.03A and -32.02A. The negative value of current implies that the battery is charging. Battery voltage was noticed increasing and reached the value 50.24V at $T=40\text{sec}$. During this period gas generator was operational in **Fig.3.33** and **Fig.3.34**.

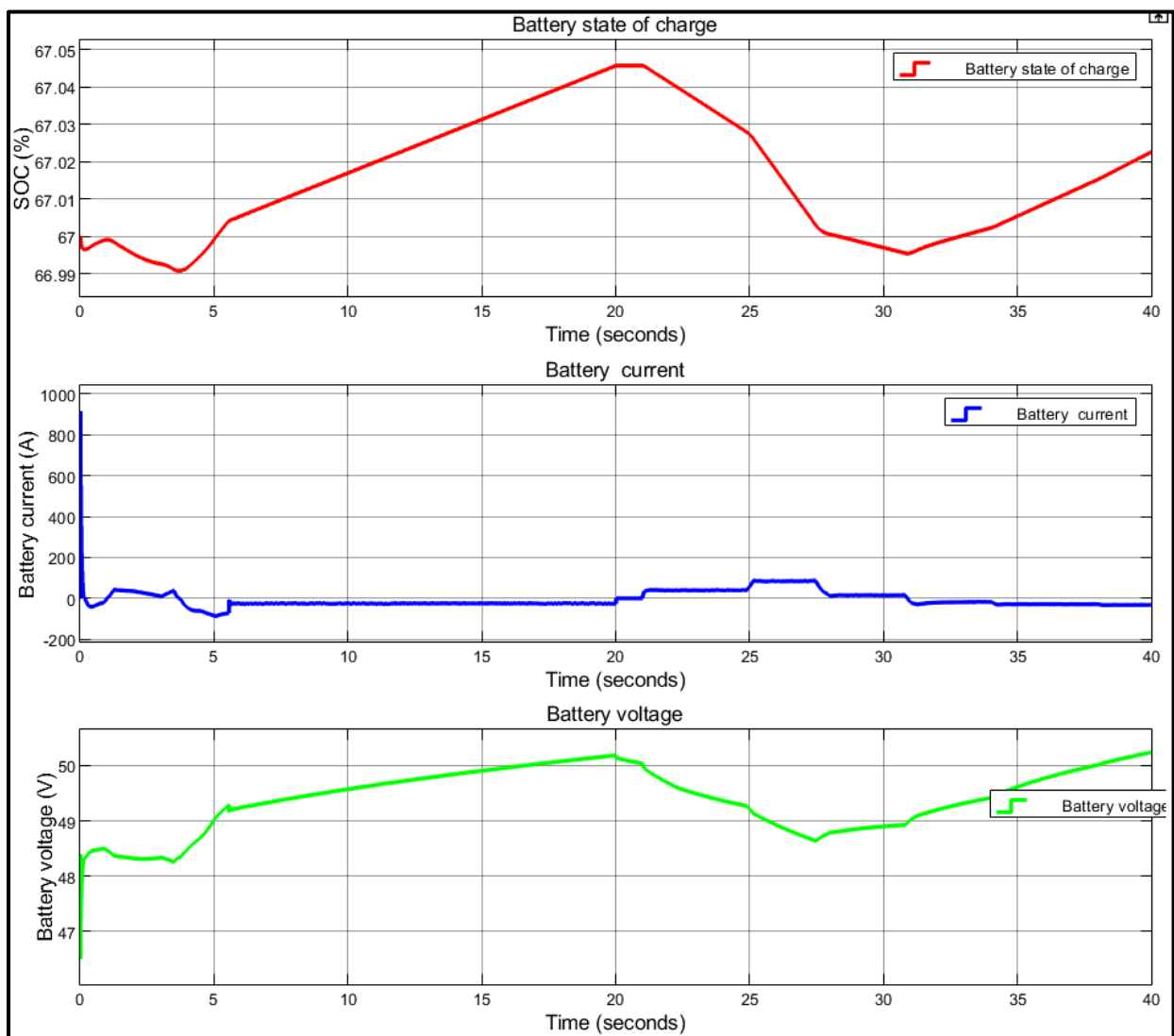


Fig.3. 31. Graph of Battery state-of-charge, i.e., SOC (%), Battery current (A), and Battery voltage (V) versus time in seconds.

The system has been designed in such a way so that PV charges the battery bank through constant current (cc) and voltage (cv) battery charger, and the gas generator charge the battery directly, i.e., bypass the charger. That is why the charging current falls into 0A at T=30sec. During partial cloud, irradiance was low, and PV produced voltage was lower than 50V, henceforth till T=4sec charger could not stabilize charging current. While PV has produced sufficient voltage, the battery charger took 2seconds to become stable and started charging the battery while T=6sec, at constant current 25A and voltage, lies between 49V and 50V. The reflection is visible in **Fig.3.32**.

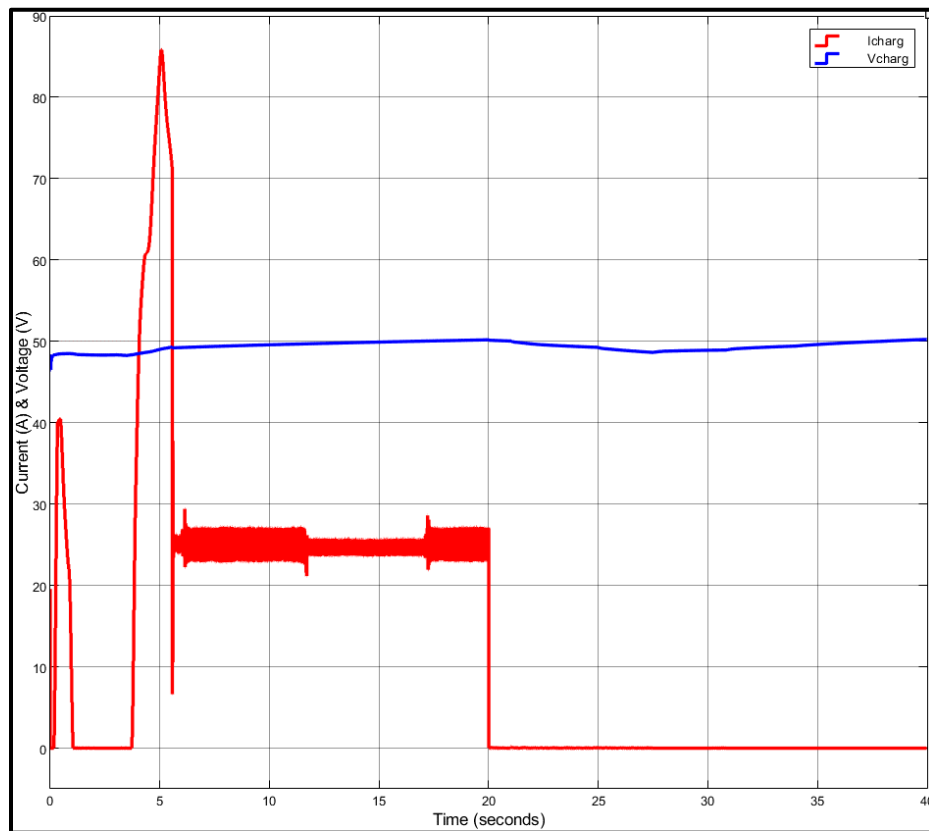


Fig.3. 32. Battery Charger Charging Current (A) and Voltage (V) versus time in second.

The gas generator was kept out of operational from T=0sec to T=30sec, and it comes into service from the instance of T=30sec till the end of simulation T=40sec. The gas generator has produced a 50V and current 33A, i.e., delivered power is equivalent to 1.65kW in **Fig.3.33** and **Fig.3.34**.

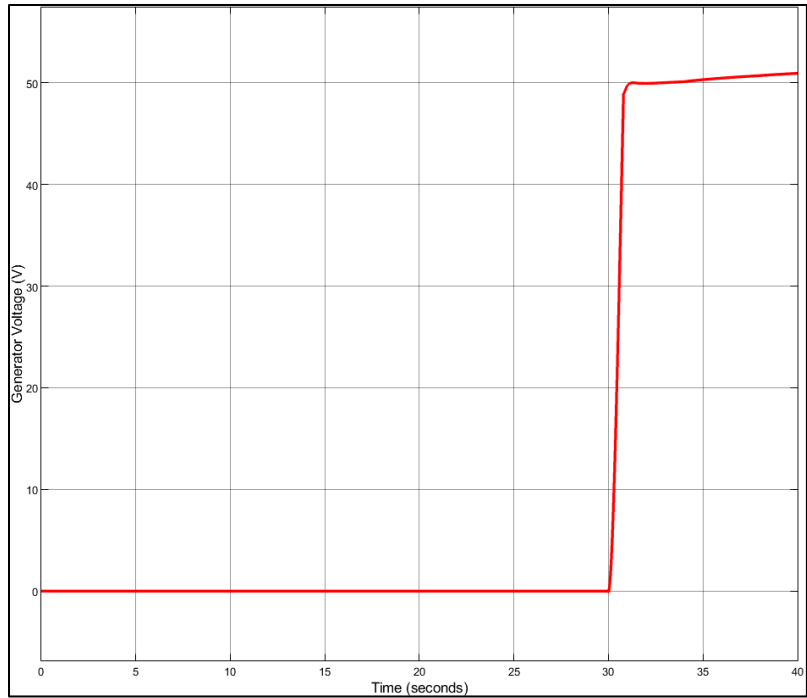


Fig.3. 33. Generator Voltage (V) versus time in second

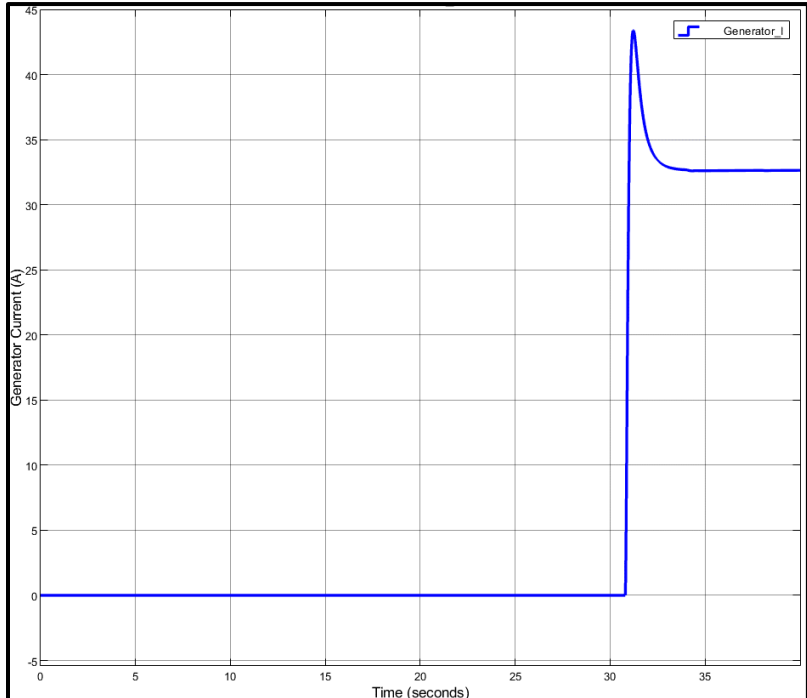


Fig.3. 34. Generator Current (A) versus time in second

3.15 Summary:

This chapter presents the optimal design and dynamic modeling and simulation of a hybrid power system for a solar boat in Bangladesh. The total system is composed of 1) hybrid power system, which consists of the photovoltaic, small-sized gas generator and battery back-up, and 2) Control system which consists of MPPT controller, battery charge controller, motor speed controller, fixed voltage controller (DC-DC converter) and battery discharge controller and 3) a permanent magnet DC motor. The dynamic performance of the system elements is evaluated thoroughly as well by considering: (i) partial cloudy weather conditions (PV & Battery), (ii) full cloudy weather (Generator & Battery), and (iii) sunny day (PV & Battery). The MATLAB simulation analysis determines that the PV produces 8.82kW power, almost equal to HOMER's required power, with only 12% variation. It could run the motor 3000rpm and charge the battery at constant current 25A and 49V simultaneously. After 3hours, the battery will be 80% charged, and 5hours after, the battery will be fully charged (100%). While the generator comes in operation and motor speed equals 500rpm, it could charge the battery with the constant 25A and 49V. The motor driver responds to the requested rpm and latches accordingly. MPPT controller response according to the required power in the system, whereas the fixed voltage controller ensures constant 49V to the motor. The battery's discharge controller discharges power according to the system requirement. Detailed dynamic simulation results are presented in this chapter. The instrumentation design will be discussed in the next chapter.

Chapter-4

Proposed Instrumentation Design and Control Mechanism

4.1 Introduction

Instrumentation design refers to using various tools for measuring, collecting, and monitoring data either for research or applying in a diversity of fields. Henceforth, all kinds of equipment will be designed to achieve superior performance and power up and navigate the boat. A boatman must know the info about their boat's equipment execution and the safe navigation atmosphere. Presently, marine electronics manufacturer offers highly performed in terms of improved accuracy and capacity electronic navigation instruments, also, facilitate of access of data from it. The battery monitoring instrument will measure battery voltage and charge level, then demonstrate in the monitor. The control mechanism is developed to manage battery charging, and motor connect and disconnect in the system consistent with the condition. This chapter is designed by considering the low cost but superior performance capable instruments.

4.2 Proposed Instruments for the Proposed System

A. Proposed Power System Instruments

10.6kW PV is connected to 150A rated copper BUS BAR through 02nos. of MPPT (70A) and the main circuit breaker (MCB), which is 150A rated. A small DC gas generator (1.6kW), which is known as an inverter, is connected to BUS BAR through a circuit breaker (CB) named CB-G (40A). The same way 48V, 440Ah rated lead-acid battery bank, Light-1, Light-2, and DC/DC converter (48V/9V) and Raymarine i70 display are connected to the BUS BAR through CB-B(150A), CB-1 (1.5A), CB-2 (1A) and CB-3 (5A) respectively. Airmar DST810 multi-sensor used to measure water depth, boat speed, and water temperature is powered from the Raymarine i70 display device. A PMDC motor (5kW, 3000rpm) is connected to the 48V bus system through a circuit breaker CB-M (135A), and an overcurrent protection relay is known as DC reversing contactor (125A).

B. Proposed Control Mechanism

The proposed control system consists of Arduino Uno programmable controller and four 5V DC relay named Relay-1, Relay-2, Relay-3, and Relay-4. It will control the PV array, battery bank, dc generator, and PMDC motor switching mechanism, and details discussed in the proposed system control section.

C. Proposed Display System Instruments (Cockpit of the boat)

The display system instruments are installed in the cockpit of the boat. It belongs to the Raymarine i70 display, which displays the boat speed, water depth, water temperature, GPS data (longitude, latitude) and navigation route, Battery voltage, and SOC monitoring display instrument, and PMDC motor driver (5kW) to regulate the motor speed by varying knob.

4.3 Proposal for Measuring, Collecting, and Displaying Data of the Proposed System

The essential sensors refer to transducers for any marine instrument system to measure battery backup status in voltage and SOC, wind speed and direction, water depth, speed-through-water, and water temperature. The transducer differentiates changes in the actual field across the boat and transforms the data into an electrical signal. After that, this signal process to display.

Many transducer types are available in the market. Airmar DST810 multi-sensor could be a good fit for measuring water depth, speed, and water temperature. The “Airmar CAST App” and Raymarine i70 multifunction display instrument is recommended to display these data.

A boatman must know about the battery charge status before and during the sail. The XCSOURCE branded 48V DC battery capacity, and voltage measurement instrument is proposed to display on the monitor. This digital Ammeter -Voltmeter comes with a display and one pair of cables. The parameter has been set by default 12V and ranged to 48V [76]. The selected device has been recommended by studying low-cost price and performance. **Fig.4.1** represents the instrument to measure and display the 48V battery capacity and voltage.



Fig.4. 1. Battery capacity and voltage measuring and display instrument.

4.4 Proposed Equipment

4.4.1 Permanent Magnet Direct Current (PMDC) Motor

In the Simulink model, a brushed Permanent Magnet DC Motor (PMDC) was simulated, driven by 48V DC & 5.0kW rated power, and produced 3000rpm while 16N.m torque applied. Henceforth, high initial torque with the same featured PMDC motor could use for the proposed solar boat; Fig. 4.2 shows a Super Motor brand 5.0kw 48V 2800RPM PMDC motor, and Table 4.1 represents the specification of the proposed PMDC motor [77].



Fig.4. 2. A Super Motor brand 5.0kW 48V 3000RPM brushed PMDC motor

Table 4. 1: Specification of the proposed PMDC motor

Model	ZT5A-48J
Brand Name	Super Motor
Output Power	5KW
Rated Voltage	48V
Rated Current	130A
Rated Speed	2800RPM
Rated Torque	17.05N.m
Commutation	Brush
Efficiency	85%
Working temperature	-25-+40 °C

4.4.2 Variable Speed Control Driver

It is compulsory to have the variable speed control driver for the selected PMDC motor to steer the boat. Moreover, the Entweg brand 5.00kW, 48V Programmable DC Motor driver has been chosen. It has an adjustable speed controller regulator with a pulse width modulation (PWM)

reversible control. This speed controller regulates the speed of a DC motor by adjusting PWM. **Fig.4.3** shows a PMDC motor PWM variable speed control driver. **Table 4.2** shows the specification of the driver.

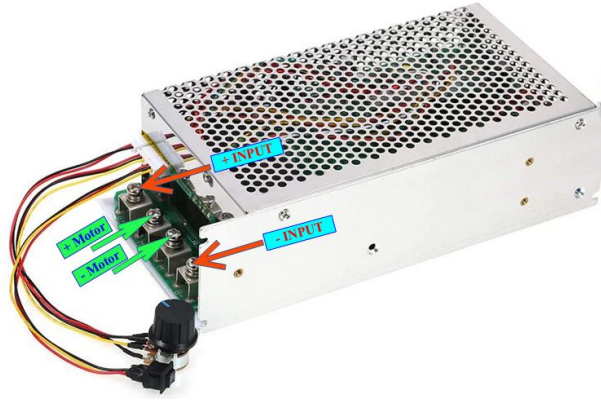


Fig.4. 3. Proposed PWM variable speed control driver for the PMDC Motor

Table 4. 2: Specification of the DC motor driver [79]

Working Voltage:	DC 10V-50V
Max. Current:	200A
continuous working current:	100A
Control Power:	0.01-5000W
Static Current:	0.05A
PWM Duty Cycle:	0%-100%
PWM Frequency:	15KHz
Control Voltage:	0-5V
Operating Temperature:	-20 to 40°C
Size:	23.5 * 11.5 * 6.5cm / 9.25 * 4.53 * 2.56in
Weight:	1.289kg

4.4.3 Maximum Power Point Tracker (MPPT)

Queenswing branded QW-JND-X Series 48V DC, 150A rated MPPT charge controller has chosen to extract power from the 10.6kW PV array, and the specification has given in the below **Table 4.3**.

Table 4. 3: Specification of the selected MPPT charge controller [78]

Rated Voltage	48VDC
Charge Current	150A
Battery terminals maximum voltage	70V
The largest pv input voltage	100VDC
Minimum pv input voltage	58VDC
The largest photovoltaic power input	24kw
Over-voltage disconnect	60V
Charging voltage limit	58V
Float charging voltage	55.2V
Under voltage disconnect recovery voltage	50V
Under voltage disconnect voltage	43.2V
Working environment temperature range	-35°C TO +55°C
Storage temperature range	-35°C TO +80°C
Humidity range	10%-90% No condensation

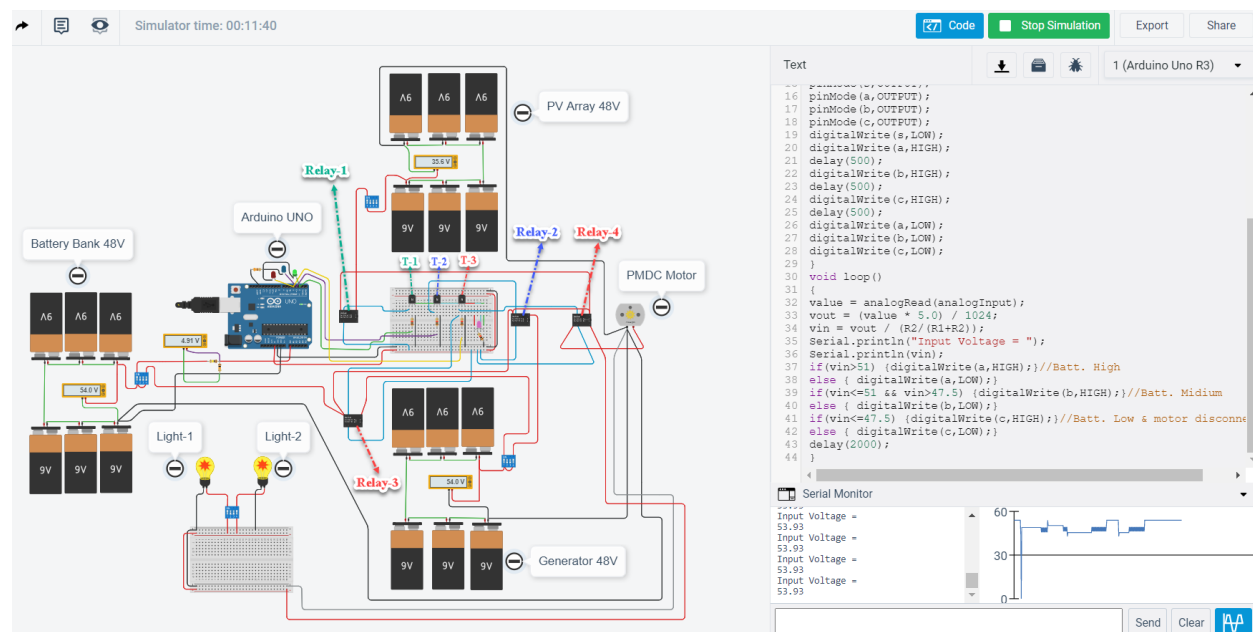
4.4.4 Proposed Main Distribution Board (MDB)

The power from the PV array, Diesel Generator, and the battery bank will come first to the proposed main distribution board (MDB) and then be supplied to loads through circuit breakers. MDB consists of the main circuit breaker (MCB) is rated 150amp, 48V DC, bus bar (150amp, 48V DC), and distributed circuit breaker. Power from the solar system is feed directly into MDB through MCB and then MCB to busbar to circuit breaker-1 (CB-1 rated 1.5amp, 48V DC), circuit breaker-2 (CB-2 rated 1amp, 48V DC), circuit breaker-3 (CB-3 rated 5amp, 48V DC), and circuit breaker-M (CB-M rated 135amp, 48V DC). Power from generator supplied to Bus bar through CB-G (40A, 48V DC). The battery to Bus bar is connected through CB-B (150amp, 48V DC). Electrical apparatus and ratings have been chosen according to the load demand in chapter -2.

4.5 Proposed Switching Control

A MATLAB function block and external signal-controlled breakers were used to automatically connect/disconnect the DC generator and PMDC motor according to the battery's

charging status during simulation in the system dynamic design. Furthermore, a programmed Arduino that will measure the battery's voltage level and report to the Arduino's digital output ports will replace the MATLAB function block. DC relays will relate to the Arduino's programmed output ports to perform the function of connecting/disconnecting. **Fig.4.4** shows the proposed control layout for switching among PV array, battery bank, dc generator, and PMDC motor based on BB voltage level, i.e., charging status. The proposed control system has been designed through Tinkercad.com and simulated to verify it. Some assumption has considered designing the planned control system, such as, (1) PV array (10.6kW), BB (440Ah) and DC generator (48V, 1.6kW) is constructed by connecting 6nos of 9V battery in series and, (2) PMDC motor (48V, 5kW) is measured as standard DC motor.



4.5.1 Proposed Physical Connection Outline

negative terminal connected to the Arduino Uno input GND terminal via 330 Ω resistor and positive terminals are connected corresponding to **Table.4.4**.

Table 4. 4: Arduino Uno functions

Case No.	Arduino Port No.	LED No.	LED status	SOC	Remarks (Measured voltage = V_{in})
Case-A: PV ON, Generator OFF & Motor ON	2	LED-G (Green)	HIGH	High	$V_{in} > 51V$, else LED status LOW
Case-B: PV OFF, Generator ON & Motor ON	3	LED-B (Blue)	HIGH	Medium	$51V \leq V_{in} > 47.5V$, else LED status LOW
Case-C: PV OFF, Generator ON & Motor disconnected.	4	LED-R (Red)	HIGH	Low	$V_{in} \leq 47.5V$, else LED status LOW

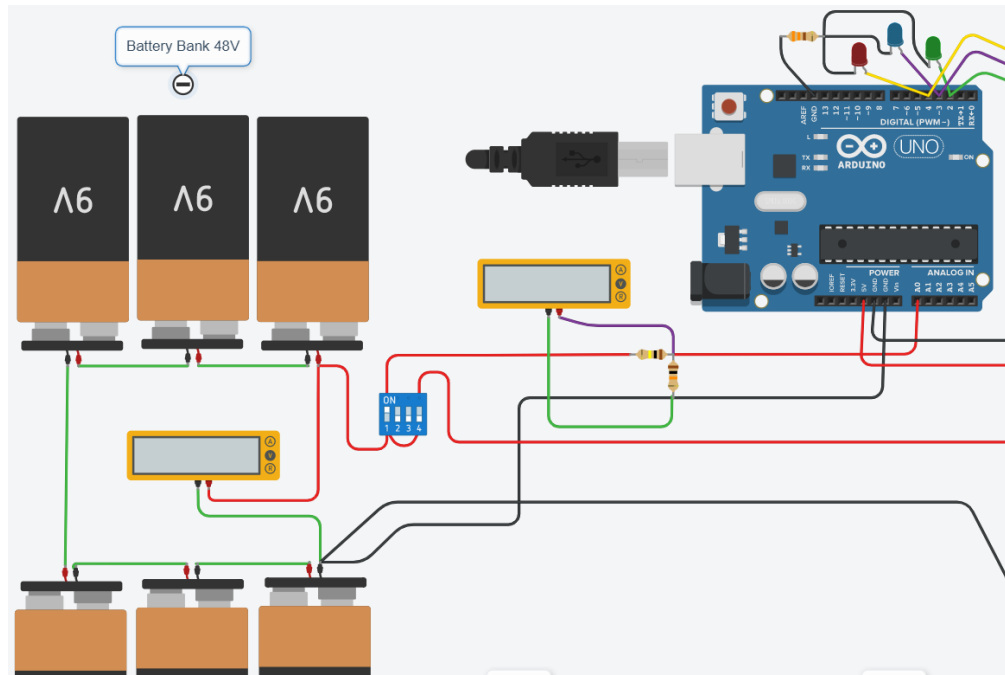


Fig.4. 5. Proposed Battery Bank to Arduino Connection for Voltage Monitoring.

Total four numbers of 5V DC relay, three numbers of transistors and three numbers of resistors (1k Ω) are used to design this proposed control mechanism and be designated as:

- (I) Relay: Relay-1, Relay-2, Relay-3, and Relay-4

(II) Transistor: T-1, T-2, and T-3.

4.5.2 Proposed Control Mechanism

The battery bank is connected to the motor through Relay-3, Relay-2, and Relay-4 in that order. Henceforth, BB will always be connected to the motor's terminal. PV is linked through Relay-1 to the motor. The generator is connected two different ways to the motor (i) Relay-3, Relay-2, and Relay-4, respectively, and (ii) Relay-3 and Relay-4, correspondingly. The proposed connection among Arduino, BB, Generator, PV, and Motor is given in **Fig.4.6**. The recommended control mechanism works according to the below description:

Case-A (PV ON, Generator OFF & Motor ON):

The Arduino Uno output digital port No. 2 (LED-G), while it goes HIGH, activates the transistor T-1 and triggers Relay-1. Henceforth, power from PV becomes available at the PMDC motor's terminal, and the motor starts to spin. LED-G turns into HIGH while Arduino's measured battery bank voltage, $V_{in} > 51V$, else LED status LOW.

Case-B (PV OFF, Generator ON & Motor ON):

The Arduino Uno output digital port No. 3 (LED-B), while it goes HIGH, activates the transistor T-2 and triggers Relay-2. As a result, the generator's power becomes available at the PMDC motor's terminal, and the motor continues to spin. LED-B turns into HIGH while Arduino's measured battery bank voltage, $51V \leq V_{in} < 47.5V$, else LED status LOW.

Case-C (PV OFF, Generator ON & Motor disconnected):

The Arduino Uno output digital port No. 3 (LED-R), while it goes HIGH, activates the transistor T-3 and triggers Relay-3 and Relay-4 simultaneously. As a result, Generator is still in operation and charging the battery bank, but the DC motor becomes disconnected from the system because of Relay-4 activation. LED-R turns into HIGH while Arduino's measured battery bank voltage, $V_{in} < 47.5V$, else LED status LOW. This case is an extreme situation, and to save the battery from deterioration, the motor is programmed to isolate from the system.

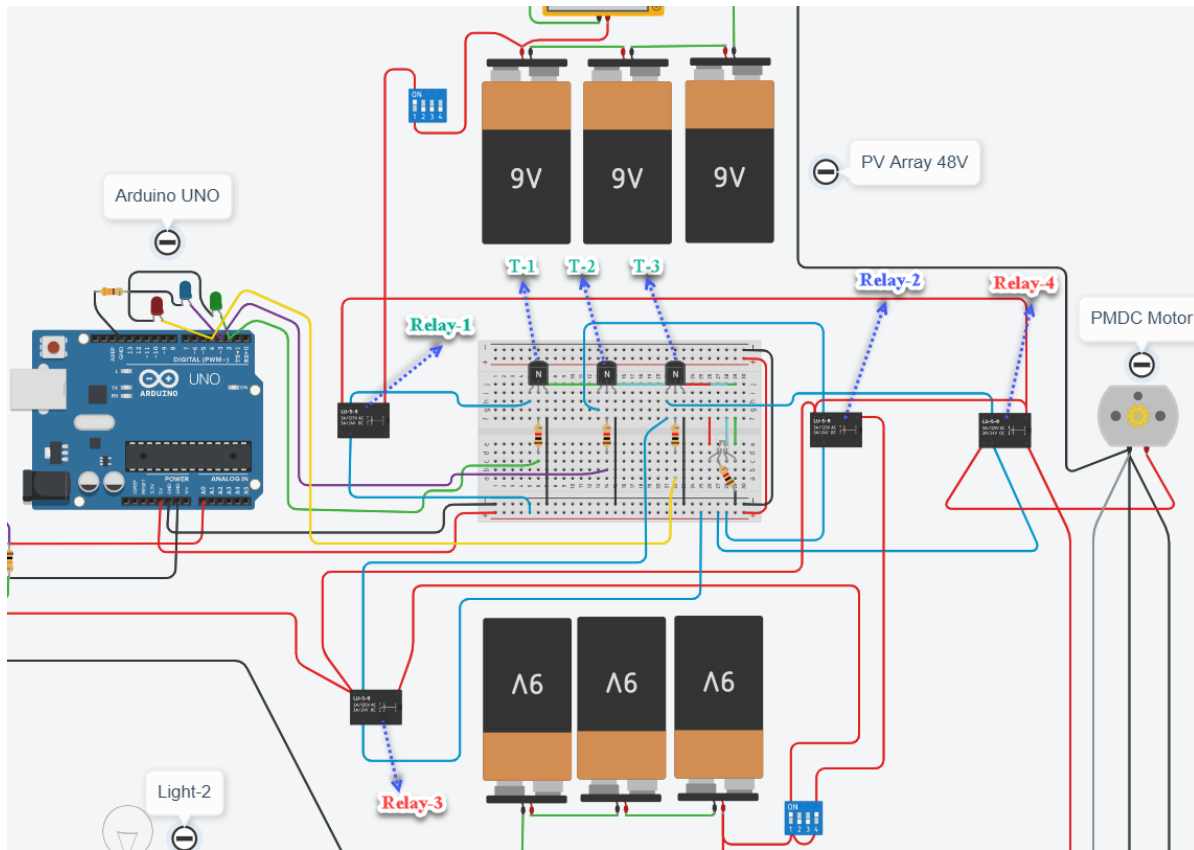


Fig.4. 6. Proposed connection among Arduino, BB, Generator, PV, and Motor.

4.6 Summary

The proposed instrumentation and Control mechanism has designed by selecting comparatively low-cost and higher-efficiency equipment but did not compromise with the quality. The proposed equipment's longevity is higher than others that are available in the market. All pieces of equipment have been chosen according to the sized data in chapter-2 and dynamic simulation in chapter-3. An overcurrent protection relay measures the dc motor protection, and circuit breakers protect other equipment. Control technology has been developed by programming Arduino Uno controller for switching generator, battery, and motor. The display system has demonstrated boat speed, water depth, water temperature, GPS location and boat navigation, battery voltage, and SOC monitoring. Also, a motor driver for driving the boat at the required speed.

(Note: Due to the Covid-19 situation, the proposed controller designed in this chapter was only simulated. It was not implemented in the lab.)

Chapter-5

Sensitivity and Socio-Economic Analysis

5.1 Sensitivity Analysis

Sensitivity analysis shows the effect of different variables on the optimized results. For sensitivity analysis, several numerical values are assigned to these variables within an acceptable range to observe their influence on the optimized system. Renewable based hybrid energy system needs a sensitivity analysis to monitor the impact of several significant variables on the system's overall cost and feasibility. In most cases, it is performed by changing the significant input variable to observe the change of the output quantity. Typically, the impact on COE and NPC gets importance in a sensitivity analysis. In HOMER, there are several kinds of technical and economic inputs such as load demand, deferrable load, solar radiation, diesel price, cost components (capital, operating, replacement, and O&M), cost multiplier, inflation rate, discount rate, renewable penetration, capacity shortage, etc. The sensitivity variables used in this study are presented in **Table 5.1**.

Table 5. 1: Sensitivity variables

Sensitivity variables	Values
Solar-scaled average (kWh/m ² /day)	4.50, 4.65*, 4.70
Diesel fuel price (\$/L)	0.70, 0.76*, 0.80
Project lifetime (years)	8, 10*, 12, 15
PV panel capital cost multiplier	0.5, 0.70, 0.8, 0.9, 1.0
Inflation rate (%)	0, 1, 2*, 3
Discount rate (%)	6, 7, 8*, 9, 10

*Baseline value

Since renewable resources are highly intermittent, uncertainties in solar radiation are considered for designing the hybrid system. The variation in solar radiation could be seasonal or annual, which covers a particular range. The annual average solar radiation in the study location is 4.65 kWh/m²/day. As a result, wide ranges of values from 4.50 to 4.70 kWh/m²/day have been

entered for sensitivity analysis. The values are chosen based on the historical data recorded in the location.

On the other hand, the diesel price has fluctuating nature and change quickly in the world market. In this study, three diesel prices range from \$0.70/L to \$0.80/L are selected for sensitivity analysis based on recent market trends. The COE and NPC of the proposed hybrid system largely depend on the project lifetime considered. In consideration of different renewable systems, four project lifetimes are set: 8, 10, 12, and 15 years. The inflation rate is set to rise from 0% to 3% considering local conditions and stable inflation in the future. There is no significant load growth for a solar boat system, as the load profile does not change based on appliances used in boat appliances during the project lifetime. Thus, the load demand is considered stable considering boat requirement conditions in the future. Moreover, no sensitivity analysis is performed on battery price because of its ongoing cost over the past few years.

5.2 The sensitivity of the PV/ Diesel/Batt system

Sensitivity analysis has been performed considering the variables presented in **Table 5.1**. This analysis aims to observe the effect of input parameters on the COE and NPC of the optimized PV/Diesel/Battery system. To investigate the stability of the proposed hybrid system, effects of varying solar radiation, diesel price, project lifetime, discount rate, and PV capital cost on the COE and NPC of optimal PV/Diesel/Battery system are analyzed. The solar radiation and diesel price's baseline value is 4.65 kWh/m²/day and 0.76\$/L, respectively. Considering all the cases, PV/Diesel/Battery is the optimized configuration shown in **Fig.5.1**. The optimized COE for the system is 0.228\$/kWh. However, the increase in solar radiation reduces the COE because of higher renewable penetration. With the increase in diesel price (in a range of 0.7 \$/L to 0.76 \$/L), COE decreases for constant solar radiation 4.65 kWh/m²/day. However, above the diesel price of 0.76\$/L, the COE follows the increasing trend.

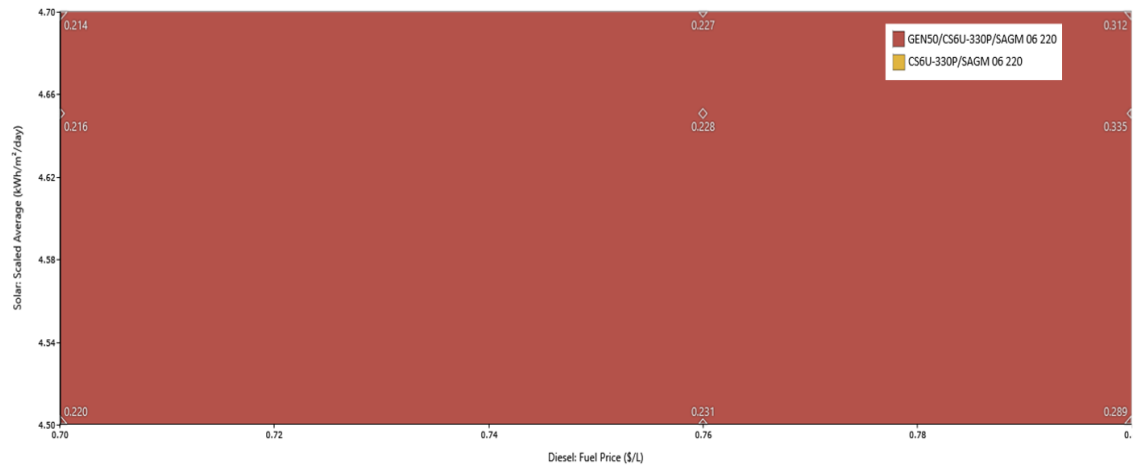


Fig.5. 1. The sensitivity of solar radiation and diesel fuel price for PV/Diesel/batt system on COE.

Sensitive variables are further exemplified for NPC through a surface plot with NPC as primary and COE as a secondary variable, as shown in **Fig.5.2**. Here NPC is represented as a colored band while the discrete points represent COE. It is found that at 0.80\$/L diesel price and 4.5 kWh/m²/day solar irradiation, the COE reached its maximum value of 0.289\$/kWh. For the same input variable, the NPC is also maximum. This is because the small contribution from PV power on demanded load results in higher diesel consumption at low solar radiation. In **Fig. 5.2**, NPC is superimposed. At the diesel price of 0.70\$/L, NPC is comparatively lower at \$14,000.

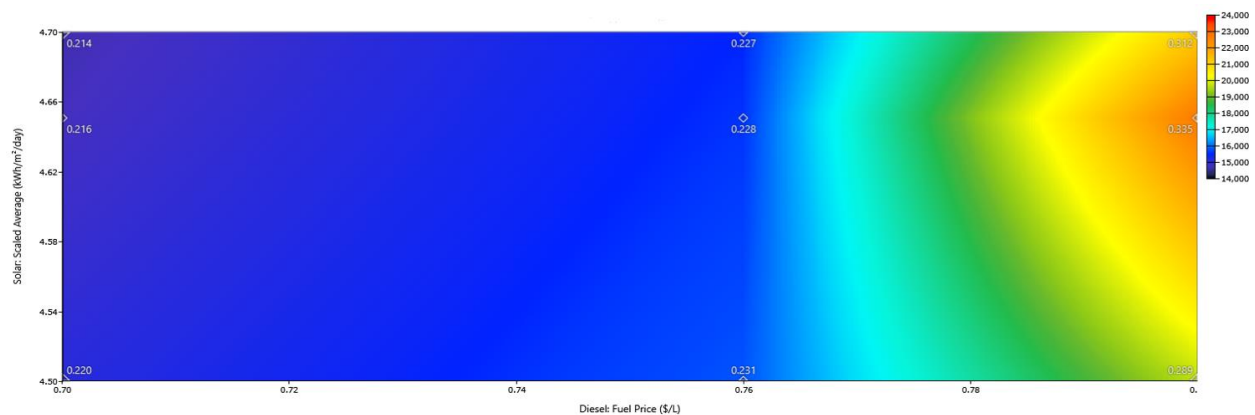


Fig.5. 2. The sensitivity of solar radiation and diesel fuel price for PV/Diesel/batt system on NPC.

On the other hand, the PV price and project lifetime significantly impact the proposed project's COE and NPC. The technological advancement in PV panels results in highly efficient panels with lower prices. The COE is again superimposed on **Fig.5.3**. It shows the optimal COE

under different PV cost multiplier and project lifetime while the other variable remains constant. It is evident that reduced PV price and a higher lifetime of project results in comparatively low COE. The lowest COE observed 0.136 while project lifetime is the highest 15years, and PV price is the lowest 0.5multiplier. It can further be noticed that the COE reduces as the project lifetime at a given PV price, and oppositely, COE increases as the PV cost increases for a given project lifetime. For the constant value of baseline PV cost multiplier 0.7, COE found 0.185 at project lifetime 10years.

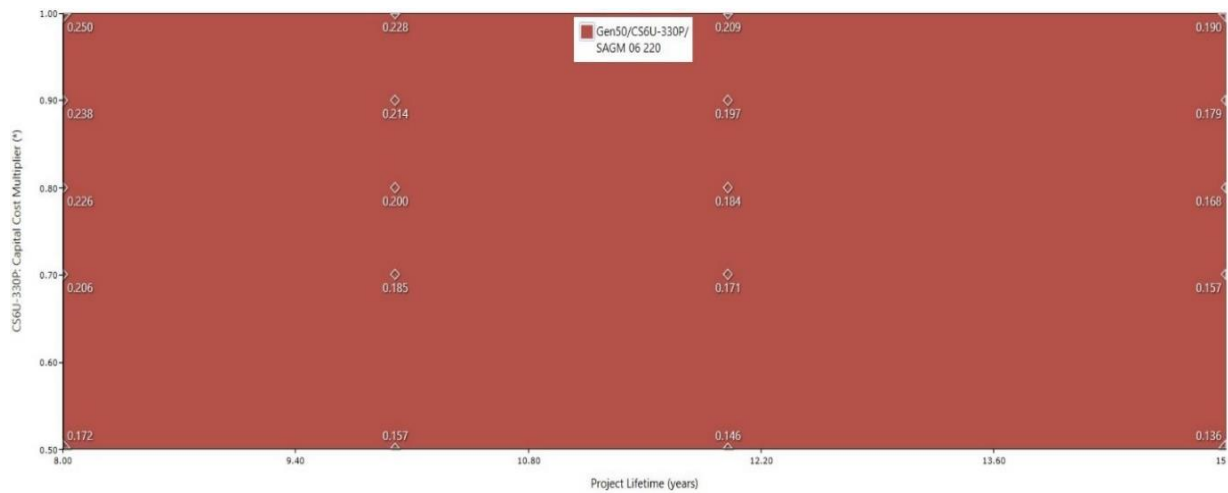


Fig.5. 3. Effects of project lifetime and PV module capital costs for PV/Diesel/batt system on COE.

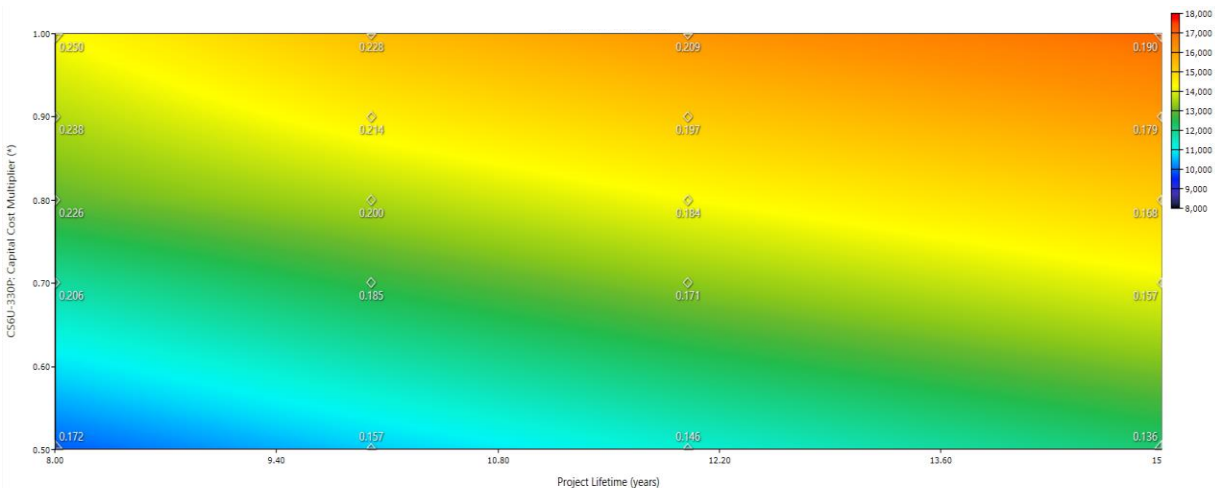


Fig.5. 4. Effects of project lifetime and PV module capital costs for PV/Diesel/batt system on NPC

The NPC is again superimposed in **Fig.5.4** for different values of PV cost multiplier and project lifetime. Once again, PV/Diesel/Battery is the most viable configuration for all cases of NPC. It can be observed that the NPC reduces when both the project lifetime and PV cost reduces. It is further observed that PV cost at a given project lifetime and similarly, project lifetime at a given PV cost increases the proposed project's NPC.

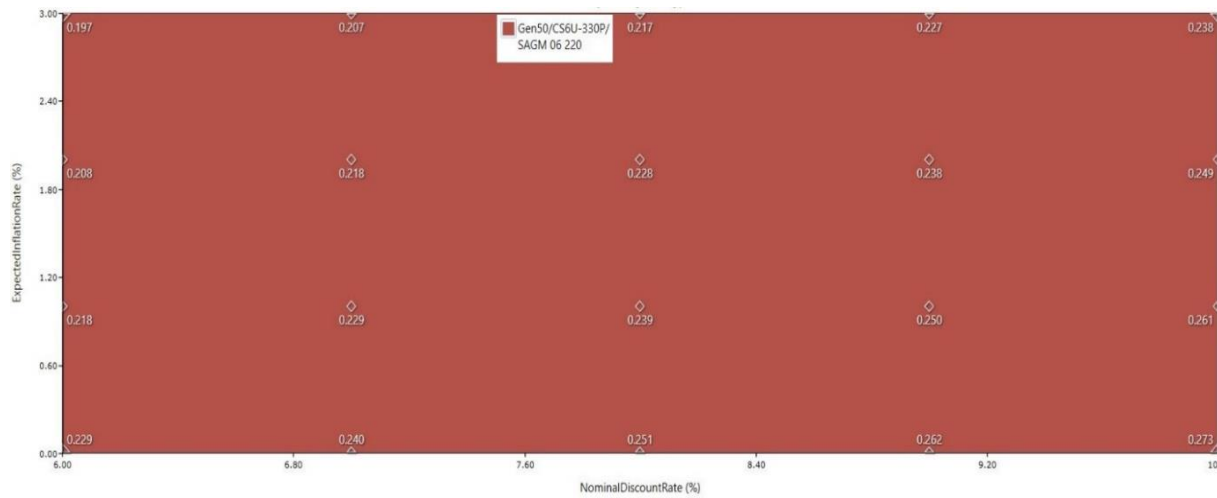


Fig.5. 5. Effects of project discount and inflation rate for PV/Diesel/batt system on COE.

The two most significant variables for any hybrid system are the discount rate and inflation rate. The discount rate is the interest rate that determines the present value of future cash flows. As a result, higher discount rates or longer delays produce lower net present value. On the other hand, the inflation rate increases or decreases in prices during a project lifetime. Low, stable, and predictable inflation is good for the project economy. A rise in the inflation rate indicates the rise of system components (PV, Diesel generator, battery, etc.). The effect of inflation and discount rate on the COE of the PV/Diesel/Battery system is shown in **Fig.5.5**. The lowest COE 0.197 \$/kWh is obtained when the inflation rate is 3%, and the discount rate is 6%. The increasing discount rate increases the COE of the system for a constant inflation rate.

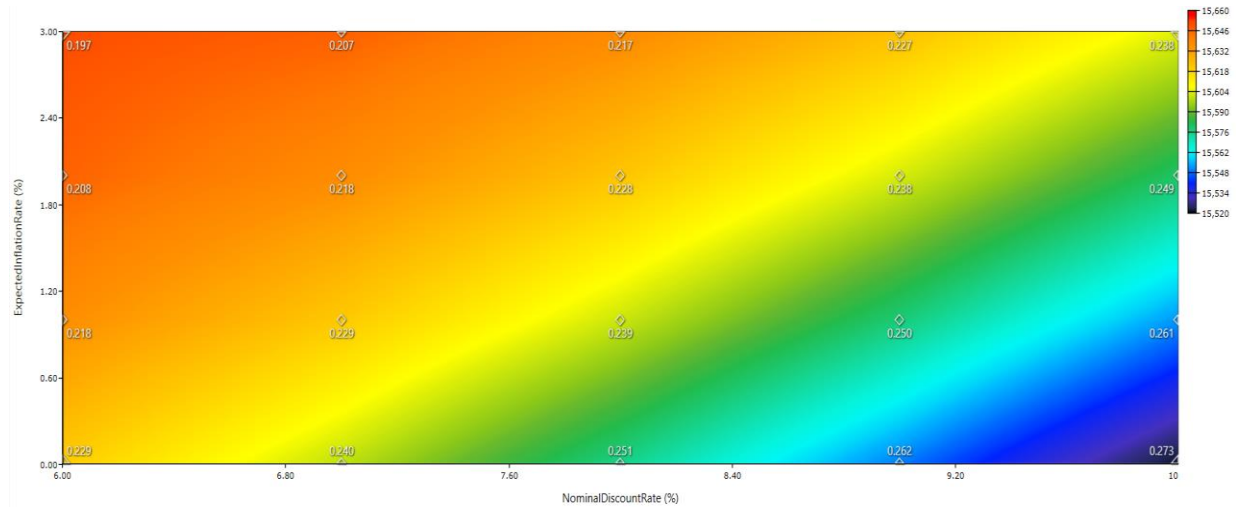


Fig.5. 6. Effects of the inflation rate and discount for PV/Diesel/batt system on NPC.

The effect of varying discounts and interest rates on the NPC is presented in **Fig.5.6**. The inflation rate varied from 0% to 3% considering a stable economy, while the discount rate is varied from 6% to 10%. A very high discount rate of 10% and 0% inflation yields a minimum NPC of \$15,520. On the other hand, the lowest discount rate with a very high inflation rate of 3% yields a maximum NPC of \$15,660.

5.3 Payback Period [61]

The economic analysis consists of estimating the simple payback period (SPBP) for the PV module, generator, and battery backup system. The proposed boat will convey 20nos of passengers per trip. The approximate trip distance is 10 km, boat speed 10km/hr (5.4 knots), the total operating period is 8hrs/day. Henceforth, the boat could travel 8trip, and the equivalent distance is 80 km in a day. If the ticket price 0.01 \$/km/person and the proposed boat operates 220days in a year, then the total annual income will be \$ 3520.00.

We found the proposed system's capital cost is \$ 13358.00, the annual operating cost is \$ 378.48, and the cost of energy (COE) is 0.228 \$/kWh from the Homer simulation result. The payback period defines the total time that it requires to recover the expenditure of financing. The proposed design's payback period, which consists of solar PV power, DG, and battery bank system, turns into a positive value of \$ 2349.6 end of the 5th year of operation. After 10years, it becomes \$18057.2, **Fig.5.3**, an excellent sign to implement this technology.

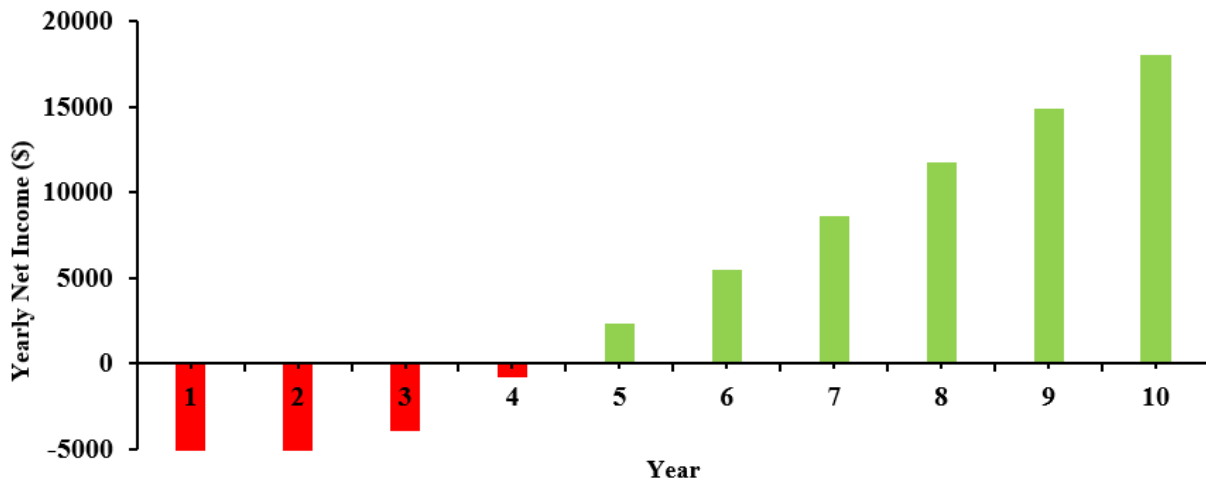


Fig.5. 7. Simple payback period (SPBP) graph of the proposed system

5.4 Environmental Benefits

The vast amount of fossil-fuel-based energy resources is the prime cause of greenhouse gas emissions, rising interest over global warming nowadays. It has encouraged research on more alternatives such as photovoltaic (PV) and wind systems for getting clean and green energy. The environmental benefits of incorporating hybrid renewable energy (PV-gas generator-battery) in the solar-powered electric boat are incredibly essential in greenhouse gas radiations. The volume of impurity radiations was assessed and contrasted with the diesel-only alternative [86]. Electricity production mainly relies on fossil fuel for the diesel-only system. As a result, its impact on the environment is adversely high. The proposed hybrid power system for the solar boat reduces CO₂, CO, UHC, PM, SO₂, and NO emissions by 7046 kg /yr, 44 kg/yr, 2 kg/yr, 0.1 kg/yr, 17 kg/yr, and 41 kg/yr respectively compared to the conventional diesel-only system since it contributes 95.6% renewable energy.

Henceforth, the following environmental crucial benefits could get from the proposed hybrid power system:

- Decreased atmosphere pollution.
- Decreased dependency on fossil fuel.
- Decreased power costs.

- Decreased water consumption and
- Slow down weather changes over

5.5 Summary

PV/diesel/battery hybrid power system was compared with green PV/battery and traditional diesel-only power system, from the economic and energy generation point of view to offer an optimal solution of an automatic solar electric boat power system with the energy storage system. The proposed hybrid power system (PV/Diesel/Battery) is cheaper than the PV/Battery and Diesel only system for long term (10Years) project. While solar radiation rises, COE decreases and stay declines if there is constant solar radiation $4.65 \text{ kWh/m}^2/\text{day}$ and an increase in diesel price (in a range of 0.7 to 0.76 \$/L). The optimized COE for the hybrid power system is 0.228\$/kWh. It has been observed that COE reduces as the project lifetime at a given PV price; contrarily, COE increases as the PV cost increases for a given project lifetime. The NPC reduces when both the project lifetime and PV cost reduces. Proposed project's NPC increases concerning fixed PV cost vs. project lifetime and fixed project lifetime vs. PV cost. The growing discount rate raises the COE of the system for a steady inflation rate. The smallest COE 0.197 \$/kWh is obtained against the inflation rate (3%) and the discount rate (6%). While the discount rate varies from 6% to 10%, the inflation rate becomes stable and lies between 0% to 3%, which turns the balanced economy. The proposed system's payback period turns into a positive value of \$ 2349.6 end of the 5th year of operation, and after 10years, it becomes \$ 18057.2. The designed hybrid power system generates negligible emissions of toxic gas, and it is a smaller amount compare to the other existing system as it contributes 93.8% renewable energy. It offers lower transportation costs and creates employment opportunities, which enhances the social life leading.

Chapter-6

Conclusion and Recommendation

6.1 Conclusion:

This research introduced the best possible resolution to replace the diesel engine boat with an automated solar-powered electric boat, which is reasonable for the minimal earner people in developing countries. For this reason, daily load data and solar global horizontal irradiance (GHI) data were collected from the existing site, where diesel engine boat operates in the Buriganga river in Bangladesh. Sizing assessment for the power system, which includes solar photovoltaic panel, dc gas generator, and battery storage, was performed in HOMER. This estimation was justified using a manual calculation.

To obtain the total electrical power requirement, firstly, the boat length was calculated as 12m and a beamwidth of 4.8m. Then based on the carrying capacity for 20 passengers, displacement of water (2400kg), boat hull speed (15.58 km/h), and boat speed 10km/h (5.4knots) were computed. Finally calculated the dc motor power 5kW to propel the boat up to 3000rpm.

A hybrid power system comprised of solar PV, gas generator, and battery bank has been proposed to supply the total load requirement of the boat. The techno-economic optimization of the hybrid system is studied and analyzed by commercially available HOMER software. HOMER optimized the system for the boat that consists of 10.6 kW PV, 1.6 kW diesel generator, 18.5 kWh storage batteries. Additionally, sensitivity analysis was performed to observe the effect of different variables such as solar irradiance, diesel fuel price, project lifetime, PV panel capital cost multiplier, inflation rate and discount rate on the COE and NPC of the proposed hybrid system. From the sensitivity analysis, it has been noticed that the optimized COE is 0.228\$/kWh for the proposed hybrid power system and the stable economy arises while discount rate is between 6%-10% and inflation rate 0%-3%. The reimbursement of the investment of the proposed system could achieve within the fifth year of operation, whereas the proposed project's lifetime was assumed ten years.

Based on HOMER optimization, dynamic modeling was performed in MATLAB Simulink to examine the dynamic behavior of the designed system, which incorporates PV (10.6kW), MPPT (140A), battery bank (48V, 440Ah), dc gas generator (1.6kW), PMDC motor (5kW, 3000rpm) with driver and controller.

The simulation has done for 40seconds duration since extended duration requires many days to compute as the system contains a few complex blocks. During the dynamic simulation, (i) partial cloudy weather, (ii) full cloudy weather, and (iii) sunny day situations were considered. The MPPT was established based on Perturb & Observe algorithm. The result was showed that the PV could produce 8.82kW equivalent power, which is almost equal to HOMER-sized 10.6kW, only 12% lesser than it. The motor was reached 3000rpm, and the speed was varied according to the reference speed. The battery was charged at a constant current of 25A and 49V. The study was showed that to charge the battery up to 80%, it takes 3hours and 5hours to full charge (100%). The dc generator was produced 1.6kW power and found that it could run the PMDC motor and charge the battery at a time. The load demand responded to the MPPT.

The proposed instrumentation and control system was designed by considering the low price but higher efficiency and better quality, so that higher instrument's longevity. The proposed Arduino uno based control system has been simulated in Tinkercad.com web-based software to verify the live functionality of the switching mechanism. Most of the boatmen in Bangladesh drive the boat without knowing the vessel's instruments' performance, boat speed, safe root for driving the boat, the submerged land in the river or pathway, and battery charge status. The recommended system is more beneficial as it is fully automated with a visual display system. Arduino Uno is used to developing control technology, and its principal function is controlling the switching among generator, battery, and motor.

The proposed design's payback period, which consists of solar PV power, DG, and battery bank system, turns into a positive value of \$2,350 end of the fifth year of operation. After ten years, it becomes \$18,057, which is an excellent sign to implement this technology. Communities' life leads improving because of the more comfortable, securer, and cheaper transportation; besides, it offers work scope for the society.

6.2 Recommendation:

Sizing PV/Generator/Bat hybrid power system, dynamic modeling, instrumentation design, and control mechanism, sensitivity, and economic analysis of a solar-powered electric boat have been described. Implementing the proposed system into a physical system is still needed to confirm the practical feasibility and use in transportation. (As mentioned, before it was not done due to the Covid-19 situation).

During rainy season and winter season solar irradiance are low in Bangladesh as a result insufficient solar power, increase the use of generator which is one of the main reasons to increase the COE, it is suggested to further work on the feasibility of implementation other renewable energy as a standby energy source.

Additionally, the Arduino Uno R3 microcontroller board was proposed to construct the switching control system among PV array, Battery bank, diesel generator, and PMDC motor. For a more complicated system, a faster processing capable microcontroller is recommended.

A wireless communication system might introduce developing a solar boat network to share their technical data and location and be monitored centrally. MATLAB dynamic simulation to observe the equipment's dynamic behavior was performed for 40seconds because of the computer's slow computing process. To overcome this problem, simulate a faster processing capable computer or an uncomplicated model for an 08hours duration is suggested. This designed solar-powered electric boat could execute in any river or lake in Bangladesh.

References

- [1] “Choosing the right Electric Propulsion Solution – Navaltboats.” <https://navaltboats.com/choosing-the-right-electric-propulsion-solution/> (accessed Sep. 10, 2020).
- [2] M. F. Hossain, S. Hossain, and M. J. Uddin, “Renewable energy: Prospects and trends in Bangladesh,” *Renew. Sustain. Energy Rev.*, vol. 70, no. C, pp. 44–49, 2017.
- [3] “Why Use Solar Energy? Why Solar Energy is Important for You.” <https://www.solar-energy-at-home.com/why-use-solar-energy.html> (accessed Sep. 10, 2020).
- [4] “Country boats in Bangladesh,” Wikipedia. Dec. 30, 2020, Accessed: Feb. 01, 2021. [Online]. Available: [https://en.wikipedia.org/w/index.php?title=Country_boats_in_Bangladesh & oldid=997208176](https://en.wikipedia.org/w/index.php?title=Country_boats_in_Bangladesh&oldid=997208176).
- [5] “Bangladesh, a beautiful ‘Country of Boats,’” Travel Bangladesh Blog, Jul. 23, 2017. <http://travel.jumia.com/blog/bd/bangladesh-beautiful-country-boats-533> (accessed Aug. 03, 2019).
- [6] P. Vorobiev and Y. Vorobiev, “Automatic sun tracking solar electric systems for applications on transport,” in 2010 7th International Conference on Electrical Engineering Computing Science and Automatic Control, Sep.2010, pp.66–70, doi: 10.1109/ICEEE.2010.5608582.
- [7] C. Sharma and A. Jain, “Simulink Based Multi Variable Solar Panel Modeling,” *Indones. J. Electr. Eng. Comput. Sci.*, vol. 12, no. 8, Art. no. 8, Aug. 2014.
- [8] “Global Solar Atlas.” <https://globalsolaratlas.info/map?c=-3.903732,-1.582031,2> (accessed Feb. 01, 2021).
- [9] “Equivalent Circuit Model - an overview | ScienceDirect Topics.” <https://sciencedirect.com/topics/engineering/equivalent-circuit-model> (accessed Feb. 01, 2021).
- [10] “Types of photovoltaic cells - Energy Education.” https://energyeducation.ca/encyclopedia/Types_of_photovoltaic_cells (accessed Feb. 01, 2021).
- [11] ZHCSolar, “MPPT vs PWM: Which Charge Controller Should You Choose?” <https://zhcsolar.com/mppt-vs-pwm/> (accessed Feb. 01, 2021).
- [12] “Maximum Power Point Tracking - Solar Power Information | Solar Quotes,” SolarQuotes. <https://www.solarquotes.com.au/inverters/mppt/> (accessed Feb. 01, 2021).
- [13] “What is the Best Battery for Solar Storage? | EnergySage.” <https://www.energysage.com/solar/solar-energy-storage/what-are-the-best-batteries-for-solar-panels/> (accessed Feb. 02, 2021).
- [14] D. O. am a writer, R. for the C. E. Sector, I. cover climate change issues, N. C. Technologies, sustainability, and green cars D. Ovy, “The Best Solar Batteries for Your Solar PV

System,” Mar. 29, 2019. <https://www.alternative-energies.net/what-are-the-best-batteries-for-solar-panel-systems/> (accessed Feb. 02, 2021).

[15] S. M. L. Kabir, I. Alam, M. R. Khan, M. S. Hossain, K. S. Rahman, and N. Amin, “Solar powered ferry boat for the rural area of Bangladesh,” in 2016 International Conference on Advances in Electrical, Electronic and Systems Engineering (ICAEES), Nov. 2016, pp. 38–42, doi: 10.1109/ICAEES.2016.7888005.

[16] “5 Best Electric Outboard Motors (Reviews Updated 2021) - Solar Sailor.” <https://www.solarsailor.com/best-electric-outboard-motor/> (accessed Feb. 02, 2021).

[17] “Solar cell efficiency tables (version 28) - Wiley Online Library,” moam.info. https://moam.info/solar-cell-efficiency-tables-version-28-wiley-online-library_59989beb1723dd97bdd00e8d.html (accessed Sep. 10, 2020).

[18] K. Mahmud, S. Morsalin, and M. I. Khan, “Design and Fabrication of an Automated Solar Boat,” *Int. J. Adv. Sci. Technol.*, vol. 64, pp. 31–42.

[19] C. S. Postiglione, D. A. F. Collier, B. S. Dupczak, M. L. Heldwein, and A. J. Perin, “Propulsion system for an all-electric passenger boat employing permanent magnet synchronous motors and modern power electronics,” in *Railway and Ship Propulsion 2012 Electrical Systems for Aircraft*, Oct. 2012, pp. 1–6, doi: 10.1109/ESARS.2012.6387441.

[20] G. C. D. Sousa, D. S. L. Simonetti, and E. E. C. Norena, “Efficiency optimization of a solar boat induction motor drive,” in *Conference Record of the 2000 IEEE Industry Applications Conference. Thirty-Fifth IAS Annual Meeting and World Conference on Industrial Applications of Electrical Energy* (Cat. No.00CH37129), Oct. 2000, vol. 3, pp. 1424–1430 vol.3, doi: 10.1109/IAS.2000.882071.

[21] W. Obaid, A.-K. Hamid, and C. Ghenai, “Hybrid Power System Design for Electric Boat with Solar Irradiance Forecasting,” in 2018 6th International Renewable and Sustainable Energy Conference (IRSEC), Dec. 2018, pp. 1–5, doi: 10.1109/IRSEC.2018.8702854.

[22] G. S. Spagnolo, D. Papalillo, A. Martocchia, and G. Makary, “Solar-Electric Boat,” *J. Transp. Technol.*, vol. 2, no. 2, Art. no. 2, Apr. 2012, doi: 10.4236/jtts.2012.22015.

[23] J. Campillo, J. A. Domínguez-Jimenez, and J. Cabrera, “Sustainable Boat Transportation Throughout Electrification of Propulsion Systems: Challenges and Opportunities,” in 2019 2nd Latin American Conference on Intelligent Transportation Systems (ITS LATAM), Mar. 2019, pp. 1–6, doi: 10.1109/ITSLATAM.2019.8721330.

[24] S. Ahmed, A. Castellazzi, and A. Williams, “Multi-source energy networks for cargo vessels,” *Trans. Environ. Electr. Eng.*, vol. 1, no. 4, Nov. 2016, doi: 10.22149/teee.v1i4.52.

[25] S. Reza, M. S. A. A. F. Shiblee, M. R. Mawla, J. N. Jein, and M. M. Rahman, “Design and Analysis of Solar PV System for Marine Fishing Trawlers in Bangladesh,” in 2018 4th International Conference on Electrical Engineering and Information Communication Technology (iCEEICT), Sep. 2018, pp. 677–680, doi: 10.1109/CEEICT.2018.8628166.

- [26] J. Hua, Y.-H. Wu, and P.-F. Jin, "Prospects for renewable energy for seaborne transportation—Taiwan example," *Renew. Energy*, vol. 33, no. 5, pp. 1056–1063, May 2008, doi: 10.1016/j.renene.2007.06.002.
- [27] C. Ghenai, I. Al-Ani, F. Khalifeh, T. Alamaari, and A. K. Hamid, "Design of Solar PV/Fuel Cell/Diesel Generator Energy System for Dubai Ferry," in *2019 Advances in Science and Engineering Technology International Conferences (ASET)*, Mar. 2019, pp. 1–5, doi: 10.1109/ICASET.2019.8714292.
- [28] C. P. Leung and K. W. E. Cheng, "Zero emission solar-powered boat development," in *2017 7th International Conference on Power Electronics Systems and Applications-Smart Mobility, Power Transfer Security (PESA)*, Dec. 2017, pp. 1–6, doi: 10.1109/PESA.2017.8277736.
- [29] S. Chakraborty, M. M. Hasan, S. Das, and M. A. Razzak, "A novel MPPT-based synchronous buck converter for solar power system in fishing trawler," in *2016 IEEE 7th Power India International Conference (PIICON)*, Nov. 2016, pp. 1–6, doi: 10.1109/POWERI.2016.8077296.
- [30] H. Liu, Q. Zhang, X. Qi, Y. Han, and F. Lu, "Estimation of PV output power in moving and rocking hybrid energy marine ships," *Appl. Energy*, vol. 204, pp. 362–372, Oct. 2017, doi: 10.1016/j.apenergy.2017.07.014.
- [31] D. Tamunodukobipi, N. Samson, and A. Sidum, "Design Analysis of a Lightweight Solar Powered System for Recreational Marine Craft," 2018, doi: 10.4236/WJET.2018.62027.
- [32] K. Mahmud, S. Morsalin, and M. I. Khan, "Design and Fabrication of an Automated Solar Boat," *Int. J. Adv. Sci. Technol.*, vol. 64, pp. 31–42.
- [33] R.-M. Chao, H.-K. Lin, and C.-H. Wu, "Solar-powered boat design using standalone distributed PV system," in *2018 IEEE International Conference on Applied System Invention (ICASI)*, Apr. 2018, pp. 31–34, doi: 10.1109/ICASI.2018.8394259.
- [34] Peter Joore and Anton Wachter, "Frisian solar boat design. A multi-level innovation analysis," in *2009 34th IEEE Photovoltaic Specialists Conference (PVSC)*, Jun. 2009, pp. 002214–002219, doi: 10.1109/PVSC.2009.5411383.
- [35] S. Das, P. K. Sadhu, and S. Chakraborty, "Green sailing of solar PV powered country boat using buck-boost chopper," in *2016 International Conference on Circuit, Power and Computing Technologies (ICCPCT)*, Mar. 2016, pp. 1–5, doi: 10.1109/ICCPCT.2016.7530283.
- [36] A. K. Sharma and D. P. Kothari, "Solar PV potential for passenger ferry boats in India's National Waterways," in *2018 2nd International Conference on Inventive Systems and Control (ICISC)*, Jan. 2018, pp. 120–130, doi: 10.1109/ICISC.2018.8399035.
- [37] W. Obaid, A.-K. Hamid, and C. Ghenai, "Wind-Fuel-Cell-Solar Hybrid Electric Boat Power Design with MPPT System," in *2019 8th International Conference on Modeling Simulation and Applied Optimization (ICMSAO)*, Apr. 2019, pp. 1–5, doi: 10.1109/ICMSAO.2019.8880330.

- [38] W. Obaid, A.-K. Hamid, and C. Ghenai, "Hybrid PEM Fuel-Cell-Diesel-Solar Power System Design with Fuzzy Battery Management System and Weather Forecasting for Electric Boats," in 2018 6th International Renewable and Sustainable Energy Conference (IRSEC), Dec. 2018, pp. 1–7, doi: 10.1109/IRSEC.2018.8702862.
- [39] W. Obaid, A.-K. Hamid, and C. Ghenai, "Hybrid PEM Fuel-Cell-Solar Power System Design for Electric Boat with MPPT System and Fuzzy Energy Management," in 2019 International Conference on Communications, Signal Processing, and their Applications (ICCSPA), Mar. 2019, pp. 1–7, doi: 10.1109/ICCSPA.2019.8713646.
- [40] S. Chakraborty, S. M. S. Ullah, and M. A. Razzak, "Quantifying solar potential on roof surface area of fishing trawlers in Chittagong Region in Bangladesh," in 2016 IEEE Innovative Smart Grid Technologies - Asia (ISGT-Asia), Nov. 2016, pp. 833–837, doi: 10.1109/ISGT-Asia.2016.7796493.
- [41] N. A. S. Salleh, W. M. W. Muda, and S. S. Abdullah, "Feasibility study of optimization and economic analysis for grid-connected renewable energy electric boat charging station in Kuala Terengganu," in 2015 IEEE Conference on Energy Conversion (CENCON), Oct. 2015, pp. 510–515, doi: 10.1109/CENCON.2015.7409597.
- [42] R. Leiner, "Solar radiation and water for emission-free marine mobility," in 2014 IEEE International Energy Conference (ENERGYCON), May 2014, pp. 1425–1428, doi: 10.1109/ENERGYCON.2014.6850609.
- [43] B. J. Dilip, D. H. Vilas, A. V. Anil, and P. N. Jaiswal, "So traction boat inland water transportation system," in 2016 International Conference on Energy Efficient Technologies for Sustainability (ICEETS), Apr. 2016, pp. 245–249, doi: 10.1109/ICEETS.2016.7582934.
- [44] T. B. Soeiro, T. K. Jappe, W. M. dos Santos, D. C. Martins, and M. L. Heldwein, "Propulsion and battery charging systems of an all-electric boat fully constructed with interleaved converters employing interphase transformers and Gallium Nitride (GaN) power FET semiconductors," in 2014 IEEE Applied Power Electronics Conference and Exposition - APEC 2014, Mar. 2014, pp. 3212–3217, doi: 10.1109/APEC.2014.6803765.
- [45] N. Fonseca, T. Farias, F. Duarte, G. Gonçalves, and A. Pereira, "The Hidrocat Project – An all-electric ship with photovoltaic panels and hydrogen fuel cells," *World Electr. Veh. J.*, vol. 3, no. 4, Art. no. 4, Dec. 2009, doi: 10.3390/wevj3040764.
- [46] M. D. Margaritou and E. Tzannatos, "A multi-criteria optimization approach for solar energy and wind power technologies in shipping," *FME Trans.*, vol. 46, no. 3, pp. 374–380, 2018, doi: 10.5937/fmet1803374M.
- [47] H. Lan, S. Wen, Y.-Y. Hong, D. C. Yu, and L. Zhang, "Optimal sizing of hybrid PV/diesel/battery in ship power system," *Appl. Energy*, vol. 158, pp. 26–34, Nov. 2015, doi: 10.1016/j.apenergy.2015.08.031.

- [48] A. Glykas, G. Papaioannou, and S. Perissakis, "Application and cost-benefit analysis of solar hybrid power installation on merchant marine vessels," *Ocean Eng.*, vol. 37, no. 7, pp. 592–602, May 2010, doi: 10.1016/j.oceaneng.2010.01.019.
- [49] R. Tang, Z. Wu, and Y. Fang, "Configuration of marine photovoltaic system and its MPPT using model predictive control," *Sol. Energy*, vol. 158, pp. 995–1005, Dec. 2017, doi: 10.1016/j.solener.2017.10.025.
- [50] R. Tang, "Large-scale photovoltaic system on green ship and its MPPT controlling," *Sol. Energy*, vol. 157, pp. 614–628, Nov. 2017, doi: 10.1016/j.solener.2017.08.058.
- [51] S. Wen, H. Lan, Y.-Y. Hong, D. C. Yu, L. Zhang, and P. Cheng, "Allocation of ESS by interval optimization method considering impact of ship swinging on hybrid PV/diesel ship power system," *Appl. Energy*, vol. 175, pp. 158–167, Aug. 2016, doi: 10.1016/j.apenergy.2016.05.003.
- [52] S. Wen et al., "Optimal sizing of hybrid energy storage sub-systems in PV/diesel ship power system using frequency analysis," *Energy*, vol. 140, pp. 198–208, Dec. 2017, doi: 10.1016/j.energy.2017.08.065.
- [53] F. Diab, H. Lan, and S. Ali, "Novel comparison study between the hybrid renewable energy systems on land and on ship," *Renew. Sustain. Energy Rev.*, vol. 63, pp. 452–463, Sep. 2016, doi: 10.1016/j.rser.2016.05.053.
- [54] C. Ghenai, M. Bettayeb, B. Brdjanin, and A. K. Hamid, "Hybrid solar PV/PEM fuel Cell/Diesel Generator power system for cruise ship: A case study in Stockholm, Sweden," *Case Stud. Therm. Eng.*, vol. 14, p. 100497, Sep. 2019, doi: 10.1016/j.csite.2019.100497.
- [55] J. Ling-Chin and A. P. Roskilly, "Investigating the implications of a new-build hybrid power system for Roll-on/Roll-off cargo ships from a sustainability perspective – A life cycle assessment case study," *Appl. Energy*, vol. 181, pp. 416–434, Nov. 2016, doi: 10.1016/j.apenergy.2016.08.065.
- [56] R. D. Geertsma, R. R. Negenborn, K. Visser, and J. J. Hopman, "Design and control of hybrid power and propulsion systems for smart ships: A review of developments," *Appl. Energy*, vol. 194, pp. 30–54, May 2017, doi: 10.1016/j.apenergy.2017.02.060.
- [57] T. Gorter, "Design Considerations of a Solar Racing Boat: Propeller Design Parameters as a Result of PV System Power," *Energy Procedia*, vol. 75, pp. 1901–1906, Aug. 2015, doi: 10.1016/j.egypro.2015.07.179.
- [58] S. Babu and J. V. Jain, "On-board solar power for small-scale distant-water fishing vessels," in 2013 IEEE Global Humanitarian Technology Conference (GHTC), Oct. 2013, pp. 1–4, doi: 10.1109/GHTC.2013.6713644.
- [59] A. Nasirudin, R.-M. Chao, and I. K. A. P. Utama, "Solar Powered Boat Design Optimization," *Procedia Eng.*, vol. 194, pp. 260–267, Jan. 2017, doi: 10.1016/j.proeng.2017.08.144.

- [60] K. Yigit and B. Acarkan, "A new electrical energy management approach for ships using mixed energy sources to ensure sustainable port cities," *Sustain. Cities Soc.*, vol. 40, pp. 126–135, Jul. 2018, doi: 10.1016/j.scs.2018.04.004.
- [61] M. A. A. A. Mehedi and M. T. Iqbal, "Optimal Sizing of a Hybrid Power System for Driving a Passenger Boat in Bangladesh," in 2020 IEEE Electric Power and Energy Conference (EPEC), Nov. 2020, pp. 1–6, doi: 10.1109/EPEC48502.2020.9319920.
- [62] "The Basics of Boat Design." <https://www.compositesworld.com/articles/the-basics-of-boat-design> (accessed Dec. 13, 2020).
- [63] "Solar Boat_Sustainable and Renewable Energy Authority (SREDA)." Accessed: Aug. 13, 2020. [Online]. Available: [http://www.sreda.gov.bd/d3pbs_uploads/files/Solar%20Boat_Write-up%20for%20SREDA%20website%20\(1\).pdf](http://www.sreda.gov.bd/d3pbs_uploads/files/Solar%20Boat_Write-up%20for%20SREDA%20website%20(1).pdf).
- [64] "Sailboat Math - pocketyachtcruising." <https://sites.google.com/site/pocketyachtcruising/sailing-references/sailboat-math> (accessed Aug. 13, 2020).
- [65] "Canadian Solar CS6U-330P 330W MaxPower Solar Panel." <https://solarelectricsupply.com/canadian-solar-cs6u-330p-330w-wholesale-maxpower-solar-panel> (accessed Feb. 01, 2021).
- [66] C. A. Hossain, N. Chowdhury, M. Longo, and W. Yaïci, "System and Cost Analysis of Stand-Alone Solar Home System Applied to a Developing Country," *Sustainability*, vol. 11, no. 5, Art. no. 5, Jan. 2019, doi: 10.3390/su11051403.
- [67] "Canadian Solar MaxPower2 CS6U-330P 330w Poly Solar Panel," Solaris. <https://www.solaris-shop.com/canadian-solar-maxpower2-cs6u-330p-330w-poly-solar-panel/> (accessed Aug. 13, 2020).
- [68] C. A. Hossain, N. Chowdhury, M. Longo, and W. Yaïci, "System and Cost Analysis of Stand-Alone Solar Home System Applied to a Developing Country," *Sustainability*, vol. 11, no. 5, Art. no. 5, Jan. 2019, doi: 10.3390/su11051403.
- [69] "Champion 1600W / 2000W Inverter Generator | Canadian Tire." <https://canadiantire.ca/en/pdp/champion-1600w-2000w-inverter-generator-0550214p.html#srp> (accessed Aug. 13, 2020).
- [70] "Trojan SAGM 06 220 AGM 6V 220Ah Battery," Solaris. <https://www.solaris-shop.com/trojan-sagm-06-220-agm-6v-220ah-battery/> (accessed Aug. 13, 2020).
- [71] "Solar Charge Controller Sizing and How to Choose One." <https://www.altenergy.org/renewables/solar/DIY/solar-charge-controller.html> (accessed Dec. 13, 2020).
- [72] "Solar Battery Charge Controller." https://www.alibaba.com/product-detail/Bluesun-12v-24v-36v-48v-96v_60461871727.html?spm=a2700.galleryofferlist.0.0.6db477ddyYywW5 (accessed Aug. 13, 2020).

- [73] R. Gupta, G. Gupta, D. Kastwar, A. Hussain, and H. Ranjan, "Modeling and design of MPPT controller for a PV module using PSCAD/EMTDC," 2010 IEEE PES Innov. Smart Grid Technol. Conf. Eur. ISGT Eur., 2010, doi: 10.1109/ISGTEUROPE.2010.5638880.
- [74] K. H. Hussein, I. Muta, T. Hoshino, and M. Osakada, "Maximum photovoltaic power tracking: an algorithm for rapidly changing atmospheric conditions," *Transm. Distrib. IEE Proc. - Gener.*, vol. 142, no. 1, pp. 59–64, Jan. 1995, doi: 10.1049/ip-gtd:19951577.
- [75] C. González-Morán, P. Arbolea, D. Reigosa, G. Díaz, and J. Gómez-Aleixandre, "Improved model of photovoltaic sources considering ambient temperature and solar irradiation," in 2009 IEEE PES/IAS Conference on Sustainable Alternative Energy (SAE), Sep. 2009, pp. 1–6, doi: 10.1109/SAE.2009.5534859.
- [76] "XCSOURCE DC 48V Acid Lead Battery Capacity Indicator Display Tester Voltmeter." https://www.amazon.ca/XCSOURCE-Capacity-Indicator-Voltmeter-MA395/dp/B01EFJPWOU/ref=sr_1_3?dchild=1&keywords=XCSOURCE+DC+12V+24V+36V+48V+60V+72V+96V+Acid+Lead+Battery+Capacity+Indicator+Display+Tester+Voltmeter%28Default+12V%29+MA395&qid=1618764253&sr=8-3 (accessed Jan. 28, 2021).
- [77] "5kw 48v Electric Dc Motor - Buy Electric Dc Motor,48v Electric Dc Motor,5kw 48v Electric Motor Product on Alibaba.com." https://www.alibaba.com/product-detail/5kw-48V-electric-dc-motor_525516727.html?spm=a2700.7724857.normal_offer.d_title.3bbf7694SYP9CS (accessed Feb. 12, 2021).
- [78] "100A/150A/200A high power solar charge controller." <http://www.queenswing.com/e-productshow/?470-100A150A200A-high-power-solar-charge-controller-470.html> (accessed Feb. 13, 2021).
- [79] "Blue Sea Systems Common BusBars - 150A." https://www.delcity.net/store/150A-Common-Bus-Bars/p_807953.h_807954 (accessed Feb. 01, 2021).
- [80] "187-Series Circuit Breaker - Panel Mount 150A - Blue Sea Systems." https://www.blueseasystems.com/products/7048/187-Series_Circuit_Breaker_-_Panel_Mount_150A (accessed Feb. 01, 2021).
- [81] "187-Series Circuit Breaker - Panel Mount 40A - Blue Sea Systems." https://blueseasystems.com/products/7038/187-Series_Circuit_Breaker_-_Panel_Mount_40A (accessed Feb. 01, 2021).
- [82] "Current-limiting Miniature Circuit Breaker: 1.5A, C curve (PN# FAZ-C1P5-1-NA-L-SP) | Automation Direct." [https://www.automationdirect.com/adc/shopping/catalog/circuit_protection_-z-_fuses_-z-_disconnects/ul_489_miniature_circuit_breakers/eaton_240vac_miniature_circuit_breakers_\(faz-na_series\)/1-pole_\(0.5a-63a\)/faz-c1p5-1-na-l-sp](https://www.automationdirect.com/adc/shopping/catalog/circuit_protection_-z-_fuses_-z-_disconnects/ul_489_miniature_circuit_breakers/eaton_240vac_miniature_circuit_breakers_(faz-na_series)/1-pole_(0.5a-63a)/faz-c1p5-1-na-l-sp) (accessed Feb. 01, 2021).
- [83] "Current-limiting Miniature Circuit Breaker: 1A, C curve (PN# FAZ-C1-1-NA-L-SP) | AutomationDirect." [https://www.automationdirect.com/adc/shopping/catalog/circuit_protection_-z-_fuses_-z-_disconnects/ul_489_miniature_circuit_breakers/eaton_240vac_miniature_circuit_breakers_\(faz-na_series\)/1-pole_\(0.5a-63a\)/faz-c1-1-na-l-sp](https://www.automationdirect.com/adc/shopping/catalog/circuit_protection_-z-_fuses_-z-_disconnects/ul_489_miniature_circuit_breakers/eaton_240vac_miniature_circuit_breakers_(faz-na_series)/1-pole_(0.5a-63a)/faz-c1-1-na-l-sp) (accessed Feb. 01, 2021).

[84] “Current-limiting Miniature Circuit Breaker: 5A, C curve (PN# FAZ-C5-1-NA-L-SP) | AutomationDirect.” [https://www.automationdirect.com/adc/shopping/catalog/circuit_protection_-z-_fuses_-z-_disconnects/ul_489_miniature_circuit_breakers/eaton_240vac_miniature_circuit_breakers_\(faz-na_series\)/1-pole_\(0.5a-63a\)/faz-c5-1-na-l-sp](https://www.automationdirect.com/adc/shopping/catalog/circuit_protection_-z-_fuses_-z-_disconnects/ul_489_miniature_circuit_breakers/eaton_240vac_miniature_circuit_breakers_(faz-na_series)/1-pole_(0.5a-63a)/faz-c5-1-na-l-sp) (accessed Feb. 01, 2021).

[85] “187-Series Circuit Breaker - Panel Mount 135A - Blue Sea Systems.” https://www.blueseasystems.com/products/7047/187-Series_Circuit_Breaker_-_Panel_Mount_135A (accessed Feb. 01, 2021).

[86] E. Akyuz, Z. Oktay, and I. Dincer, “Energetic, environmental and economic aspects of a hybrid renewable energy system: a case study,” *Int. J. Low-Carbon Technol.*, vol. 6, no. 1, pp. 44–54, Mar. 2011, doi: 10.1093/ijlct/ctq041.

List of Publications

Refereed Journal Article and Conference Publications:

- [1] M. A. A. A. Mehedi and M. T. Iqbal, "Optimal Design, Dynamic Modeling and Analysis of a Hybrid Power System for a Catamarans Boat in Bangladesh," *Eur. J. Electr. Eng. Comput. Sci.*, vol. 5, no. 1, Art. no. 1, Feb. 2021, doi: 10.24018/ejece.2021.5.1.294.
- [2] M. A. A. A. Mehedi and M. T. Iqbal, "Optimal Sizing of a Hybrid Power System for Driving a Passenger Boat in Bangladesh," in 2020 IEEE Electric Power and Energy Conference (EPEC), Nov. 2020, pp. 1–6, doi: 10.1109/EPEC48502.2020.9319920.
- [3] A. Sharan, M. Zamanlou, M. Rahman, and M. Al-Mehdi, "Centralized Power Generation of Solar Parks using Wireless Controlling," *Int. J. Curr. Eng. Technol.*, vol. 9, Aug. 2019, doi: 10.14741/ijcet/v.9.3.9.

Regional Conference Publication:

- ✓ Mohammad Abu Abdullah Al Mehedi, M. Tariq Iqbal, "Design of a PV system for a small boat for use in Bangladesh," presented at the 28th Annual IEEE NECEC conference, St. John's, NL, Canada, November 19th, 2019.